INFORMATION TO USERS

This reproduction was made from a copy of a document sent to us for microfilming. While the most advanced technology has been used to photograph and reproduce this document, the quality of the reproduction is heavily dependent upon the quality of the material submitted.

The following explanation of techniques is provided to help clarify markings or notations which may appear on this reproduction.

1. The sign or "target" for pages apparently lacking from the document photographed is "Missing Page(s)". If it was possible to obtain the missing page(s) or section, they are spliced into the film along with adjacent pages. This may have necessitated cutting through an image and duplicating adjacent pages to assure complete continuity.

2. When an image on the film is obliterated with a round black mark, it is an indication of either blurred copy because of movement during exposure, duplicate copy, or copyrighted materials that should not have been filmed. For blurred pages, a good image of the page can be found in the adjacent frame. If copyrighted materials were deleted, a target note will appear listing the pages in the adjacent frame.

3. When a map, drawing or chart, etc., is part of the material being photographed, a definite method of "sectioning" the material has been followed. It is customary to begin filming at the upper left hand corner of a large sheet and to continue from left to right in equal sections with small overlaps. If necessary, sectioning is continued again—beginning below the first row and continuing on until complete.

4. For illustrations that cannot be satisfactorily reproduced by xerographic means, photographic prints can be purchased at additional cost and inserted into your xerographic copy. These prints are available upon request from the Dissertations Customer Services Department.

5. Some pages in any document may have indistinct print. In all cases the best available copy has been filmed.

University Microfilms International
300 N. Zeeb Road
Ann Arbor, MI 48106

1327642

Finley, Ray E.

DESIGN OF TUNNELS IN ROCK USING STRAIN ENERGY AND LIMIT STATE CONCEPTS

The University of Arizona M.S. 1986

University
Microfilms
International 300 N. Zeeb Road, Ann Arbor, MI 48106

PLEASE NOTE:

In all cases this material has been filmed in the best possible way from the available copy. Problems encountered with this document have been identified here with a check mark __✓__.

1. Glossy photographs or pages _____
2. Colored illustrations, paper or print _____
3. Photographs with dark background _____
4. Illustrations are poor copy _____
5. Pages with black marks, not original copy _____
6. Print shows through as there is text on both sides of page _____
7. Indistinct, broken or small print on several pages ✓
8. Print exceeds margin requirements _____
9. Tightly bound copy with print lost in spine _____
10. Computer printout pages with indistinct print _____
11. Page(s) _____ lacking when material received, and not available from school or author.
12. Page(s) _____ seem to be missing in numbering only as text follows.
13. Two pages numbered _____. Text follows.
14. Curling and wrinkled pages _____
15. Dissertation contains pages with print at a slant, filmed as received _____
16. Other _____

_____

_____

University
Microfilms
International

DESIGN OF TUNNELS IN ROCK USING STRAIN ENERGY AND LIMIT STATE CONCEPTS

by

Ray Edward Finley

A Thesis Submitted to the Faculty of the

DEPARTMENT OF MINING AND GEOLOGICAL ENGINEERING

In Partial Fulfillment of the Requirements
For the Degree of

MASTER OF SCIENCE
WITH A MAJOR IN GEOLOGICAL ENGINEERING

In the Graduate College

THE UNIVERSITY OF ARIZONA

1 9 8 6

STATEMENT BY AUTHOR

This thesis has been submitted in partial fulfillment of requirements for an advanced degree at The University of Arizona and is deposited in the University Library to be made available to borrowers under rules of the Library.

Brief quotations from this thesis are allowable without special permission, provided that accurate acknowledgement of source is made. Requests for permission for extended quotation from or reproduction of this manuscript in whole or in part may be granted by the head of the major department or the Dean of the Graduate College when in his or her judgement the proposed use of the material is in the interests of scholarship. In all other instances, however, permission must be obtained from the author.

SIGNED: Ray E. Finley

APPROVAL BY THESIS DIRECTOR

This thesis has been approved on the date shown below:

I. W. Farmer
Professor of Mining and
Geological Engineering

1-9-86
Date

ACKNOWLEDGEMENTS

I would like to thank the US Army Corp of Engineers, Waterways Experiment Station, Vicksburg, Mississippi for providing the funding for this research.

I am indebted to Dr. Ian Farmer, my thesis director, Dr. Jaak Daemen, and Dr. Charles Glass for their helpful criticism and encouragement throughout this study and my entire graduate program.

I would also like to express my love and appreciation to my wife and children who made all the work worthwhile.

TABLE OF CONTENTS

TABLE OF CONTENTS--Continued

LIST OF ILLUSTRATIONS

LIST OF ILLUSTRATIONS--Continued

LIST OF ILLUSTRATIONS--Continued

LIST OF TABLES

ABSTRACT

The design of tunnels in rock based strictly on strength characteristics is unrealistic. The initial redistribution of stresses, or strain energy, will commonly exceed the rocks resistance to fracture along at least a portion of the tunnel boundary. Therefore, a more reasonable approach would be to define allowable or limiting states of deformation and then control the deformation, with supports, to that limit state.

Tunnel boundary deformations occur as a result of fracture in the surrounding annulus. The energy stored in the annular rocks as a result of tunnel development is released onto fracture surfaces as kinetic energy. The resulting change in energy is manifested as tunnel boundary displacements. Initiation of fracture in the annulus is itself influenced by the rocks fracture toughness, incorporating both strength and elastic characteristics.

Common laboratory tests may not adequately model the conditions the rock will encounter in the tunnel annulus. Laboratory tests should be evaluated in terms of strain energy and alternate testing programs initiated.

CHAPTER 1

INTRODUCTION

The design of tunnels in rock can be based on various criteria describing the behavior of rock and its influence on the performance of the tunnel. These criteria can range from simple destructive or nondestructive tests to quite complex classification systems aiming to divide rocks into groups which behave in similar ways. The need for some kind of characterization is evident, since too little is known about the behavior of rock masses to allow engineers to design underground structures with confidence. Nevertheless, the basis of many attempts at characterization is such as to raise genuine questions about the philosophy of engineering design in rock on which they are based. The reason for this is that implicitly or explicitly they contain assumptions about rock and rock mass behavior which may not be wholly sound.

For example, the most common approaches to design of underground structures are based on:

(a) Empirical relations between case histories in similar types of rock usually defined on the basis of rock mass structure.

(b) Relations between stress distributions and ultimate limit states such as "strength."

While acceptable in engineering practice, neither of the these approaches are entirely satisfactory. For instance, case history and

empiricism rely on a presumption that all rock behavior can be predicted from previous experience. In a complex and variable rock mass this is not always the case. Similarly, ultimate limit states are based on an assumption of idealized behavior, usually precluding, or describing only poorly, rock fracture mechanics.

The initial redistribution of stresses, or development of excess strain energy, around underground openings commonly results in exceeding the rocks resistance to fracture along at least a portion of the tunnel boundary. The excess strain energy developed by this redistribution will be expended in rock fracture and dilation, the amount of which will depend on the energy release characteristics of the rock itself. Underground missile bases, such as those being considered in the MX "deep basing" concept, must additionally be designed to resist the dynamic energy associated with the detonation of nuclear warheads. The success or failure of the design being not necessarily controlled by the strength characteristics but more importantly by the deformational characteristics of the rock.

Inherent in this concept is the idea of performance. Common design procedure is to evaluate tunnel performance based on the rocks strength characteristics. The tunnel support is usually designed to resist deformation and is based on the common strength criteria. A more reasonable approach would be to establish tolerable limiting states of deformation and to design the support to control the deformation to these tolerable levels. A limit state design approach, commonly used in reinforced concrete design, is ideally suited to the

design of structures in rock. This approach evaluates the design performance of structural concrete based on the attainment of certain limit states, the most important of which for structures in rock, are the ultimate limit state, based on strength excess, and serviceability limit states, based on tolerable deformations.

Previous Work

There is a significant body of technical literature dealing with the subject of rock fracture around underground openings, and tunnel support required to satisfy the design performance standards of tunnels. A complete accounting of this literature is beyond the scope of this report, however, some of the more important developments should be addressed.

The behavior of rock around underground openings has historically been described through the use of theoretical or empirical models. Simple geometries and simple field stresses can be treated analytically but more complex geometries require numerical solutions.

The most commonly addressed problem is that of a circular tunnel in a hydrostatic ($\sigma_1 = \sigma_2 = \sigma_3$) stress field. The assumptions used in developing this analytical solution are; that the rock is isotropic, homogeneous, and continuously linear elastic and that the opening deforms according to plane strain conditions. Stress and radial displacement for this situation are derived in Jaeger and Cook (1979) to be:

$$\sigma_\theta = P_o(1 + a^2/r^2)$$

$$\sigma_r = P_o(1 - a^2/r^2)$$

$$U_r = ((1 - \nu)/G)P_o a$$

where: r = radial distance from the tunnel centerline

a = tunnel radius

P_o = hydrostatic ($\sigma_1 = \sigma_2 = \sigma_3$) field stress

G = shear Modulus

ν = Poisson's ratio

σ_θ = tangential (major principal) stress

σ_r = radial (minor principal) stress

U_r = radial displacement of the tunnel boundary

Inherent in this solution is the assumption that the strength is not exceeded by the redistributed stresses (σ_θ, σ_r). This assumption is probably not valid except for unusual instances in which openings are developed in very strong rocks at shallow depth so that the stress is small compared to the strength. The solution does, however, provide useful insight which can be utilized by the more realistic solutions.

Many other solutions to the circular tunnel in a hydrostatic stress field problem allow for the development of a zone of broken rock around the tunnel periphery. Five common solutions to this problem are described below.

Fenner (1983) modeled both the broken and intact rock as a Coulomb material ($\tau = c + \sigma\tan\theta$) in which the intact and residual strengths were identical. Hobbs (1970) carried out tests on broken rock and developed a broken-intact model in which the fractured material obeyed a curved failure envelope. Ladanyi (1974), in possibly the most widely quoted method, developed a procedure by which the broken material behaved plastically, obeying a flow rule from the theory of plasticity relating plastic strain deformation to the associated stress. Wilson (1977) assumed the broken material acted as a granular material without cohesion. Wilson (1980) also developed a model in which the broken material acts as a Coulomb material with some residual cohesion. Fenner's (1938) and Ladanyi's (1974) approach yield the least broken thickness, whereas Wilson's (1977, 1980) developed the greatest broken zone around a circular tunnel. The approximate relationship between the various methods is illustrated in Figure 1. In all cases the intact rock is assumed to behave elastically and body forces are ignored.

Closures or boundary deformations, can be determined using Ladanyi's (1974) approach. This method makes use of the average plastic dilation due to fracturing of the rock and the opening of the discontinuities. Hoek and Brown (1981) utilize Ladanyi's (1974) approach and an empirical failure criterion based on numerous laboratory experiments and the authors extensive experience to estimate both closure and support requirements.

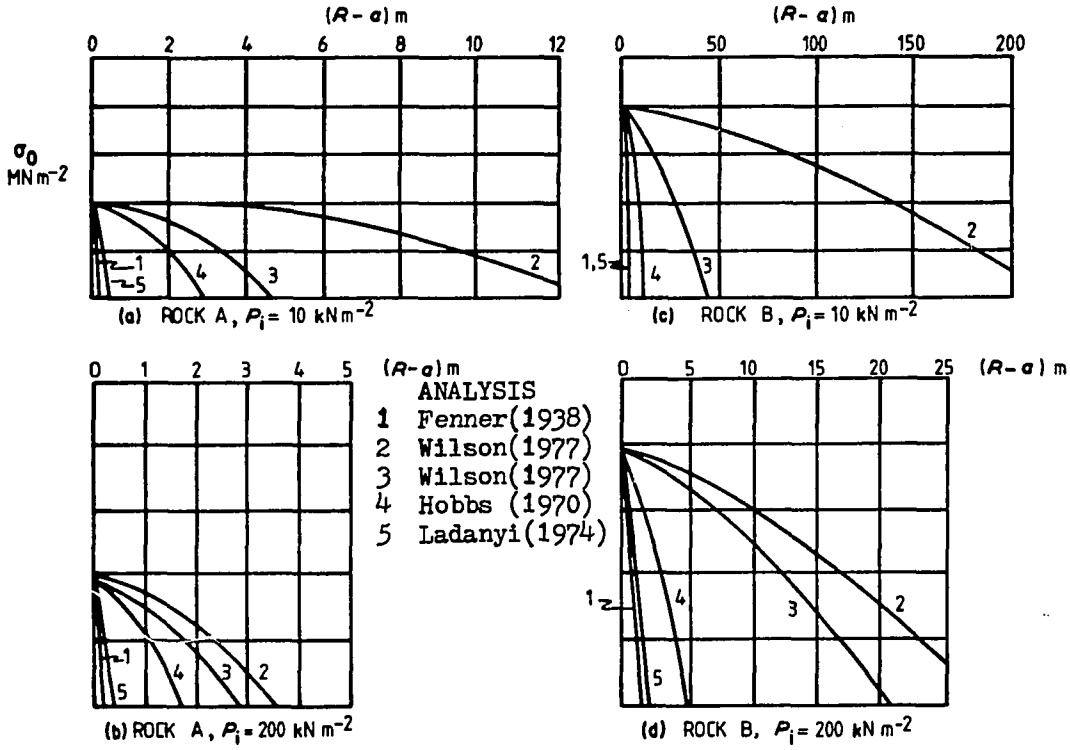

Figure 1. Comparison of Fracture Zone Widths from Two Support Pressures (10 and 200 KN/m^2) and Two Hypothetical Rock Types. (Farmer, 1985)

Tunnel support requirements are commonly analyzed by the use of ground response curves (Daemen, 1977; Brown, et al. 1983), or empirical methods (e.g. Barton, Lien and Lunde, 1974; Bieniawski, 1973). These curves, developed for specific projects, illustrate the way in which tunnel support interacts with the deforming tunnel periphery to achieve equilibrium. The equilibrium point can be controlled, to a certain degree, by the support stiffness. A yielding or soft support will deform significantly before it reaches its ultimate strength, whereas stiff supports will mobilize ultimate strengths at small deformations. Hoek and Brown (1981) have developed an elaborate rock-support interaction analysis with ground characteristics determined through an empirically modified Ladanyi (1970) approach as previously described. This method is very sensitive to the selection of the empirical residual rock parameters and as such requires some experience to be successfully used.

Little information is available which describes the energy changes resulting from the development of underground openings. Cook (1967) and Jaeger and Cook (1979) include some information on the subject but make no specific recommendations on rock fracture and fracture resistance or on tunnel support requirements. Wiebols and Cook (1968) have developed a polyaxial failure criterion for rock based on the maximum shear strain energy. This approach requires numerical methods and makes certain assumptions about the number and orientation of micro-cracks and as such has limited applicability. The energy required to satisfy new fracture surface area in rock has

been studied by Friedman, Handin and Alani (1972) and Krech (1974) for rock samples in uniaxial tension. The results do not correlate well with surface energy requirements of single crystals, but the discrepancies may be related to fracture surface topographic effects. Brady and Brown (1981) as well as other authors use some energy considerations and the boundary element method to analyze rockburst susceptibility.

The dynamic stability of tunnels and underground openings has been considered by many workers. Tunnel damage has been related to peak surface accelerations (Dowding 1978), peak free-field velocity (Owen, Scholl and Brekke 1979), and peak free-field strain (Joachim, 1979). The conclusion, in general, is that underground installations are less sensitive to dynamic energy inputs than surface structures and that dynamic energy in the seismic range must be great for damage to occur at all. For defense installation subject to nuclear attack loading, damage will probably occur as a result of the high pressure shock wave. The structure should be designed to withstand the shock wave (possibly through the use of special backpacked liners (Dickenson and Lindberg, 1984) or be moved beyond the range of shock wave influence. In summary, the principal governing factor in the design of underground installations to withstand nuclear attack loading, is the estimate of the expected shock or seismic pulse from the surface blast. The amount of energy transmitted as a shock or seismic wave is dependent on, the amount of energy released at the surface (explosive yield), the lithology through which the energy will be transmitted,

the moisture content (saturation), the in-situ stress regime, and the orientation and size of the installation.

Objective

This thesis is not meant to be a "cookbook" for design but rather conceptual in nature, illustrating the importance of the ideas considered. The strain energy concepts have been developed to interface with a strain based tunnel failure criterion under development at the Waterways Experiment Station. Limit state design concepts are introduced to provide a link with strain energy and to suggest a basic framework by which a better approach to design may be developed.

CHAPTER 2

ENERGY CONCEPTS

Energy is a fundamental concept in science and engineering and occurs in two forms: kinetic and potential. Changes in the kinetic and potential energy in the annulus of a tunnel can directly affect the tunnels performance. Kinetic energy is the energy of motion, and, for the case of tunnels, is most commonly initiated by earthquakes, rockbursts, or explosive blasts. Potential energy is the energy associated with position and is generated by gravitational forces. Strain energy can be considered a form of potential energy and the development of an underground opening will alter the distribution of strain energy in the annulus of a tunnel. The changes associated with both potential (strain) and kinetic energy can create conditions in which the fracture resistance of the rock in the tunnel annulus is exceeded. Fracturing will generate the tunnel boundary deformations which control tunnel performance.

Strain Energy Principles

The concept of strain energy, although not commonly employed in rock mechanics, is frequently used in structural analysis and allows for the solution of otherwise indeterminate problems. A thorough treatment of basic strain energy principles can be found in most books on elasticity or advanced mechanics of materials

(Timoshenko and Goodier 1951; Timoshenko, 1958). Jaeger and Cook (1979) also provide some basic strain energy relationships, some of the more useful of which are outlined below.

Basic Concepts

In mechanics, energy is the capacity to do work, and work is the product of force and the distance in the direction the force moves. In solid deformable bodies, stress multiplied by areas are forces and deformations are distances. The product of force and distance (or stress x area and deformation) is the internal work done in a body by externally applied forces. This internal work is stored in a body as strain energy.

The physical significance of strain energy is illustrated in Figure 2. In this figure, a block of rock of unit volume is loaded uniaxially in the x-direction producing the indicated stress-strain curve. The strain energy per unit volume stored in the rock block is the shaded area under that curve and is expressed as:

$$W = 1/2\ \varepsilon_x \sigma_x \tag{1}$$

or since $\varepsilon_x = \sigma_x/E$

$$W = 1/2\ \sigma_x^2/E \tag{2}$$

In the case of uniaxial loading to failure, when $\sigma_x = \sigma_c$ (the unconfined compressive strength), so that equation (2) becomes.

$$W = 1/2\ \sigma_c^2/E \tag{3}$$

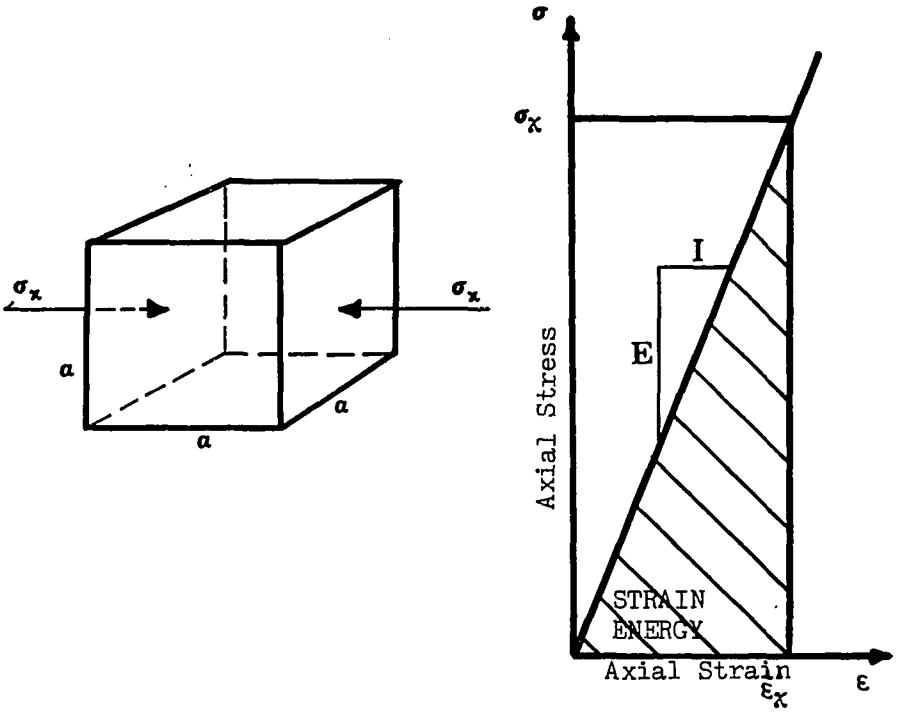

Figure 2. Definition of Strain Energy in Uniaxial Compression.

W in equations (1), (2), (3) is referred to as the energy density since it represents the energy per unit volume in the rock block. The total energy for the block, assuming a volume a^3 would be:

$$W_{Total} = (a^3/2)\ \varepsilon_x \sigma_x \tag{4}$$

The uniaxial case is, as expected, much simpler than the triaxial loading condition. Under triaxial loading, there will be a contribution to the total stored strain energy as a result of the stresses σ_2 and σ_3 acting over the side areas a^2. As a result of this additional contribution, the total strain energy in the rock block will be given by:

$$W_{Total} = a^3/2\ \varepsilon_1 \sigma_1 + a^3/2\ \varepsilon_2 \sigma_2 + a^3/2\ \varepsilon_3 \sigma_3 \tag{5}$$

or

$$W_{Total} = a^3/2\ (\varepsilon_1\sigma_1 + \varepsilon_2\sigma_2 + \varepsilon_3\sigma_3) \tag{6}$$

The energy density is:

$$W = 1/2\ (\varepsilon_1 \sigma_1 + \varepsilon_2 \sigma_2 + \varepsilon_3 \sigma_3) \tag{7}$$

which was obtained by dividing the total energy by the unit volume. Another useful form of equation (7) is:

$$W = (1/(2E))(\sigma_1^2 + \sigma_2^2 + \sigma_3^2 - 2\nu\ (\sigma_2\sigma_3 + \sigma_1\sigma_3 + \sigma_1\sigma_2)) \tag{8}$$

which was obtained from the inverse formulae:

$$E\,\varepsilon_1 = \sigma_1 - \nu\,(\sigma_2 + \sigma_3)$$

$$E\,\varepsilon_2 = \sigma_2 - \nu\,(\sigma_1 + \sigma_3) \qquad (9)$$

$$E\,\varepsilon_3 = \sigma_3 - \nu\,(\sigma_1 + \sigma_2)$$

Equation (8) illustrates the complexity of triaxial energy calculations and also emphasizes the importance of Young's modulus (E) and Poisson's ratio (ν) in determining strain energy.

Equation (3) for the strain energy in a uniaxial specimen: $W = 1/2\ \sigma_c^2/E$ contains a term σ_c^2/E sometimes referred to as the rocks fracture toughness which can be thought of as a measure of the rocks resistance to fracture. Fracture toughness is an important rock characteristic and can graphically be represented as in Figure 3. Rock A has an unconfined strength σ_A and rock B has an unconfined strength σ_B. Rock B requires a greater strain, ε_B, to mobilize its maximum strength. The strain energy required to fracture each rock is shown crosshatched in the figure. Therefore, rock A is a stronger rock, however, rock B is a tougher rock, since a greater energy input is required to fracture it. The fracture toughness is a measure of the energy required to fracture the rock and this energy is the area under the stress-strain curves for rocks A and B respectively.

Fracture Toughness

Fracture toughness (σ_c^2/E) was defined in the preceeding

section. Figure 3 illustrates the importance of not solely considering strength as the criterion for failure. Obviously, the rocks fracture toughness can also be used as a criterion.

Deere and Miller (1966) showed that a linear relationship existed between Young's Modulus (E) and unconfined compressive strength (σ_c) for many rocks. This was later confirmed by Hobbs (1974) for Lias and Trias rocks. The data envelopes from these two sources are shown in Figures 4 and 5, and have been replotted in σ_c^2 - E space in Figure 6. This figure shows that most generic rock types (granite, limestone, etc.) fall within a range of fracture toughnesses. In general, sedimentary rocks have a very wide range of fracture toughness values, ranging from σ_c^2/E values greater than 1 to σ_c^2/E values less than 0.01. This illustrates the difficulty in describing rocks by generic classifications. Igneous rocks, on the other hand, exhibit a much narrower fracture toughness range of values, from σ_c^2/E about equal to 1 to σ_c^2/E about 0.1. Basalts and other flow rocks exhibit a broader and lower fracture toughness band. Chalk tends to have a uniformly low fracture toughness. The wide range of fracture toughnesses for some generic rock types occurs as a result of not being able to adequately describe rocks generically. For instance, "basalt and other flow rocks" encompasses a wide range of rock types from basalt to rhyolite. What Figure 6 does illustrate, is that differences in fracture toughness do occur for various generic rock types. Additionally, some weak rocks such as mudstones or weak sandstones will have a similar or even higher resistance to fracture,

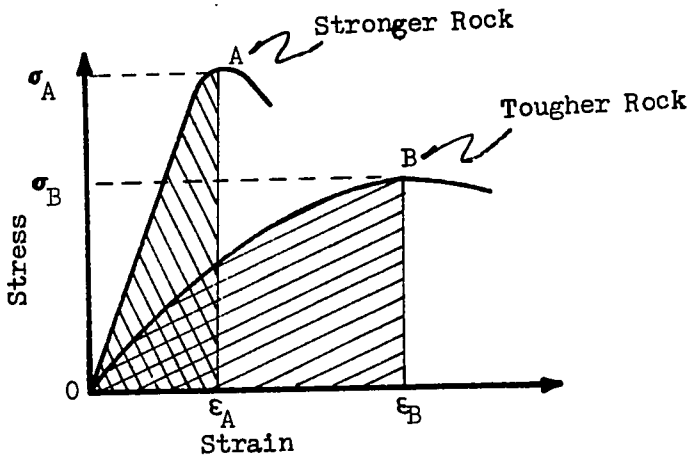

Figure 3. Definition of Fracture Toughness.

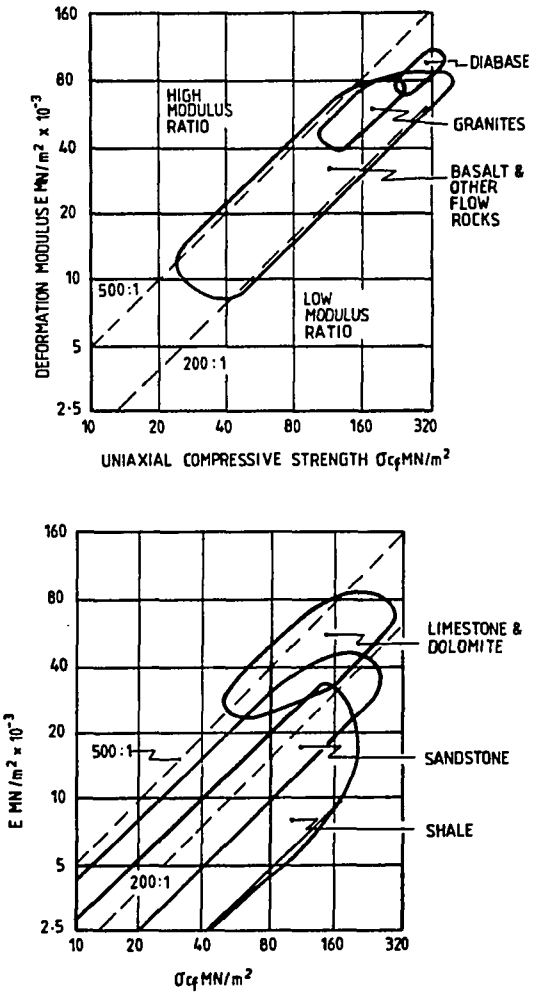

Figure 4. Modulus Ratio Ranges for Typical Igneous and Sedimentary Rocks. (after Deere and Miller, 1966)

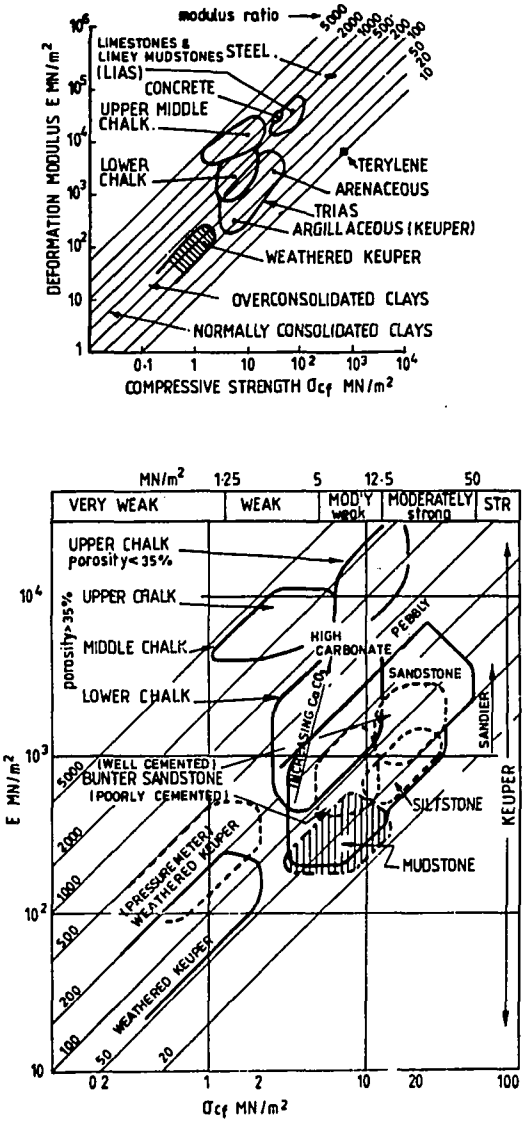

Figure 5. Modulus Ratio Ranges for Some Chalk, Lias and Trias Rocks, Together with Some Typical Engineering Materials and Overconsolidated Clays. (after Hobbs, 1974)

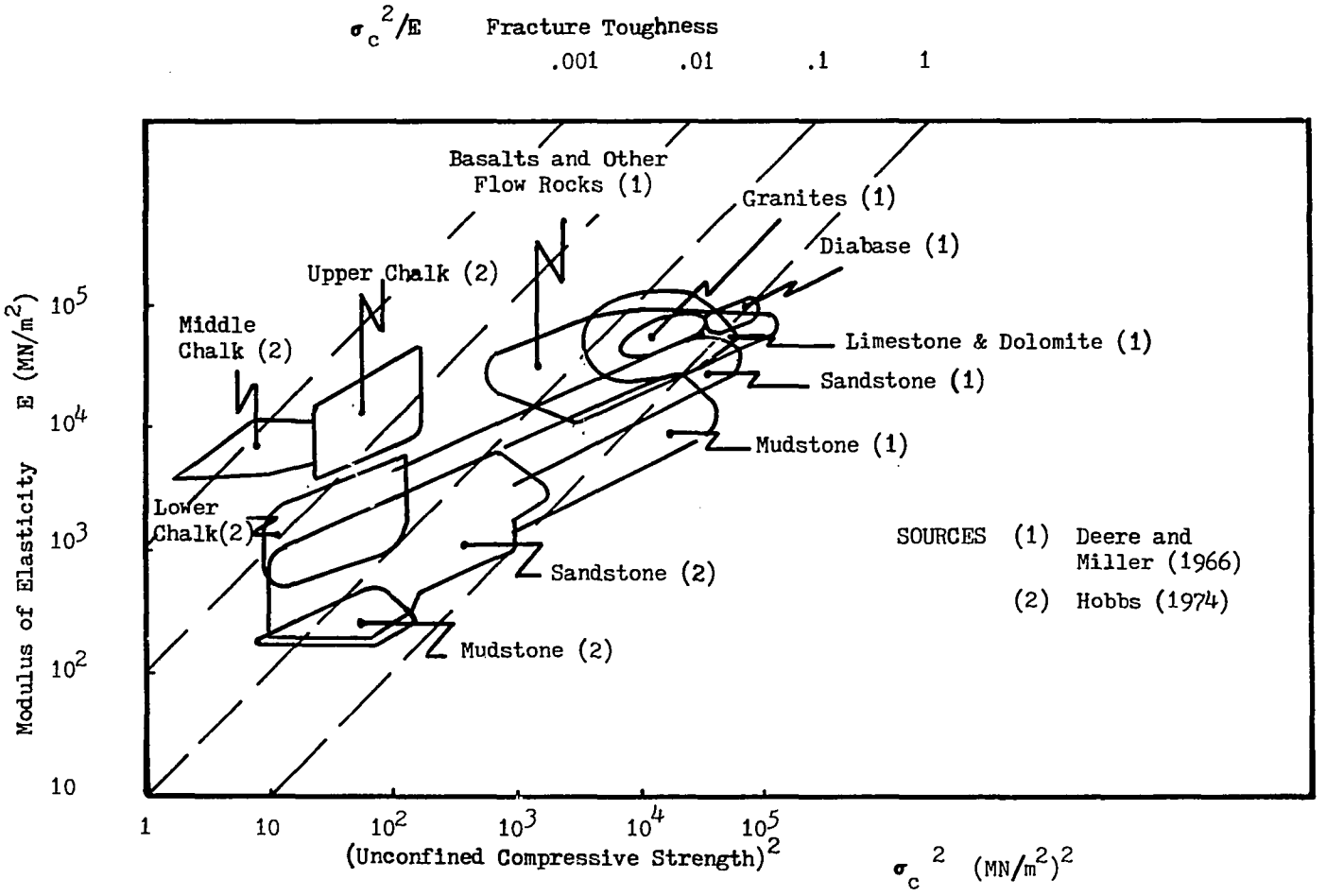

Figure 6. Fracture Toughness Bands, Superimposed on Strength/Modulus Ranges Proposed by Hobbs (1974) and Deere and Miller (1966) for Various Rock Types.

or fracture toughness, than some strong igneous rocks. These "weak" rocks might be expected to resist fracture an equal or greater amount than some "strong" rocks when they appear in the periphery of a tunnel. The range of expected fracture resistances can be used to estimate rock behavioral characteristics around tunnels.

Strain Energy Around Tunnels

Cook (1967) and Jaeger and Cook (1979) have considered a strain energy approach to tunnel design. The approach is proposed to evaluate rock burst susceptibility in deep level mines. The concepts are equally valid in shallower tunnels in which the energy storage capability of the rocks are not so great.

The maximum amount of energy which can be released by any excavation is:

$$W_{Rmax} = \sigma_o V \tag{10}$$

where σ_o = the maximum virgin stress around the excavation

v = the volume of the excavation

This maximum energy release will only be realized if the opening closes on itself so that opposite sides of the excavation touch and produce stresses equal to the in-situ field stress. Alternatively, assuming opposite sides do not touch, the energy released will be:

$$W = 1/2 \int_{a_1} \sigma_1 u_1' da_1 + 1/2 \int_{a_2} \sigma_2 u_2' da_2 + 1/2 \int_{a_3} \sigma_3 u_3' da_3 \tag{11}$$

which shows the contribution of released energy by the three principal stresses (σ_1, σ_2, σ_3) acting on the surface of the excavation,

where: da_1 = the unit excavation surface area perpendicular to σ_1

da_2 = the unit excavation surface area perpendicular to σ_2

da_3 = the unit excavation surface area perpendicular to σ_3

u_1' = displacement due to σ_1

u_2' = displacement due to σ_2

u_3' = displacement due to σ_3

The changes in energy can best be understood considering the following figures.

Figure 7 illustrates the pre and post-excavation condition. The field stress is hydrostatic and everywhere equal to P_o. The dotted lines enclosing the tunnel indicate the proposed position of the tunnel. As was stated previously, a certain amount of energy will be released and will be equivalent to the amount of elastic closure Figure 7b. In addition, changes in potential energy will occur as a result of far-field displacements in the horizontal and vertical planes. The change in horizontal potential energy is given by:

$$W_H = P_o V_2 + P_o V_3 \qquad (12)$$

where: P_o = the in-situ field stress (hydrostatic)

V_2, V_3 = the volume change in the vertical planes due to movement toward the excavation

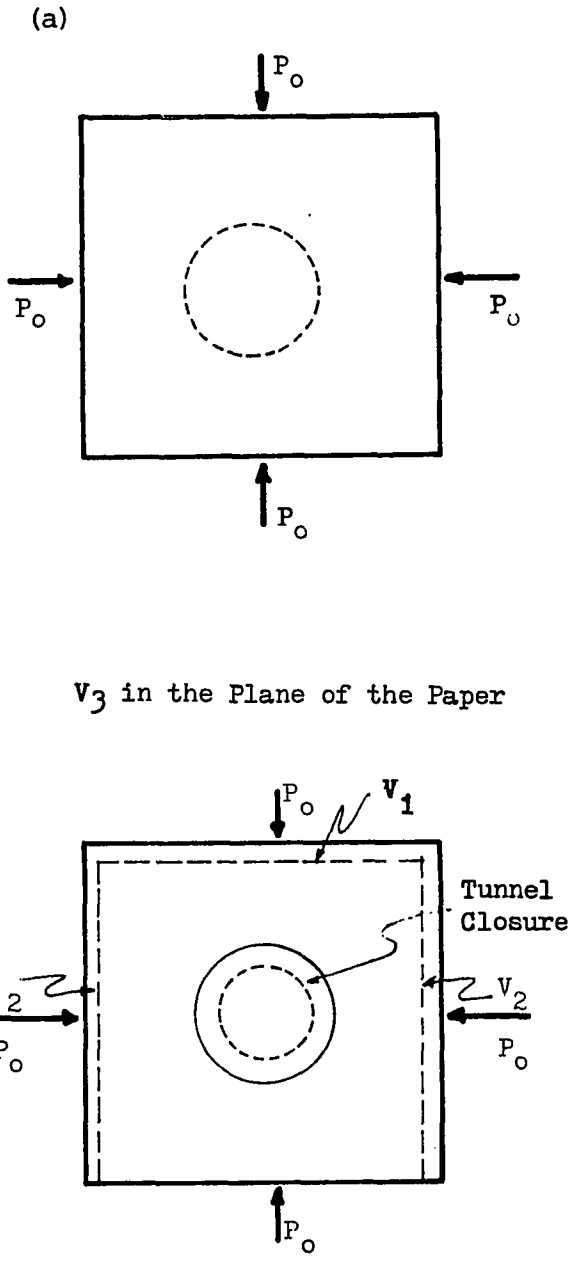

Figure 7. Stresses and Volume Changes Associated with Tunnel Development. (a) Pre-excavation Condition, (b) Post-excavation Condition.

The change in gravitational potential energy is:

$$W_G = P_o V_1 \tag{13}$$

where: V_1 = the volume change due to the movement of the horizontal surface toward the center of the earth

Finally, there is an energy change due to the rock removed by mining which is denoted by W_v.

The total energy change is given by:

$$\Delta W_{To} = W_G + W_H = 2W_R + 2W_v = W_R + W_I + 2W_v \tag{14}$$

where $W_I = W_R$ = the energy induced in the rock due to the induced stresses and W_v = the energy originally in the volume of rock removed by mining.

The stored energy is the difference between the total energy change and the energy released and is:

$$W_s = W_I + 2W_v \tag{15}$$

In elastic rock, the released energy, W_R, and the induced energy, W_I, are equal if the rock does not fracture. If fracture does occur, then the released energy increases and the induced energy decreases. This is illustrated in Figure 8 which shows the energy changes that occur as the stresses on the surface of the excavation are reduced, by mining, from P_o to zero. As these stresses are reduced, energy is released, and this release is manifested as

volumetric closure. The abscissa on Figure 8a and b shows how the volume of the excavation will change, from V_o immediately prior to excavation, to V_f, the equilibrium volume.

For the case of a circular tunnel (the simplest case), the stored energy per unit length is given by:

$$W_s = \pi P_o^2 a^2 (1 + \nu) (3 - 4\nu)/E \tag{16}$$

The induced energy is:

$$W_I = \pi P_o^2 a^2 (1 + \nu)/E \tag{17}$$

The energy due to the rock originally in the tunnel is:

$$W_v = \pi P_o^2 a^2 (1 + \nu) (1 - 2\nu)/E \tag{18}$$

so that the total energy change per unit length of tunnel is:

$$\Delta W_{Tot} = W_R + W_I + 2W_v$$

or

$$\Delta W_{Tot} = 4\pi P_o^2 a^2 (1 - \nu^2)/E \tag{19}$$

These equations (16-19) make two useful statements about the changes in energy which occur as a result of excavation. The first, is that fracture toughness σ_c^2/E (P_o^2/E) is important in creating conditions for energy release. The second, is that the stored and induced energy is related to the volume of the rock excavated. The maximum stored or released (induced) strain energy which is possible without inducing fracture in the tunnel annulus may be calculated and

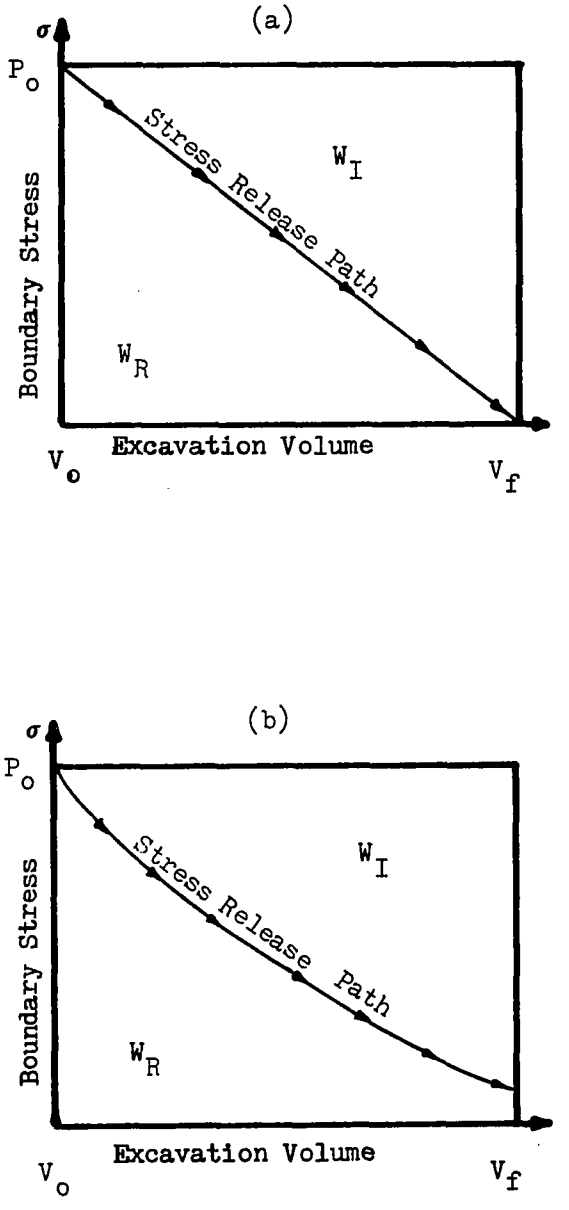

Figure 8. Released Energy and Induced Energy for: (a) Perfectly Elastic Rocks (No Fracture), (b) with Rock Fracture.

plotted using equations (16, 17). This is done in Figure 9 for several rock qualities and tunnel radii. Not unexpectedly, the highest quality rocks ($\sigma_c^2/E = 1$) showed the highest capability to accept energy changes (W_S and W_I) at all radii, but also ($\sigma_c^2/E = 1$) increased in this capability more rapidly. It is evident that the strain energy which might be tolerated by some tunnel annuli is significantly larger than others.

Strain Energy Distribution in the Tunnel Annulus

The development of a circular tunnel in an initially elastic rock mass will result in the release of energy and will induce strain energy in the tunnel annulus. Prior to excavation, the energy density in the rock will be the same everywhere (for a given horizontal plane).

Given a tunnel of initial radius a in an initially elastic rock mass and assuming that the energy changes created by the tunnel are instantaneously transmitted to the rock around the opening, the strain energy can be calculated using the previously described method outlined in Jaeger and Cook (1979).

The initial strain energy (prior to excavation) can be calculated by:

$$W_i = \pi (1 + \nu) (1 - 2\nu) P_o^2 (R_2^2 - a^2)/E \qquad (20)$$

The terms are defined as in Figure 10. Figure 11 and 12 illustrate the initial energy conditions in the tunnel annulus prior to driving the tunnel. The energy density is constant and is equal to $(1 + \nu) (1 - 2\nu) P_o^2/E$. The total energy in the annular sections

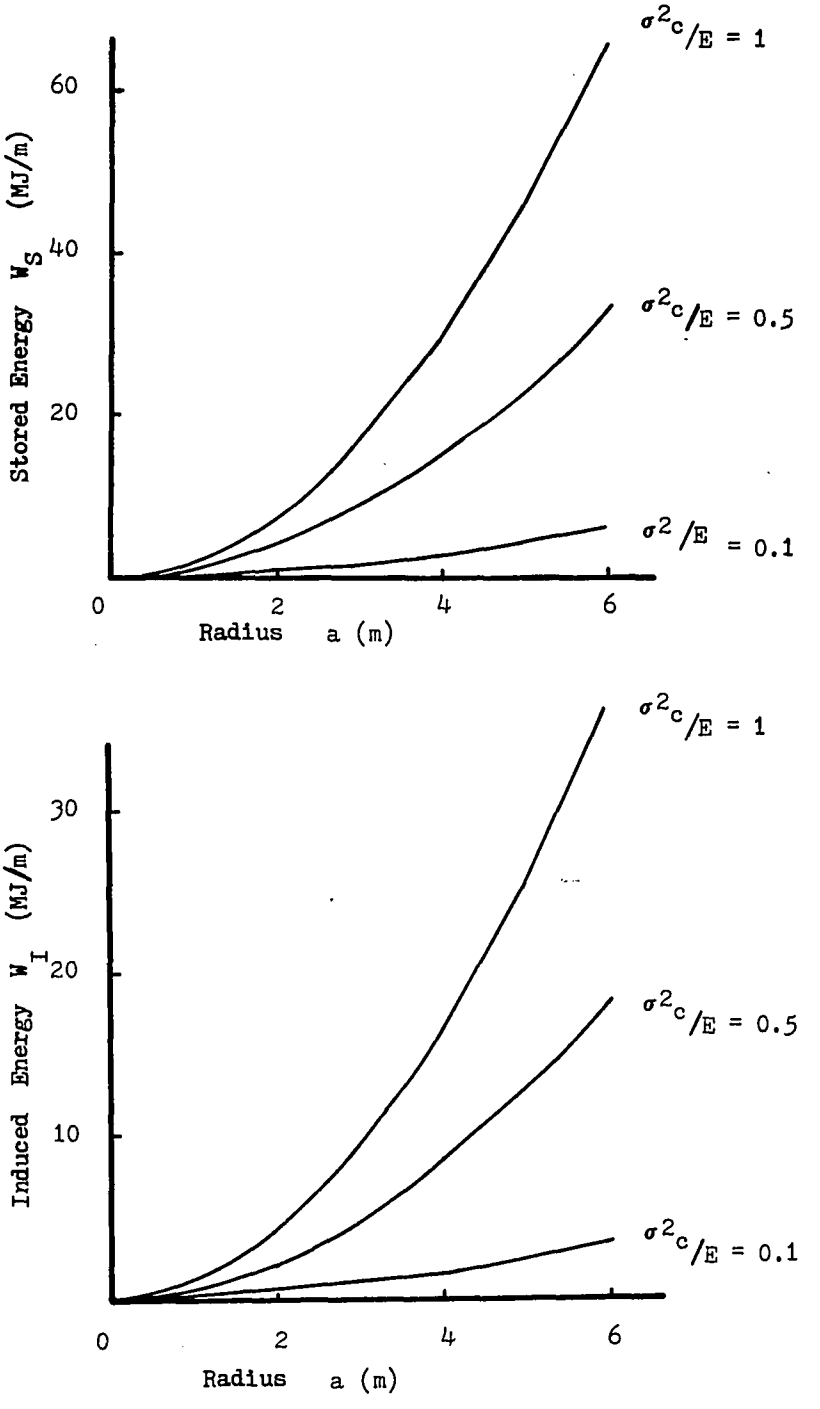

Figure 9. Maximum Stored and Induced Energy in an Annulus of Varying Radius.

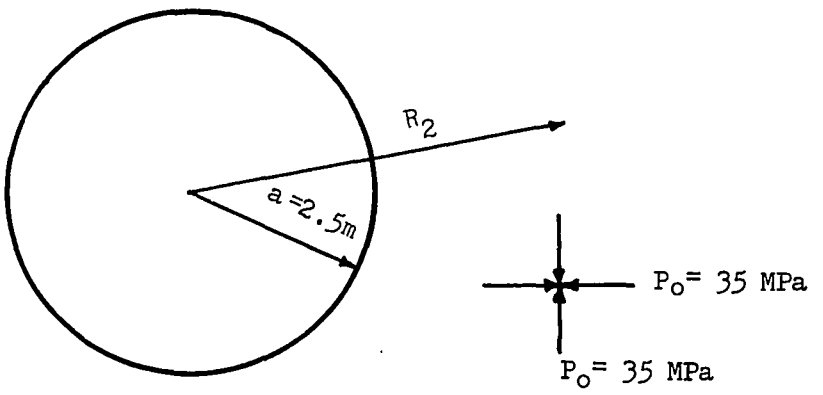

W = Total strain energy in annulus, defined by a and R_2
a = Tunnel radius
R_2 = Radial distance from tunnel centerline

Figure 10. Definition of Terms Used in Equation (20).

ν = 0.3
E = 20 GPa
P_o = 35 MPa
a = 2.5m
R_2 = Varies from 2.5m to 7.5m

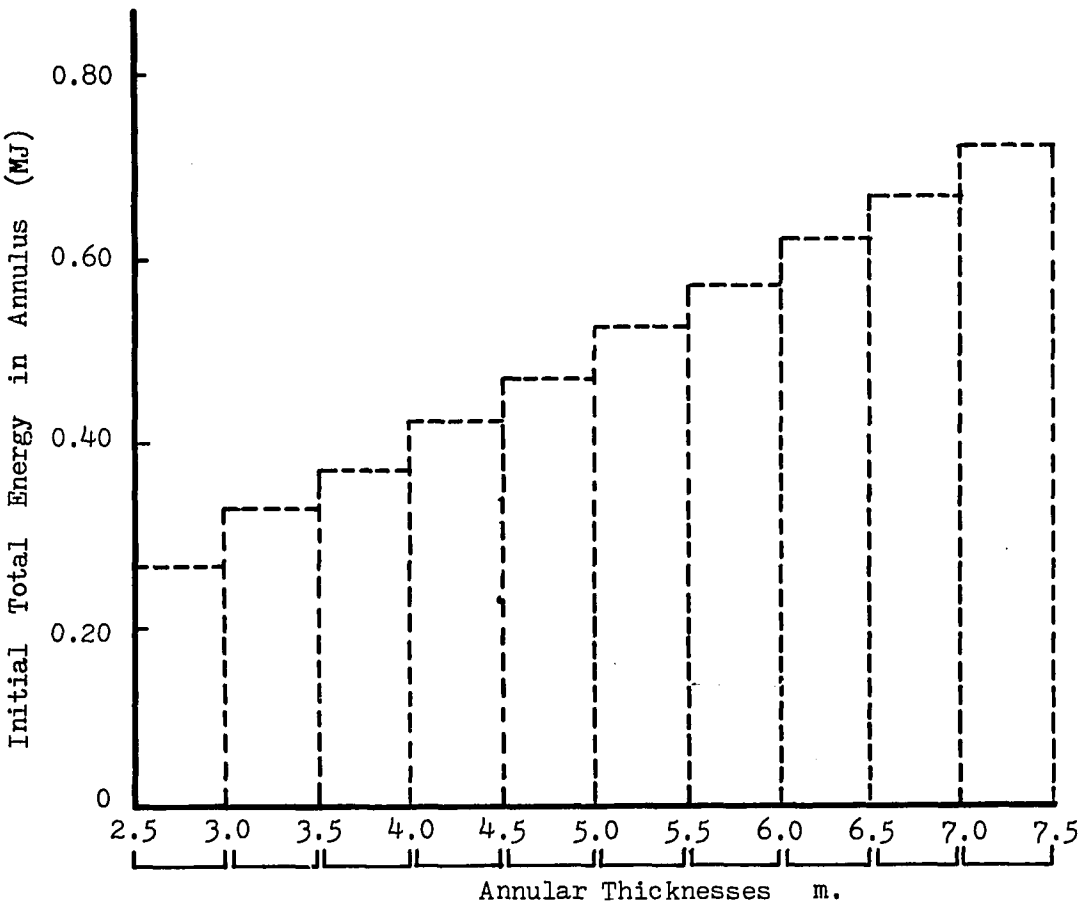

Figure 11. Total Initial Strain Energy in Annular Sections.

ν = 0.3
E = 20 GPa
P_o = 35 MPa
a = 2.5m
R_2 = Varies from 2.5m to 7.5m

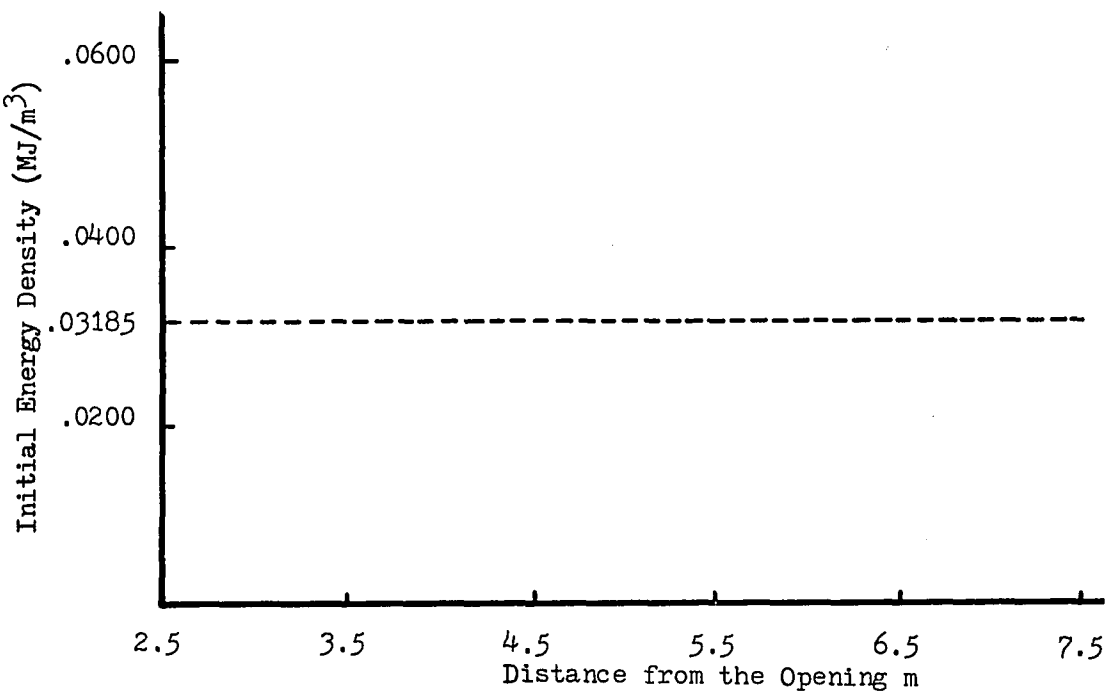

Figure 12. Initial Energy Density Throughout the Annulus.

increases with distance from the tunnel boundary due to the volume increase of each annular section.

Figure 13 illustrates the way in which the energy changes as a result of developing the tunnel. Strain energy was calculated for 1/2 meter annular thicknesses. Interestingly, the total strain energy initially decreases for the 1/2 meter sections and then begins to increase about 4.5 meters from the tunnel boundary. The strain energy density, however, decreases quickly from a maximum at the tunnel boundary and asymptotically approaches the initial (pre-excavation) energy density. At a radial distance 3 times the tunnel radius, the excess strain energy density has decreased to a value less that 4% greater than the in-situ value. The energies were calculated for the tunnel conditions previously described in Figure 10.

Strain Energy Required To Initiate Fracture in the Tunnel Boundary

Having established, in the previous section, some of the ways in which the strain energy is developed and distributed around a circular tunnel, and some of the ways in which changes occur in that distribution, it is now necessary to determine how the strain energy can fracture the intact rock around an excavation.

Assuming the rock into which the tunnel will be driven is initially elastic and unfractured, then the energy distribution will be as shown in the previous section. According to the Kirsch (1898) solution, the stresses on the boundary of a circular hole in an infinite plate subjected to a hydrostatic stress field will be:

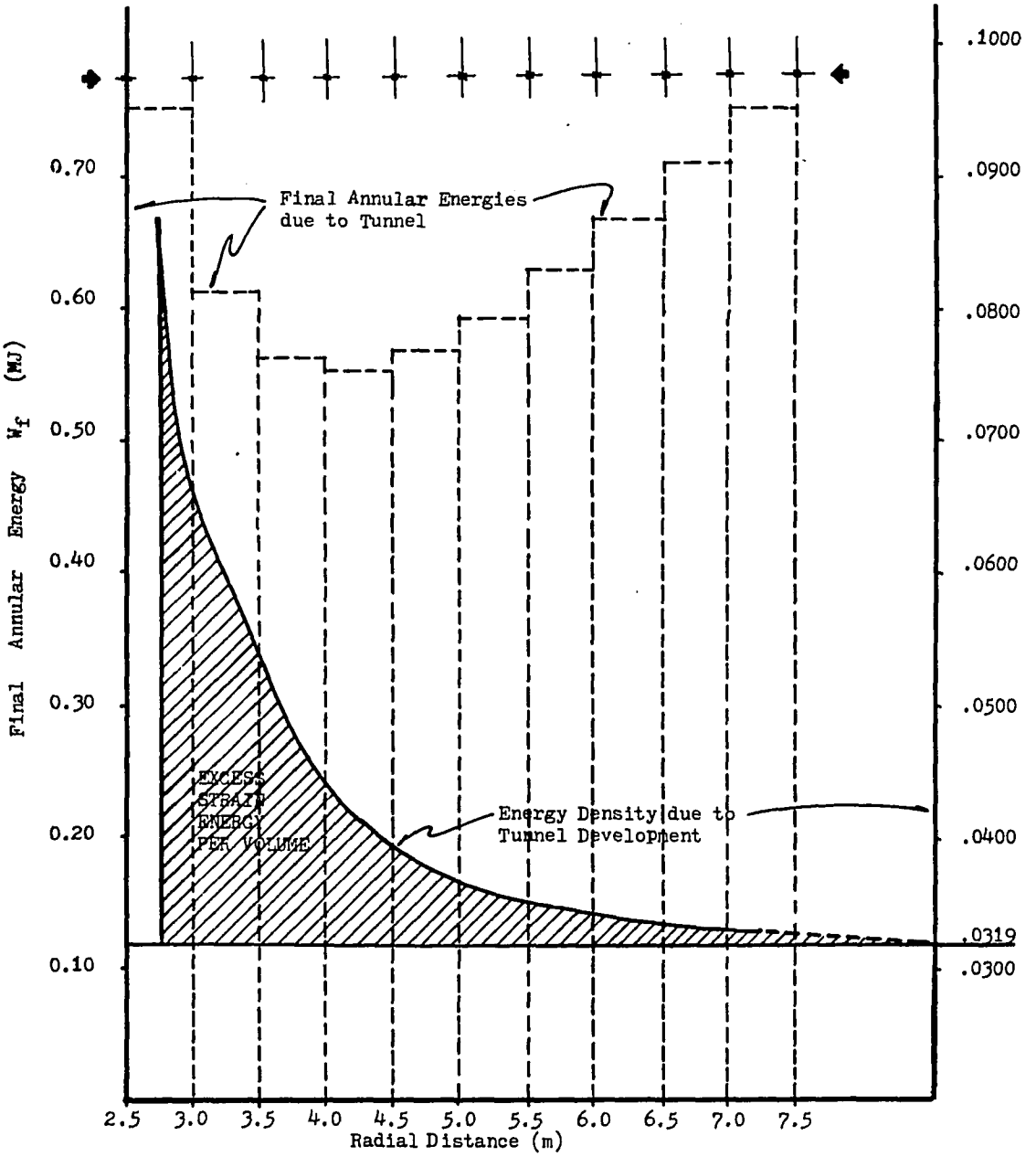

Figure 13. Distribution of Initial Strain Energy and Post-excavation Energy Density.

$$\sigma_1 = \sigma_\theta = 2P_o$$

$$\sigma_2 = P_o$$

$$\sigma_3 = \sigma_r = 0$$

Assuming no support, the loading condition, in a 2-dimensional sense, is similar to the uniaxial case. The radial stress acting on the exterior boundary of the infinitesimal layer will be very small with respect to the tangential stress which approaches the theoretical maximum value of $2P_o$. The radial stress can therefore be neglected. In this case, at failure, the major principle stress $\sigma_1 = 2P_o$ must equal the unconfined compressive strength σ_c so that the strain energy density at the initiation of rock fracture in the tunnel boundary layer will be:

$$W = 1/2E\ (\sigma_c^2) = 1/2\ (\sigma_c^2/E)$$

Therefore, the initiation of boundary layer failure is directly related to the quantity, fracture toughness σ_c^2/E, as previously defined.

The popular rock tunnel boundary failure models used this type of 2-dimensional loading to estimate the rocks behavior (see Ladanyi, 1974; Hoek and Brown, 1981). This suggests that the intermediate principle stress σ_2 has little or no influence on rock failure characteristics. The validity of such an argument is questionable. The true state of stress in the tunnel sidewall (assuming the Kirsch (1898) equations are valid) is the plane stress or biaxial stress

condition where $\sigma_1 \neq 0$, $\sigma_2 \neq 0$, $\sigma_3 = 0$. In this case, $\sigma_1 = \sigma_\theta = 2P_o$, $\sigma_2 = P_o$, and $\sigma_3 = 0$ (for no support). This is obviously not a 2-dimensional problem but rather a true 3-dimensional problem. The influence of the intermediate principle stress, σ_2, has been considered by many workers including Wiebols and Cook (1968) whose results indicate that the intermediate principle stress does influence the strength of the rock. Figure 14 from Wiebols and Cook (1968) shows the σ_B/σ_c ratio versus μ, the coefficient of friction. The term σ_B is the so-called biaxial strength ($\sigma_1 = \sigma_2$, $\sigma_3 = 0$) and σ_c is the unconfined compressive strength ($\sigma_1 \neq 0$, $\sigma_2 = \sigma_3 = 0$).

In the case of the circular tunnel with hydrostatic in-situ stress, the stress condition with $\sigma_1 = 2P_o$, $\sigma_2 = P_o$ and $\sigma_3 = 0$, the strength of the rock will be intermediate between σ_B and σ_c. The exact value of the tunnel boundary layer rock strength is, however, difficult to determine. The use of the unconfined compressive strength σ_c in the biaxial loading condition will produce conservative results since Figure 14 suggests the strength will be somewhat greater.

The strain energy at the initiation of rock fracture in the tunnel boundary layer is:

$$W = 1/(2E)\ (\sigma_1^2 + \sigma_2^2 - 2\nu\sigma_1\sigma_2)$$

at failure $\sigma_1 = \sigma_c$ (the conservative estimate) $= 2P_o$ $\therefore$ $\sigma_c = 2P_o$ and $\sigma_2 = 1/2\sigma_c$.

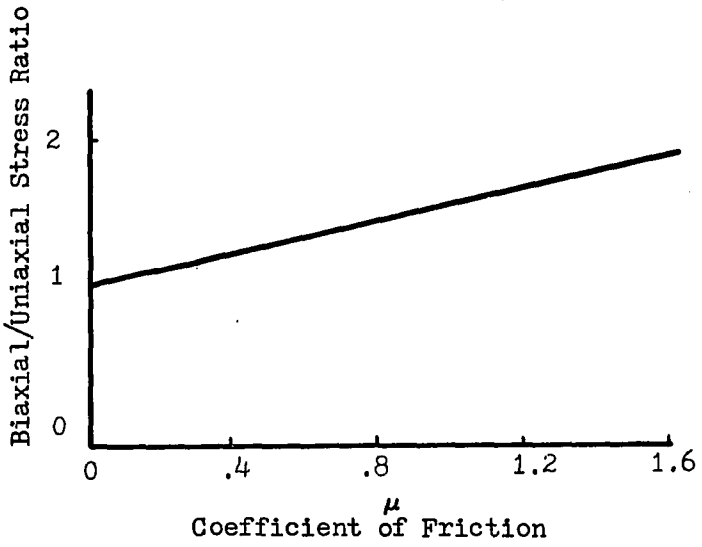

Figure 14. The Ratio Between the Biaxial Plane Strength and Uniaxial Compressive Strength as a Function of μ. (from Wiebols and Cook, 1968)

Therefore,

$$W = 1/(2E)\ (\sigma_c^2 + (\sigma_c/2)^2 - 2\nu\ (\sigma_c)\ (\sigma_c/2))$$

or

$$W = \sigma_c^2/E\ ((5 - 4\nu)/8) \qquad (21)$$

which is the strain energy density in the tunnel boundary layer at the initiation of rock fracture there. This is a conservative estimate of the energy density since the strength is probably greater than σ_c. The energy (at failure in the immediate boundary layer) can be plotted for various fracture toughnesses (σ_c^2/E) related to generic rock types, such as those from Figure 6. Figure 15 is such a plot of fracture toughness versus strain energy density. Included in the figure is a range of Poisson's ratios which might be expected for rock. Three fracture toughnesses were used: $\sigma_c^2/E = 1$ representing the range of strain energy required to initiate fracture in the tunnel periphery of rocks of the highest quality (all groups), $\sigma_c^2/E = 0.1$ representing the range of energy required to initiate fracture in the tunnel periphery of basalts, weaker igneous rocks, mudstones, etc., and $\sigma_c^2/E = 0.01$, which represents the energy required to initiate fracture in the tunnel boundary layer of chalks, weak limestones, and weak fine-grained clastic rocks.

The boundary layer strain energy is a function of the in-situ stress and the rock characteristics. These two parameters are plotted in Figure 16. The highest quality rocks ($\sigma_c^2/E = 1$) as expected show the highest energy density for the adjusted hydrostatic field stress

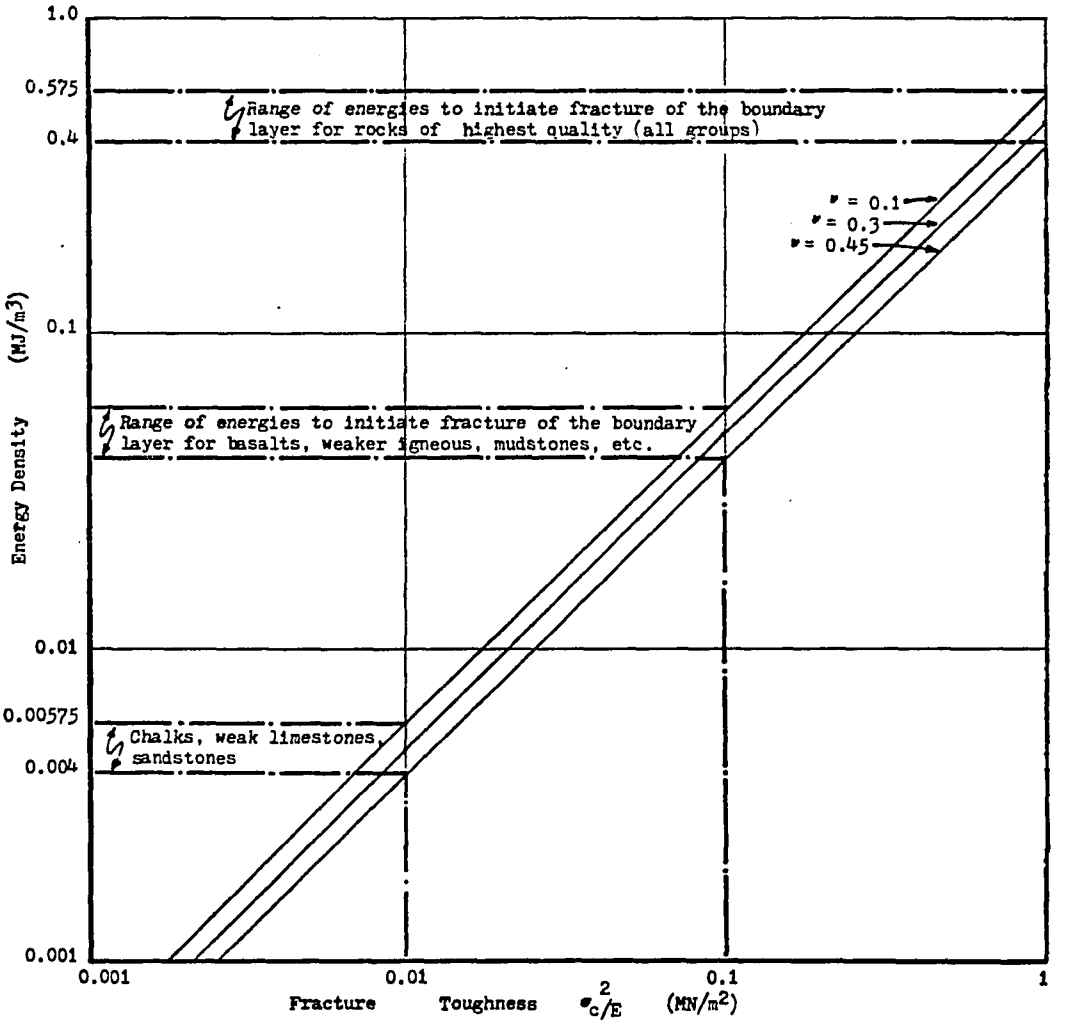

Figure 15. Strain Energy Density Required to Initiate Fracture in the Tunnel Boundary Layer.

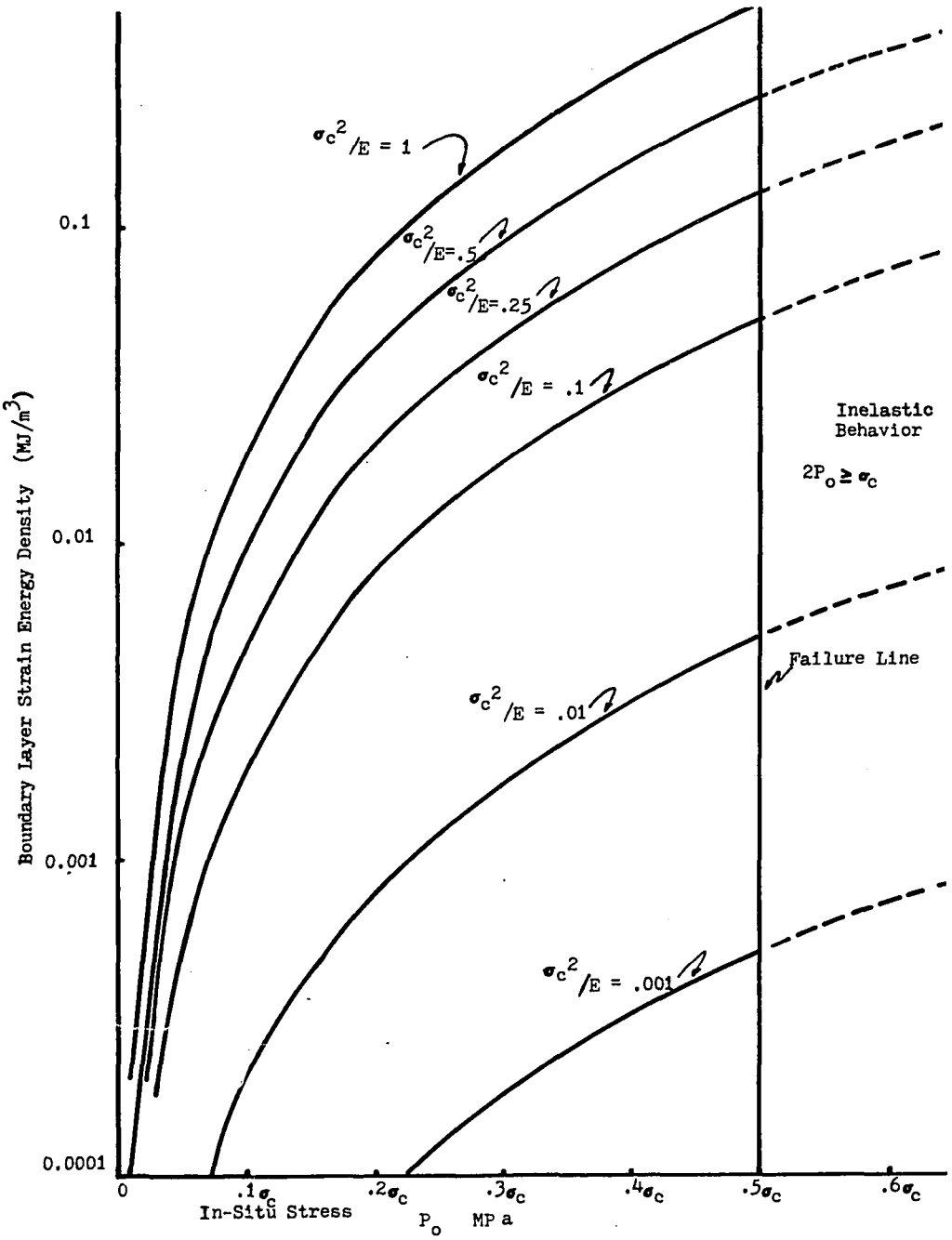

Figure 16. Variation of Boundary Layer Strain Energy with In-situ Stress and Rock Characteristics.

P_o/σ_c. Again, the conservative estimate of tunnel boundary layer failure of σ_c was used and the in-situ hydrostatic field stress required to cause this failure is equal to $0.5P_o$. The energy density storage capability increases dramatically from a low stress condition ($P_o = 0\sigma_c$) to the failure condition ($P_o = \sigma_c/2$) shown as a line between elastic and inelastic behavior.

Rock Fracture Beyond the Tunnel Boundary Layer

The strain energy in excess of the threshold energy for a given rock will result in rock fracture and dilation. Even after fracture and dilation, a rock mass will not completely lose its ability to store energy (unless the broken material falls, under the influence of gravity, into the opening, or moves into the opening in a violent rockburst condition). In this way, broken rock provides some support to the rock beyond the opening, increasing its strength from a pseudo-unconfined state to that of a polyaxial specimen. This rock fracturing and broken rock energy storage will be a reciprocal relationship (the strain energy in the unbroken rock will attempt to fracture the rock and the fractured rock's energy strength will attempt to limit the development of these fractures).

As was mentioned previously, the development of a tunnel or excavation in rock will result in changes in the energy distribution in the vicinity of the opening. If the energy changes are such that the fracture resistance of the rock in the tunnel annulus is exceeded, then fracture and dilation will occur causing additional changes in

the energy distribution. Assuming that the stiffness of the intact rock is great relative to the stiffness of the broken rock, then rockburst type activity will probably not occur and the energy changes can be considered stable. In this case, the broken rock will retain some energy storage capability and will provide some support for the unbroken rock beyond, both of which will depend upon the energy release characteristics of the rock. The stored strain energy will be dissipated until a pseudo-equilibrium condition is reached. The energy changes in the annulus can roughly be described as in Figures 17-20. The initial strain energy density prior to excavation will be constant throughout the annulus (Figure 17). Fracturing will begin initially in the tunnel boundary layer when the strain energy density reaches the threshold energy at the boundary. The threshold energy is the minimum amount of energy which will cause fracturing of the rock for any confinement situation. Energy will be released until the residual energy density for that rock at the confinement is reached. If energy is available to cause more interior points to reach their threshold energy density, then that annulus will fracture according to its fracture resistance, confinement, and residual energy characteristics. Figure 18 shows the energy distribution immediately following excavation (before fracture can occur). In this case, the redistributed strain energy exceeds the threshold energy throughout a thickness of the tunnel annulus. Realistically, this would not occur since attainment of the threshold energy density is theoretically the maximum energy density which the rock can sustain. However, this

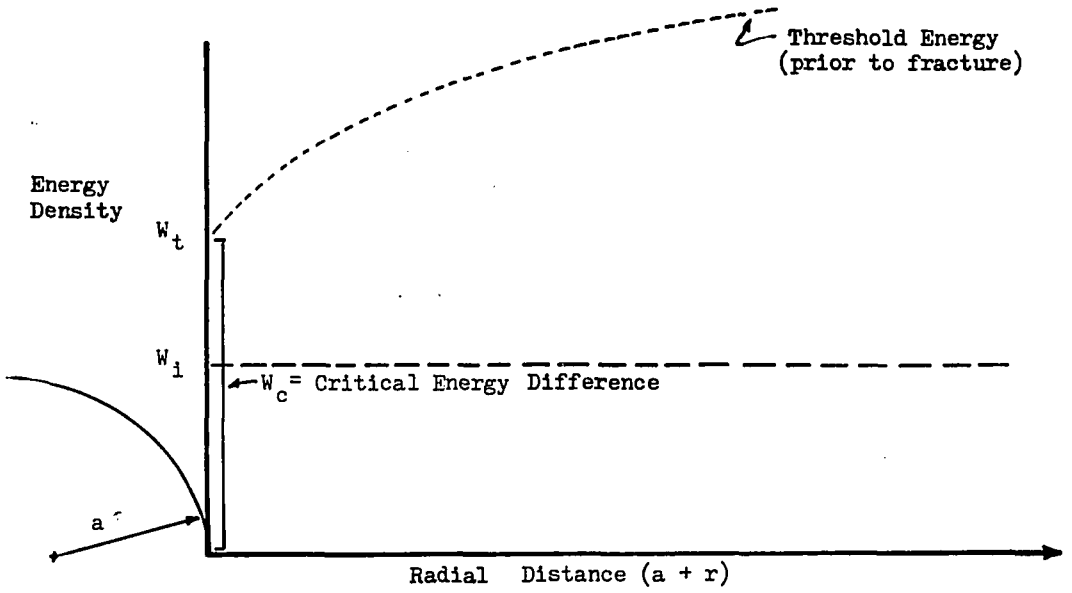

Figure 17. Initial Pre-excavation Energy Density.

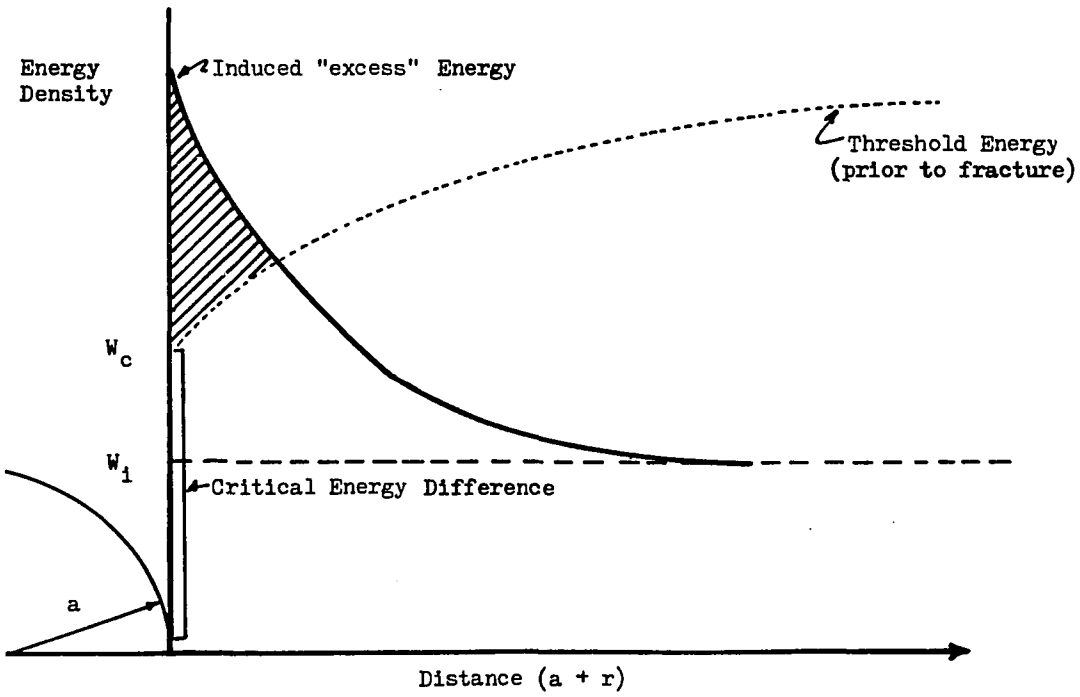

Figure 18. Energy Conditions Just Prior to Fracture.

concept allows for illustration of the energy changes. The figures show the threshold energy density, the input energy density due to the original initial energy density, the residual energy stored in the rock, and the so-called confining energy which represents the energy in the fractured rock. Confining energy is the lowest potential energy in a volume adjacent to the volume of rock under consideration. The confining energy at the tunnel-rock boundary is thus the potential associated with atmospheric pressure to do work on the boundary layer rock. This potential is, for all practical purposes, equal to zero. The residual energy stored in the rock just fractured will be the "confining" energy for the intact rock radially outward. It is assumed that the tunnel-rock system will tend toward an equilibrium state eventually, in which the energy density is everywhere the same for a given horizontal plane passing through the annulus. This suggest that the excess strain energy stored in the tunnel annulus will be abstracted toward the opening, so that the "confinement" provided by the rock on the tunnel side of the rock being considered will be the recipient of this energy change (neglecting energy escaping the local system through seismic activity and heat radiation). In other words, the energy will move from an area of high potential toward the area of lowest potential. Lowest potential will always be toward the tunnel opening. This is the justification for the use of confining energy as described above. The excess energy density represents the energy in excess of the minimum amount required to fracture the rock and is shown shaded in the

figure. As the rock begins to fracture due to the "excess" energy, some of the original excess energy will be expended (shown cross-hatched) in fracturing the rock and subsequent dilation. Figure 19 is illustrative of an intermediate condition prior to achievement of energy equilibrium. The total energy density which has gone into rock fracture is outlined as before. The original excess energy has dissipated slightly since some has been abstracted to increase the original input energy density level to the threshold energy level which itself has increased due to increased confinement. There is still enough potential excess strain energy (greater than threshold) to continue the process of rock fracture. The final figure (Figure 20) illustrates the pseudo-equilibrium condition where the original excess strain energy has been abstracted radially outward to fracture the intact rock there. The crosshatched area shows the final total amount of energy which has gone into rock fracture and dilation. The bottom portion of the confining energy curve on Figure 20 occurs as a result of relaxation of the broken rock. More precisely, the rock at all radial points, fractures when the threshold energy is reached at the confining energy of the intact rock. Therefore, the energy going into rock fracture and "immediate" dilation is the difference between the threshold energy and the residual energy instantaneously at the confining energy of failure. The portion of the confining energy curve is caused by the fracture and immediate dilation of the rock beyond which essentially pushes the near-tunnel broken rock toward the opening. This added strain-softening type motion continues to break

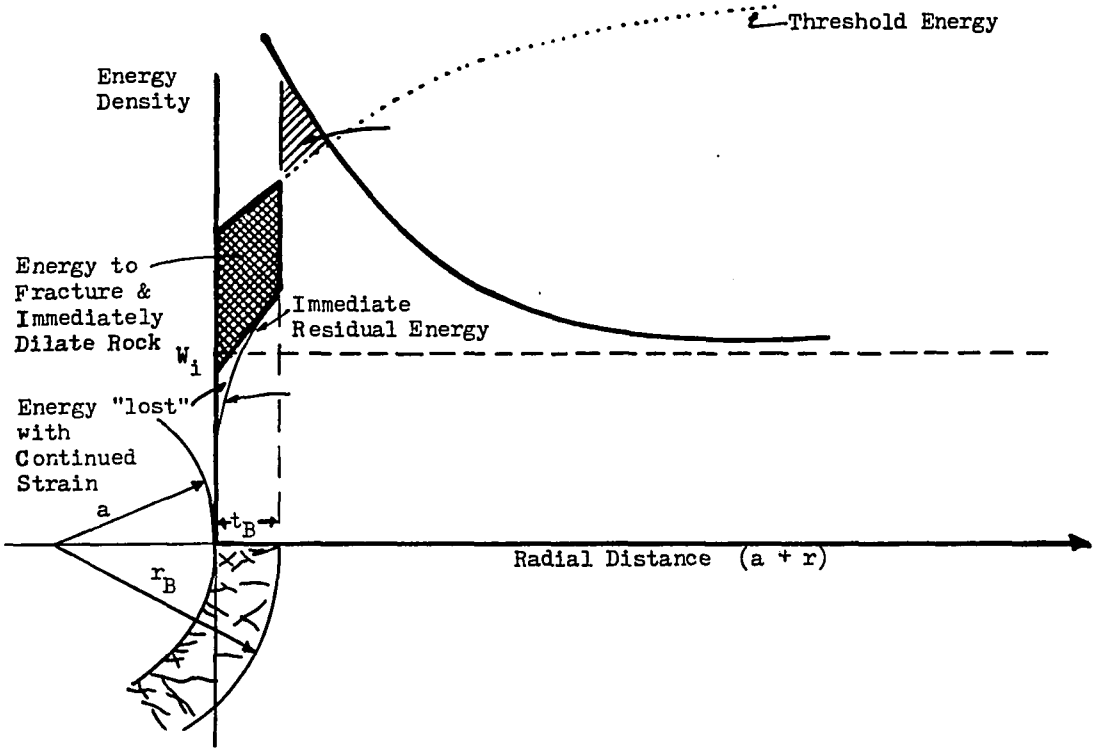

Figure 19. Intermediate Condition Prior to Equilibrium.

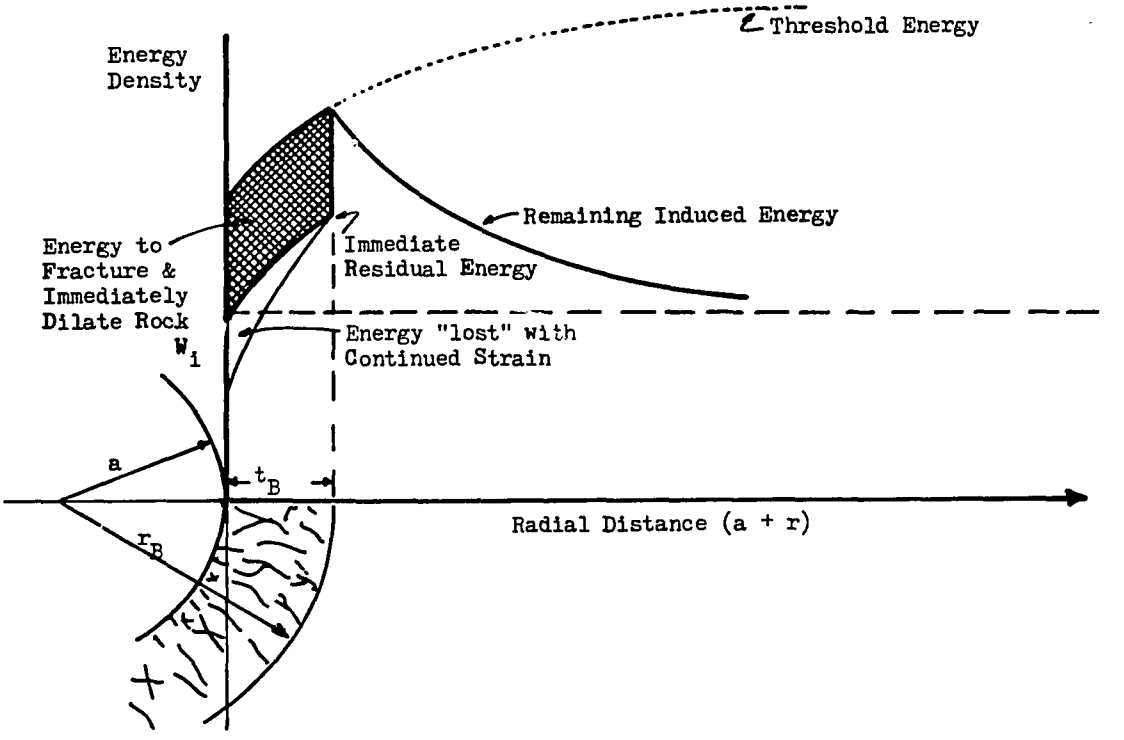

Figure 20. Final Equilibrium Condition.

down the strength of the broken rock (destroying any "cohesion" if it existed). This essentially corresponds to the "strain-softening" behavior associated with actual rock fracture and deformation as described in Brady and Brown (1985) and elsewhere. The amount of energy released in this strain-softening behavior will be manifested in continued tunnel boundary displacements, frictional heat loss due to relative block movement along fracture contacts, and acoustic emissions. Therefore, the total inelastic closure occurs as a result of:

a. initiation of fractures in the annular section being considered.

b. initiation of fractures in the rock beyond that being considered. This "pushes" the broken rock in the tunnel boundary inward causing more dilation. (strain-softening)

Threshold Energy Characteristics of Some Generic Rock Types

The threshold strain energy density as defined previously, is the total strain energy density at the initiation of macro fracture of rock at any confinement. Hoek and Brown (1981) describe triaxial ($\sigma_1 \neq 0$, $\sigma_2 = \sigma_3$) data for a large number of generic rock types. The data is normalized by dividing the major principal stress (σ_1) and minor principal stress (σ_3) by the unconfined compressive strength σ_c. Some of these generic triaxial failure curves (σ_1/σ_c vs σ_3/σ_c) are reproduced in Appendix A. This data redefined into strain energy terms, along with the fracture toughness data from Figure 6 can be

used to develop a rough threshold energy criterion for some generic rock types.

The threshold energy density for any stress situation can be calculated using equation (8).

$$W = 1/2E\ (\sigma_1^2 + \sigma_2^2 + \sigma_3^3 - 2\nu\ (\sigma_1\sigma_2 + \sigma_2\sigma_3 + \sigma_1\sigma_3)) \qquad (8)$$

For the case of triaxial testing by Hoek and Brown (1981) $\sigma_2 = \sigma_3$ so that (8) becomes:

$$W = 1/2E\ (\sigma_1^2 + 2\sigma_3^2 - 2\nu\ (2\sigma_1\sigma_3 + \sigma_3^2)) \qquad (22)$$

In terms of σ_c with

$$a = \sigma_1/\sigma_c$$

and

$$c = \sigma_3/\sigma_c$$

$$\sigma_1 = a\sigma_c \text{ and } \sigma_3 = c\sigma_c$$

Therefore:

$$W = 1/2E\ (a^2\sigma_c^2 + 2c^2\sigma_c^2 - 2\nu\ (2ac\sigma_c^2 + c\sigma_c^2))$$

or:

$$W = \sigma_c^2/2E(a^2 + 2c^2 - 2\nu\ (2ac + c^2)) \qquad (23)$$

where: a = a constant describing the relationship between the major principal stress σ_1, and the unconfined compressive strength σ_c.

c = a constant describing the relationship between the minor principal stress σ_3 and the unconfined compressive strength σ_c.

The final equation (equation 23) is the most general and from it the energy thresholds for various confining pressures (energies), in terms of a and c, can be determined. The threshold energies for granite, limestone, sandstone, and mudstone have been computed for various confining energies. Confining energy is the strain energy associated with the intermediate and minor principal stresses σ_2 and σ_3 and is given by:

$$W = 1/2E(\sigma_2^2 + \sigma_3^2 - 2\nu\ (\sigma_2\sigma_3))$$

or, since $\sigma_2 = \sigma_3$ in triaxial testing,

$$W = \sigma_3^2/E(1 - \nu) = c\sigma_c^2/E(1 - \nu) \qquad (24)$$

In triaxial testing, the fluid (hydraulic oil), being itself not able to store strain energy, provides a pressure (stress) on the rock sample which can be thought of as restricting the outward displacement of the rock. In other words, the fluid displaces the rock sample inward from the position it would have assumed without annular support. Therefore, the fluid can be thought of as containing potential strain energy equivalent to the contribution of $\sigma_2 = \sigma_3$ into the rock. The fluid does not "feel" the influence of σ_1 which the rock feels, since the pressure in the fluid is hydrostatic.

In an actual rock mass, strain energy will be stored as a result of all three principal stresses and should provide a lower energy gradient between the broken rock and the adjacent intact rock. This would result in rock being apparently stronger in the tunnel annulus than would be expected from triaxial testing.

The information from Deere and Miller (1966) and Hobbs (1974) suggest that there are bounds for the behavioral characteristics σ_c^2/E, σ_c, and E for the generic groups granite, limestone, sandstone, and mudstone. These bounds are listed in Table 1.

Using the information from Table 1 and the triaxial data from Hoek and Brown (1981), Appendix A, Figures 21-24 have been developed. These figures represent the range of threshold energies (total strain energy density at failure) for a range of confinements for granite, limestone, sandstone, and mudstone.

The question arises again as to the influence of the intermediate principal stress, σ_2, on rock fracture. Figures 21-24 were developed for the conservative case of $\sigma_2 = \sigma_3$. As such, they represent the minimum strain energy density that a rock in a tunnel annulus can withstand since, as is shown in Figure 14, the strength will most probably increase with an increase in σ_2 from $\sigma_2 = \sigma_3$ to $\sigma_2 > \sigma_3$. Figures 21-24 do show that there is a wide range of rock response to strain energy inputs. Figure 25 shows this variation for granite and limestone. This highest quality limestone, with σ_c^2/E, σ_c, and E, very similar to the highest quality granite responds much differently to confining pressure than does the granite. The

Table 1. Range of σ_c^2/E, σ_c, and E for Four Generic Rock Types

Rock Type	Fracture Toughness σ_c^2/E MPa(MJ/m^3)		Compressive Strength σ_c MPa		Young's Modulus E GPa	
	high	low	high	low	high	low
Granite	1.0	0.25	275	105	76.0	11.0
Limestone	1.0	0.10	245	50	44.0	25.0
Sandstone	2.0	0.05	255	17	32.5	6.0
Mudstone	0.5	0.025	10	2.5	0.25	0.25

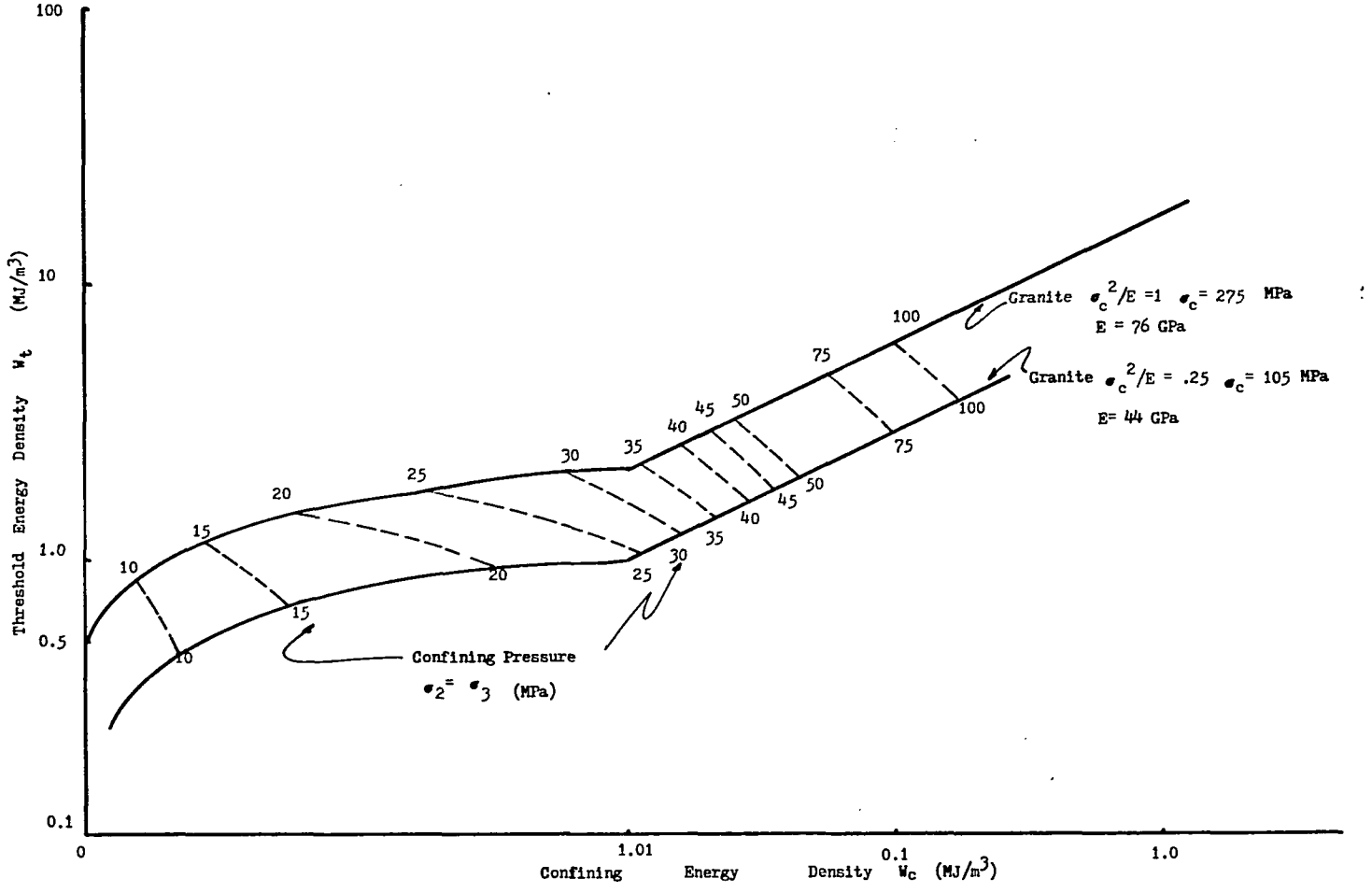

Figure 21. Range of Threshold Energy with Variation in Confinement: Granite.

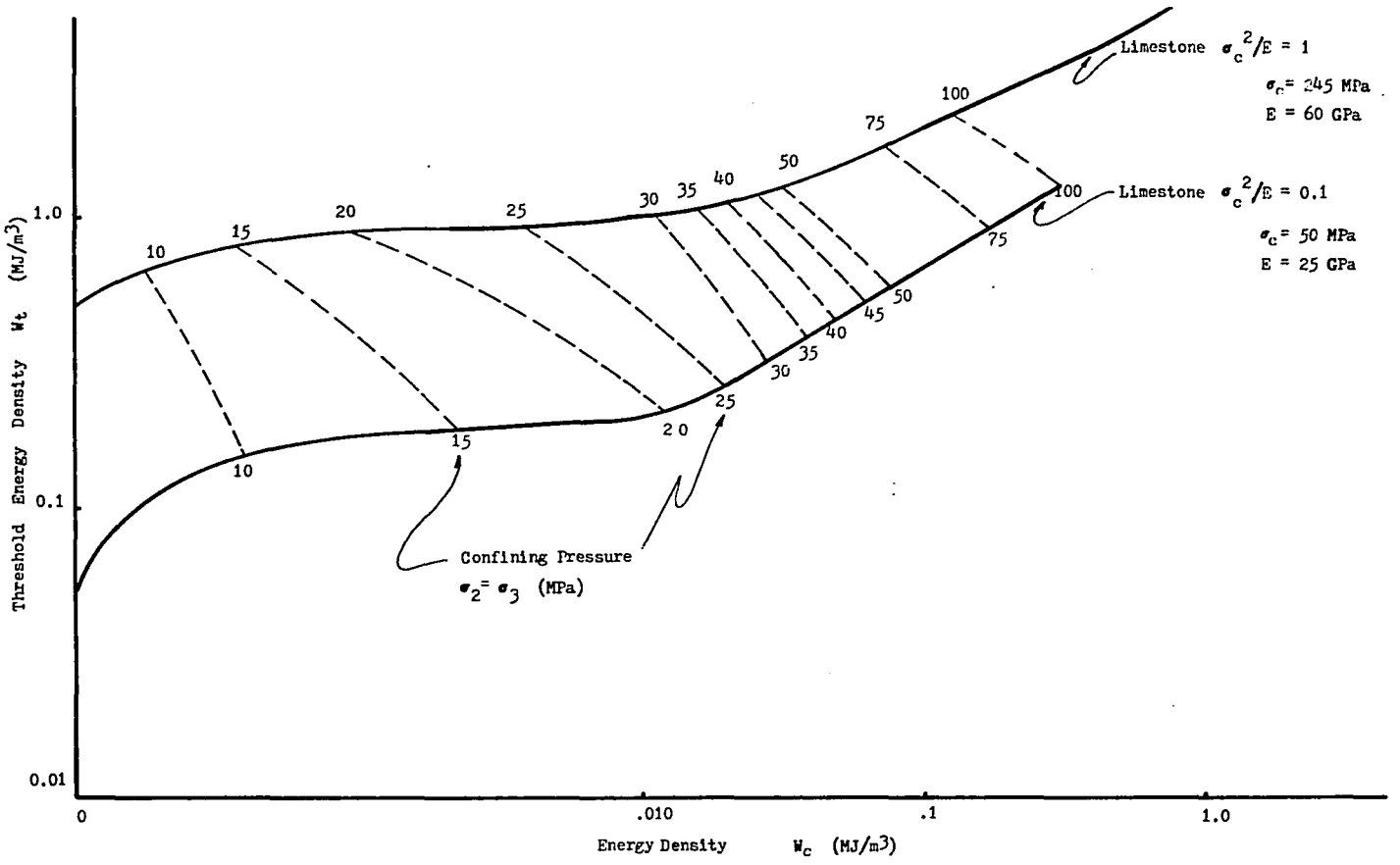

Figure 22. Range of Threshold Energy with Variation in Confinement: Limestone.

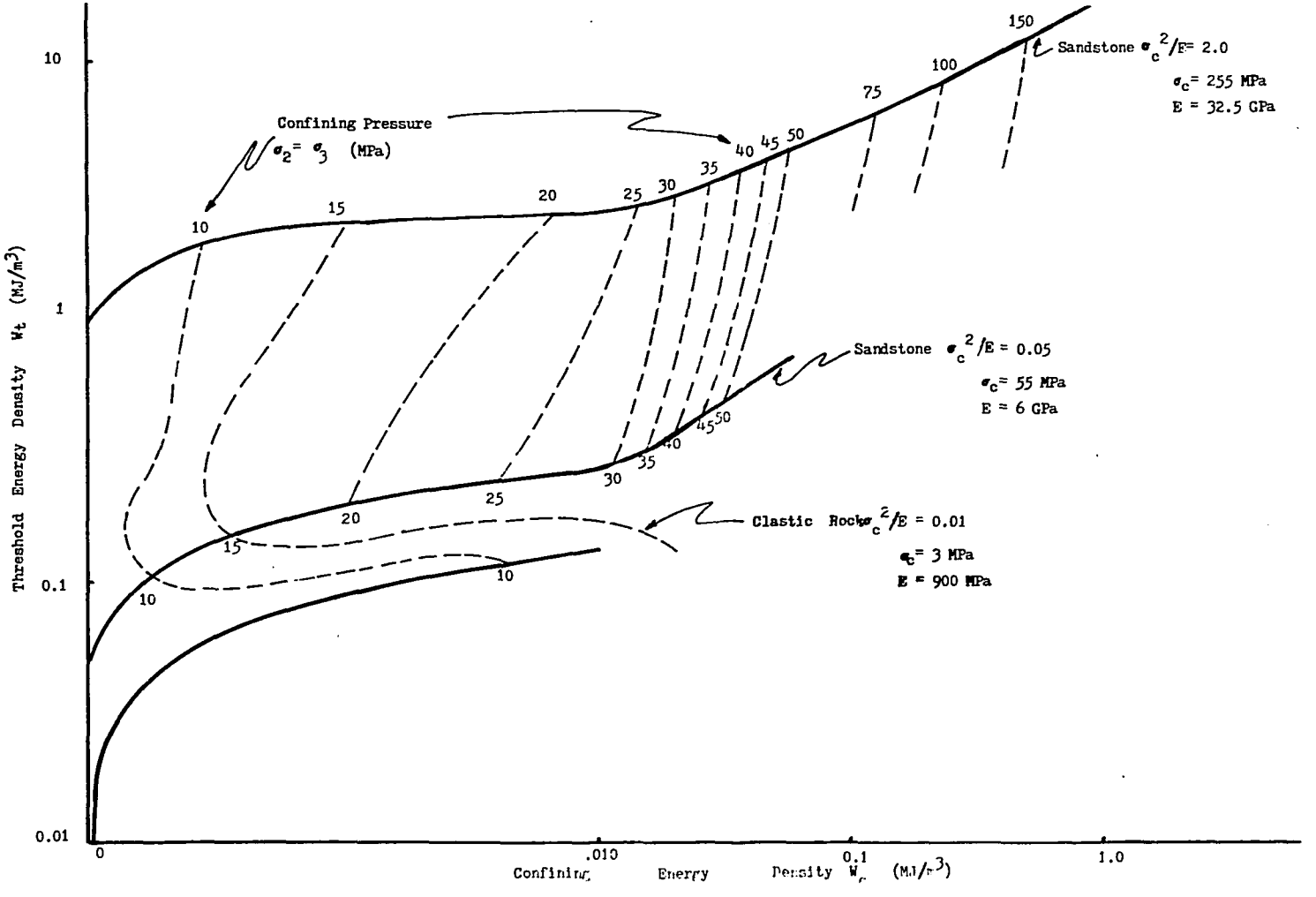

Figure 23. Range of Threshold Energy with Variation in Confinement: Sandstone.

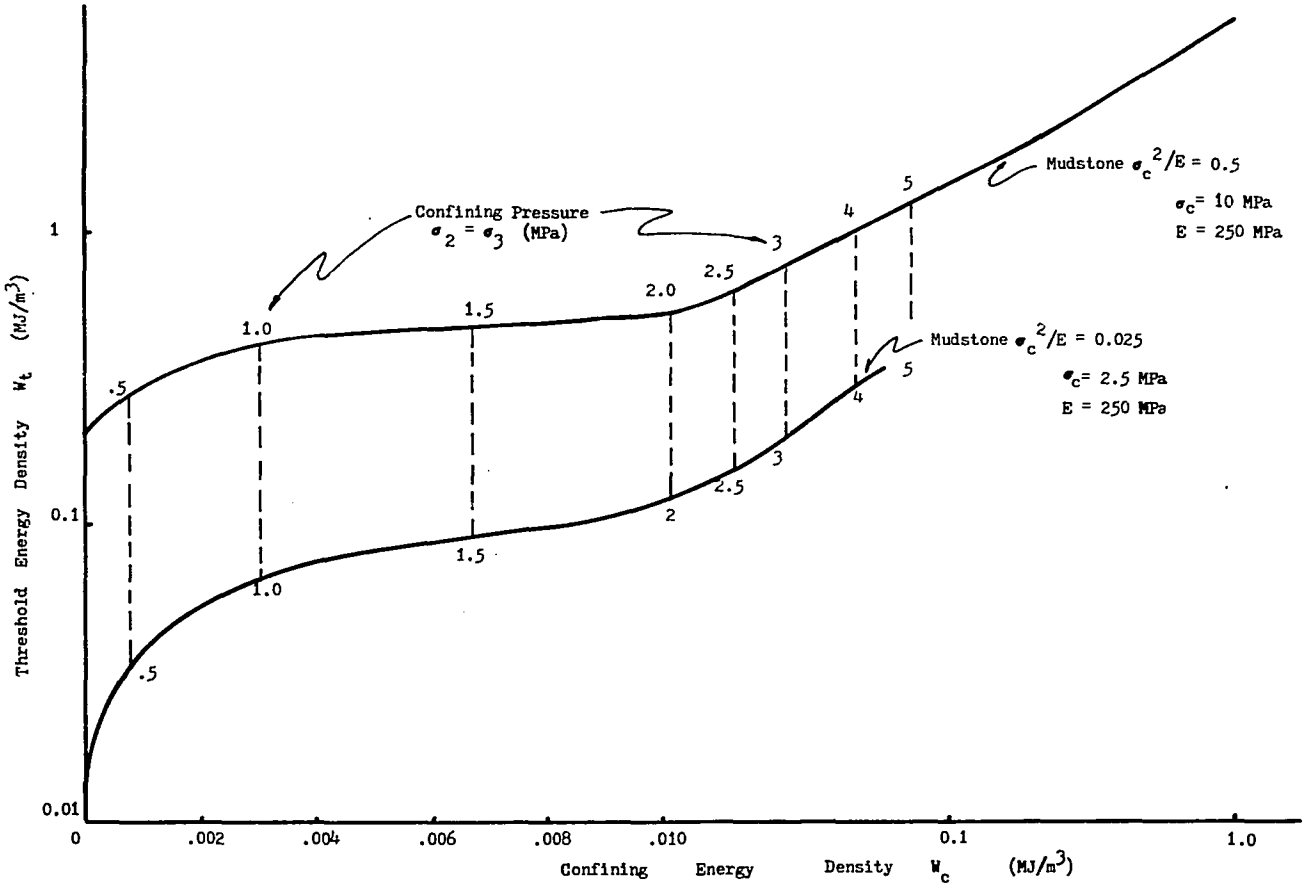

Figure 24. Range of Threshold Energy with Variation in Confinement: Mudstone.

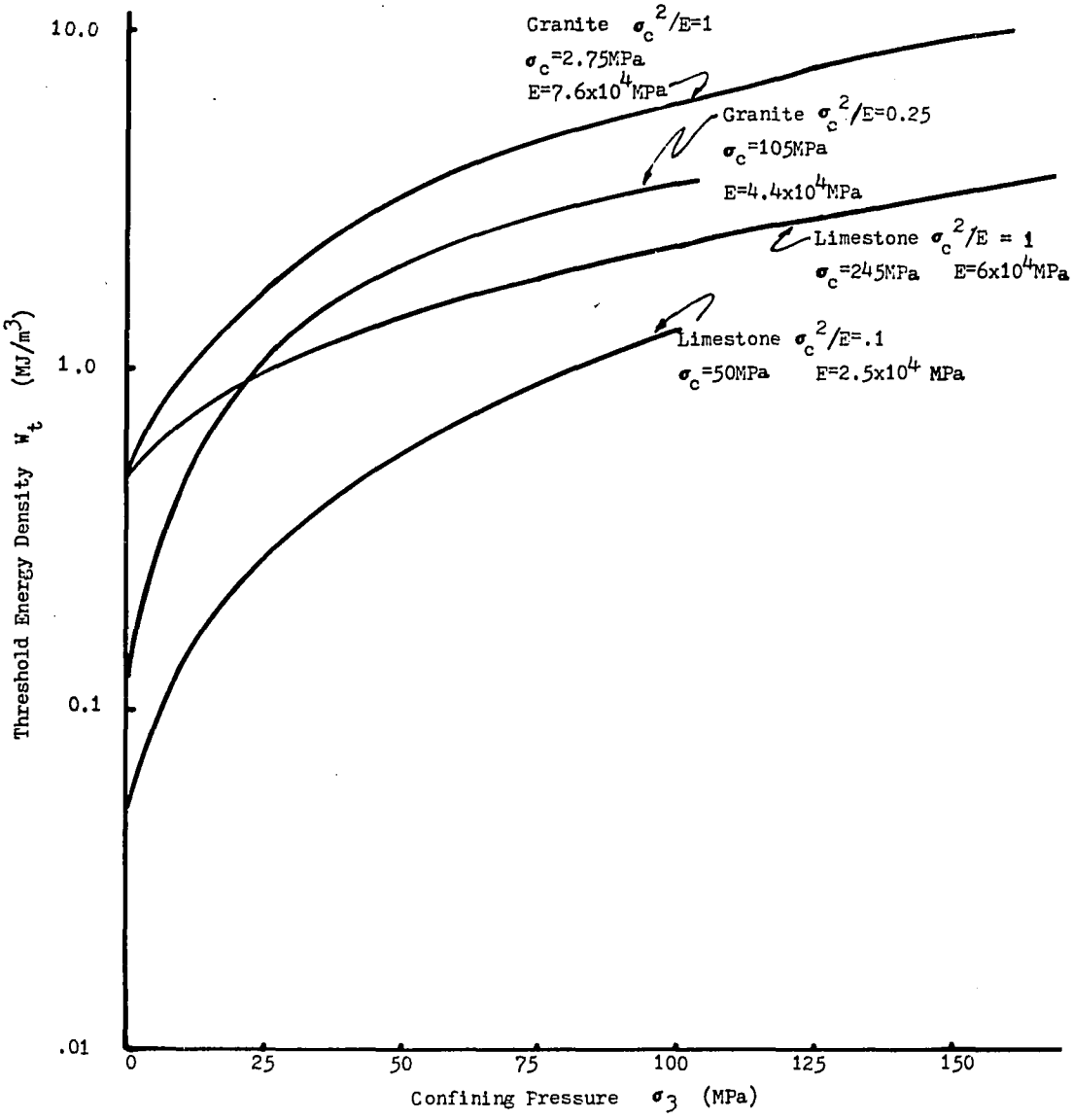

Figure 25. Variation Between Threshold Energy and Confining Pressure: Limestone and Granite.

limestone does not increase in strength as significantly. The lower bound limestone and granite both begin with much lower boundary layer (unconfined) strain energy densities than their upper bound counterparts, but gain fracture resistance much more quickly. The lower quality granite, although originally with much lower fracture resistance than the high quality limestone, will, with a small increase in confinement, become more fracture resistant. This all suggests that tunnels developed in "lower bound" rocks will exhibit boundary layer fracture at a much shallower depth than "upper bound" rocks, but will approach "upper bound" fracture resistance with an increase in confinement. In other words, the zone of fracturing around tunnels in "low quality" (low σ_c^2/E) rocks will develop a smaller fractured annulus than might be expected.

Elastic Closure in Strain Energy Terms

The theory of elasticity predicts that the development of an opening in an elastic rockmass will induce energy changes around that opening. The manifestation of these energy changes (for energy changes below the fracture resistance of the rock), will be in movement of the annulus toward the center of the excavation. This movement, or straining of the rock, induces strain energy in the annulus and is the origin of the stress changes there.

In simplest terms, the radial closure (deformation) occurring as a result of the development of a circular tunnel in a hydrostatic stressfield is, assuming plane strain, from Muskhelishvili (1953):

$$u_r = 2P_o a(1 - \nu^2)/E \qquad (25)$$

where a = the radius of the tunnel

P_o = the hydrostatic field stress

The variation of maximum elastic closure (at the instant the boundary layer begins to fracture) can be calculated as a function of fracture toughness (σ_c^2/E), since at failure:

$$\sigma_\theta = \sigma_c = 2P_o \quad \text{or} \quad P_o = \sigma_c/2 \quad \text{(the conservative case)}$$

Therefore (25) becomes:

$$u_r = [\sigma_c/E]a\ (1 - \nu^2) \qquad (26)$$

or

$$u_r^2 = [\sigma_c^2/E^2]a^2(1 - \nu^2)2 = \sigma_c^2/E\ a^2(1 - \nu^2)^2/E$$

so that

$$u_r = (1 - \nu^2)\ a/\sqrt{E}\ (\sqrt{\sigma_c^2/E}) \qquad (27)$$

The variation of maximum elastic closure can then be plotted against unconfined compressive strength and related to various rock classification schemes (e.g. Farmer, 1983). As can be seen from Figures 26-28, the elastic closure increases with an increase in fracture toughness. This might not seem correct (since increases in σ_c^2/E represent an improvement in rock quality), but increasing σ_c^2/E and maintaining E constant simply means that the in-situ stress at failure has increased. These figures were developed for the specific tunnel cross-section of 2.5 meter radius (corresponding closely with

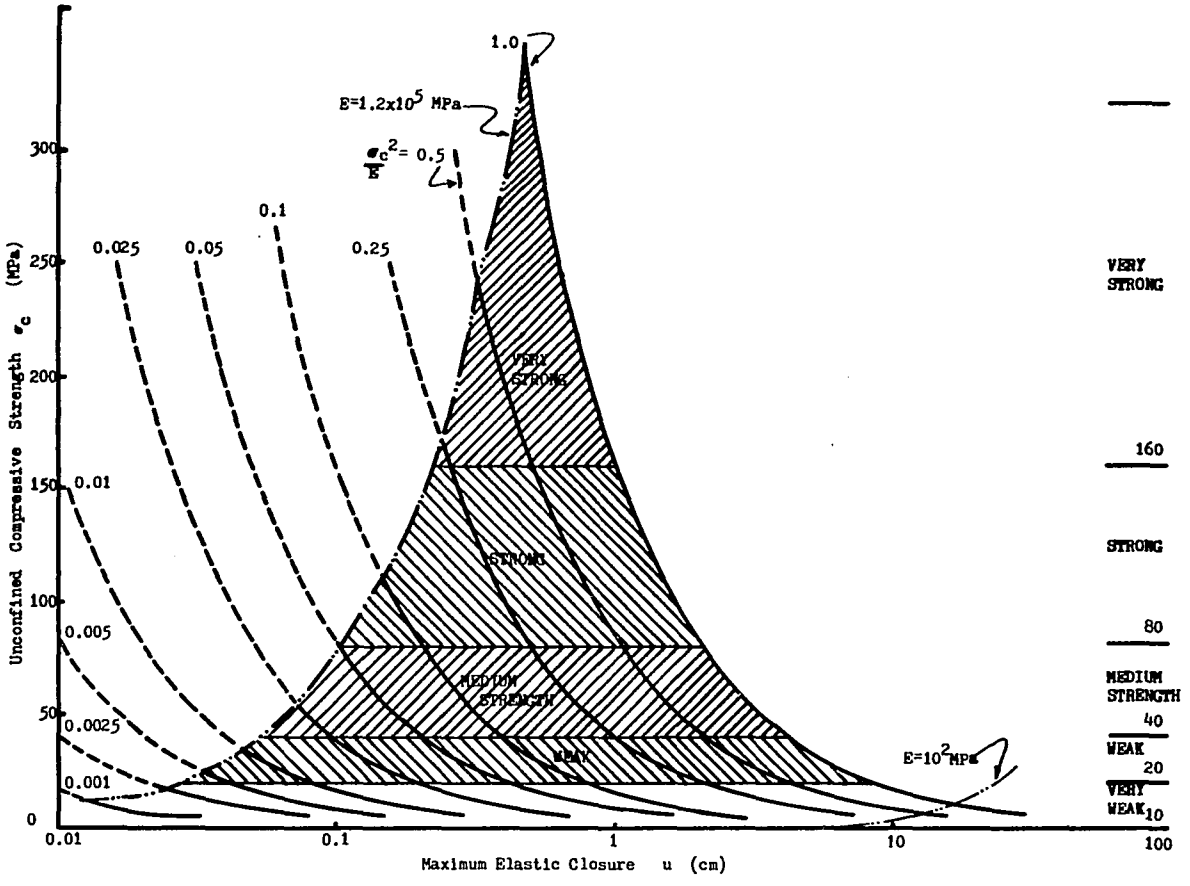

Figure 26. Variation of Maximum Elastic Closure (at Initiation of Boundary Layer Failure) for $\nu = 0.3$, $r_i = 2.5$ m.

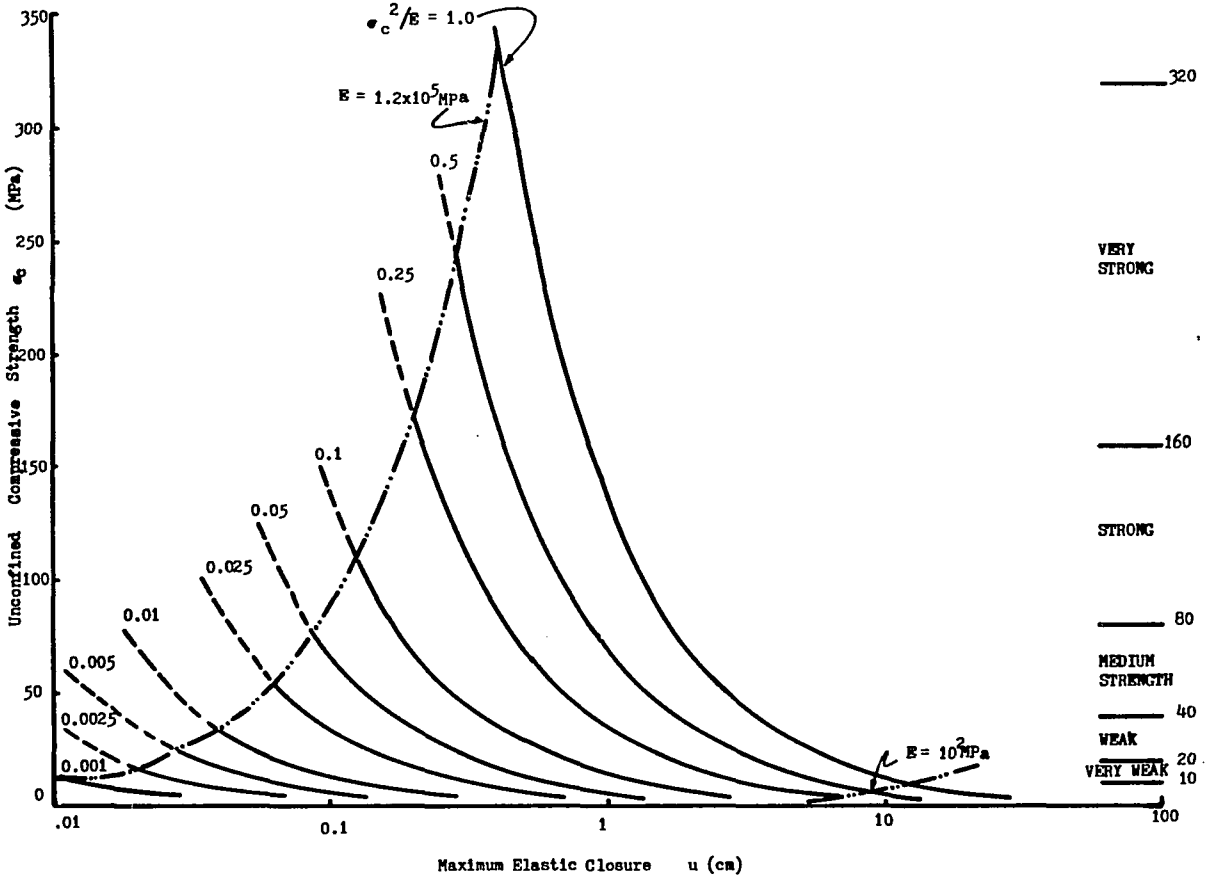

Figure 27. Variation of Maximum Elastic Closure (at Initiation of Boundary Layer Failure) for $\nu = 0.1$, $r_i = 2.5$ m.

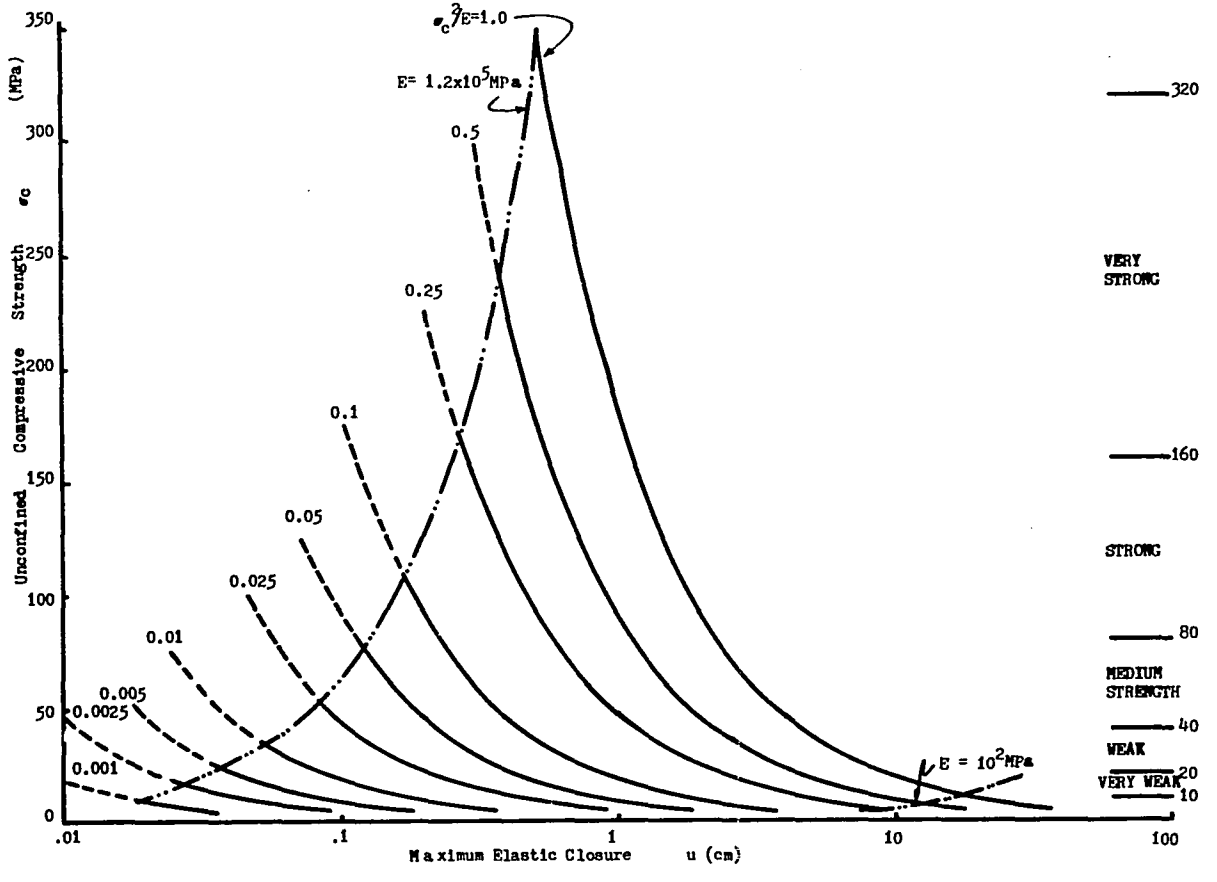

Figure 28. Variation of Maximum Elastic Closure (at Initiation of Boundary Layer Failure) for $\nu = 0.45$, $r_i = 2.5$ m.

the size of the proposed MX access and network tunnels). The influence of Poisson's ratio (ν) is seen to have little influence on the maximum elastic closure (Figures 26-28). Variations in the Modulus of Elasticity, on the other hand, can change the maximum elastic closure (for materials of equal fracture toughness) by a large factor. Obvious from Figures 26-28 is that "failure" criteria for tunnels based on deformation of the tunnel boundary, cannot be defined by strength characteristics alone, especially for rocks of low strength. What may not be obvious from Figures 26-28 is that rocks of equal compressive strength can allow a wide range of radial closures depending on the elastic characteristics. Fracture toughness incorporates both strength and elastic characteristics and may therefore be considered to describe better the behavior of rock in the annulus of a tunnel.

As was determined previously, the strain energy density at the initiation of rock fracture in the tunnel annulus is given by equation (21).

$$W = (\sigma_c^2/E)((5 - 4\nu)/8)) \qquad (21)$$

The elastic closure is from equation (27)

$$u_r = [a(1 - \nu^2)/\sqrt{E}][\sqrt{\sigma_c^2/E}] \qquad (27)$$

and the volumetric closure is $\Delta V/V_i$,

where ΔV = the change in volume

V_i = the initial tunnel volume

$$\Delta V = \pi(a^2 - (a - u_r)^2)$$

and

$$V_i = \pi a^2$$

so that

$$\Delta V/V_i = \pi(a^2 - (a - u_r)^2)/\pi a^2$$

$$\Delta V/V_i = \frac{\pi a^2 - \pi a^2 [1 - (1 - \nu^2)\sigma_c/E]^2}{\pi a^2}$$

$$\Delta V/V_i = \{1 - [1 - (1 - \nu^2)\sigma_c/E]^2\} * 100\%$$

$$\Delta V/V_i = \{1 - [1 - ((1 - \nu^2)/\sqrt{E})(\sqrt{\sigma_c^2/E})]^2\} * 100\% \qquad (28)$$

Equation (28) gives the volumetric closure (%) at the instant of fracture in the tunnel boundary. This can be superimposed on a curve of (E, $\sqrt{E}$) vs (σ_c,σ_c^2) as shown in Figure 29. This figure illustrates in a more satisfying manner, the variation of maximum elastic volumetric closure. Superimposed on the curve is Farmer's (1983) unconfined compressive strength criterion and the data from Deere and Miller (1966) and Hobbs (1974) replotted in σ_c^2/E space.

General points about Figure 29:

a. The maximum volumetric closure increases with a decrease in σ_c and a decrease in E.

b. The quantity fracture toughness (σ_c^2/E), influences the maximum volumetric closure to a great degree.

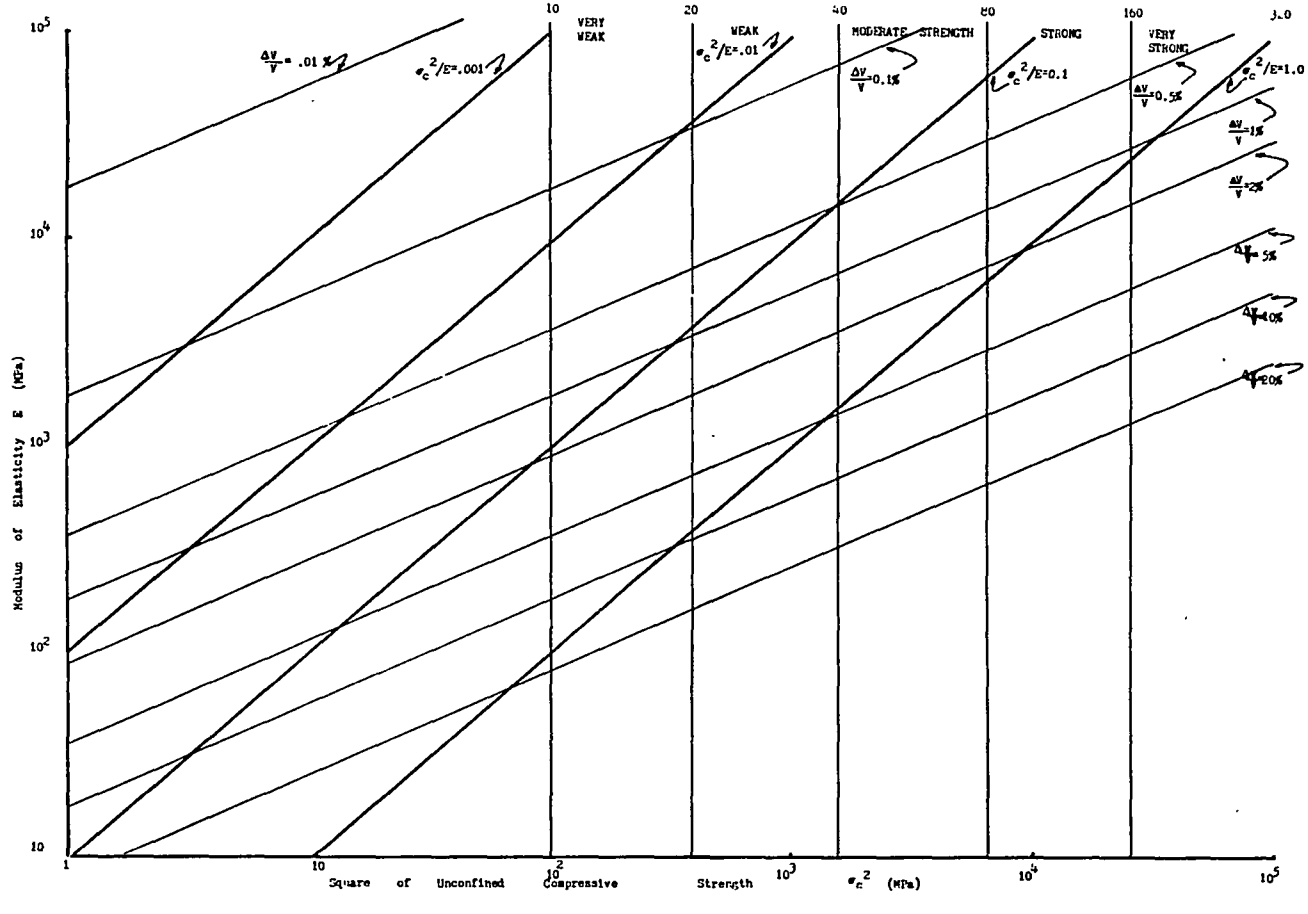

Figure 29. Variation of Maximum Elastic Volumetric Closure with Fracture Toughness.

c. For brittle rocks (low ν), equation (28) may be approximated as

$$\Delta V/V_i = \{1 - [1 - (\sqrt{\sigma_c^2/E})(1/\sqrt{E})]^2\} * 100\%$$

since $((1-\nu^2) = 1$ for low ν (ie $\nu < 0.3$).

Apparent from Figure 29 is that the highest quality rocks can sustain the largest and the poorest quality rocks the least amount of elastic volumetric closure. This is true, undoubtedly, because the field stress $P = \sigma_c/2$ at failure is much lower for these rocks.

The problem still remains, however, as to how the energy changes (from an initial non-tunnel rockmass to one with a tunnel through it) affect the displacements of the tunnel boundary in a qualitative "limit-state" manner.

The energy density around a tunnel is not a function of the size of the tunnel. This is true in non-dimensional terms but is not true in absolute terms. For instance, the energy density at a distance equal to two tunnel radii will be equal for tunnels of radius 2 meters and 10 meters. However, the energy density 5 meters from a 2 meter radius tunnel will not equal the energy density 5 meters from a 10 meter tunnel. This non-dimensional similitude can allow for energy-rock quality-closure comparisons for tunnels.

The strain energy density around any circular tunnel in a hydrostatic stress field can be determined from the following equation:

$$W = (P_o^2/2E)[3(1 - 2\nu) + (2a^4/r^4)(1 + \nu)] \qquad (29)$$

Which was derived from equation (8) with

$$\sigma_\theta = \sigma_1, \qquad \sigma_r = \sigma_3, \qquad \text{and} \quad P_o = \sigma_2$$

also

$$\sigma_\theta = P_o (1 + (a^2/r^2))$$
$$\sigma_r = P_o (1 - (a^2/r^2))$$

From which the energy density at the tunnel boundary is (with r = a):

$$W = (P_o^2/2E)(5 - 4\nu) \quad \text{which is the same as (21)}$$

This is a much more general approach to the strain energy density solution (for the circular tunnel in a hydrostatic stress field case) than that previously introduced and allows exact determinations of strain energy density for any radial distance. It also further illustrates the non-dimensional aspects of the strain energy-tunnel radius relationships.

The volumetric closure at the initiation of boundary layer fracture, in terms of the strain energy density, can be developed from equations (21) and (28) as:

$$\Delta V/V_i = \{1 - [1 - (2(1 - \nu^2)(\sqrt{2W})/(\sqrt{E(5 - 4\nu)}))]^2\} * 100\% \qquad (30)$$

Once a rock's characteristics (σ_c^2/E, σ_c, E, ν) are known, then it is a simple matter to calculate the elastic volumetric closure:

from a given boundary layer strain energy ($W = (P_o^2/2E)(5 - 4\nu)$). If these values are compared to allowable values of volumetric closure for different tunnels and different tunnel functions, then the adequacy of the tunnel for that purpose can be evaluated. Under most circumstances, the volumetric closure due to elastic energy release will be less that 10% (probably less than 1%). Therefore, only the most critical structures will be unfavorably affected by this elastic behavior.

Closure Due to Rock Fracture and Dilation

More important than the elastic closures, from a limit state design point of view, will be the closures associated with rock fracture and dilation. As discussed previously, the development of a tunnel can create conditions in which the redistributed strain energy exceeds the rocks fracture resistance in a thickness of rock in the tunnel annulus. An amount of this redistributed energy will be released, manifesting itself as boundary relaxation, which in turn induces additional strain energy in the annulus. A point will be reached in which the amount of energy which can be released through relaxation will be exceeded. At this point the tunnel boundary layer will begin to fracture. Strain energy will be released onto newly formed fracture surfaces until a pseudo-equilibrium condition is reached. Pseudo-equilibrium refers to the point when the fracture resistance of the intact rock just exceeds the amount of energy which is stored in that volume. The energy released as a result of fracture will be of the following forms:

(1) KINETIC ENERGY - energy moving the rock in the annulus to a lower potential energy state, i.e., increased closure.

(2) SEISMIC ENERGY - energy released at the moving crack tip, some of which is transmitted to areas beyond the tunnel annulus.

(3) HEAT ENERGY - energy due to the movement and friction caused by the release of potential energy onto the fracture surface.

The energy differences between the highest and lowest potentials will be greatest at the tunnel boundary and that difference will continue to be the greatest on the tunnel side of the annulus. The strain energy will be released in the direction of maximum energy gradient, toward the tunnel, since potential energy will tend toward its lowest state eventually, and the lowest state will be when the tunnel is completely closed. Complete closure will occur when opposite sides of the excavation touch and produce stresses there equal to the in-situ field stresses.

A great deal of difficulty arises attempting to partition the amounts of energy in each of the aforementioned forms. For a macroscopic crack to form at all, the strain (potential) energy stored in the rock must be great enough to satisfy the surface energy requirements of the potential fracture. Opposite sides of the fracture will be moved apart as the crack opens. Energy will be released seismically at the crack tip, kinetically as the opposite sides move apart, and as heat as friction between blocks occurs.

Krech (1974), Friedman et al. (1972), and others have studied fracture surface energy requirements of rocks. The results indicate that a specific value of this energy may be determined. A knowledge of this energy requirement is paramount as a first step in developing an energy approach to rock fracture around a tunnel annulus and will be expanded upon.

The fracture-surface energy of rocks has traditionally been determined by propagating a stable tensile fracture through the specimen and then measuring the area of the fracture surface (Friedman et al., 1972). The loading arrangement is that of a notched or unnotched rock beam loaded in a simply supported arrangement in a stiff loading device. Early work in this area yielded fracture surface energy requirements greater than the constitutent minerals. This is physically impossible since fracturing takes place both through and around crystals and as such should theoretically be less than the surface energy requirements of the constitutent minerals. Friedman et al. (1972) studied the fracture surface itself and concluded that fracture surface topography and the occurrence of a "zone" of strained crystals adjacent to the macrofracture must be considered in the surface energy calculations. The total strain energy stored in the sample at fracture was used in the calculation and assumed that the energy lost to heat and sound at fracture was small. The adjusted surface energy calculations conform well with the surface energy requirements of single crystals. The use of this logic in a compressive stress field is suspect, however, since energy will

be lost closing unfavorably oriented microcracks and in frictional sliding (McClintock and Walsh, 1962). The actual surface energy requirements, however, may remain the same since the macrofracture will fail principally in tension, that is, the new surface will be created by the energy doing work to separate adjacent atoms a distance equal to the thickness of the crack. This work will be performed by the kinetic energy released as the crack tip advances through the rock. Coincident with the separation of the fracture surfaces will be the development of seismic energy which will travel spherically outward from the crack tip.

The surface energy requirements of rocks found in the tunnel annulus may hold promise in determining the residual energy storage capability and inelastic closures in the annulus. Unfortunately, the capability does not yet exist to allow measurement of the actual area of fracture development in compressively fractured samples. The volumetric strain, being a function of the rocks ability to do work against the confinement in creating the fractures, appears to depend upon the surface energy requirements, confinement and total available energy, and the rocks propensity to develop a certain area of fracture surface given the preceding conditions. The residual potential energy stored in the rock sample will be a fraction of the original strain energy stored in the sample prior to fracture. The kinetic energy released onto the fracture surface will be transformed into potential energy (some going into the fractured portion of the rock in the annulus), seismic energy, and some into heat energy. The amount of

energy contributing to potential energy in the fractured rock is of utmost importance, as it will control the behavior of the intact rock adjacent to it. It is not clear what controls the area of fracture surface created at the threshold energy value for a given rock. Triaxial tests can provide relative relationships but the test itself may not properly model the conditions in the annulus.

Rock samples loaded compressively commonly form more than one single fracture surface and triaxial tests indicate that the "confinement" contributes to the extent and nature of the fractures thus formed. It is obvious that attempting to determine the area of fracture surface from such tests is, in general, unacceptable. Complete stress-strain curves (Figures 30-33) illustrate the manifestation of the energy changes which took place as the fractures developed in the rock. For these samples, work was done in fracturing the rock, and that fracturing and any other immediate kinetic effects are exhibited as immediate (at the point of fracture) volumetric strain. The amount of potential energy retained in the confined samples (indeed, potential energy exists since stresses still act on the sample) corresponds to the residual energy, described earlier for a tunnel annulus. The residual energy for the triaxial samples in Figures 30-33 is, at this time, incalculable since the elastic properties (E, ν) of the broken rock are not known, and it is not even known if the broken material will behave elastically at all, since the post-failure strains are large and by definition, elastic behavior is defined in terms of small strains.

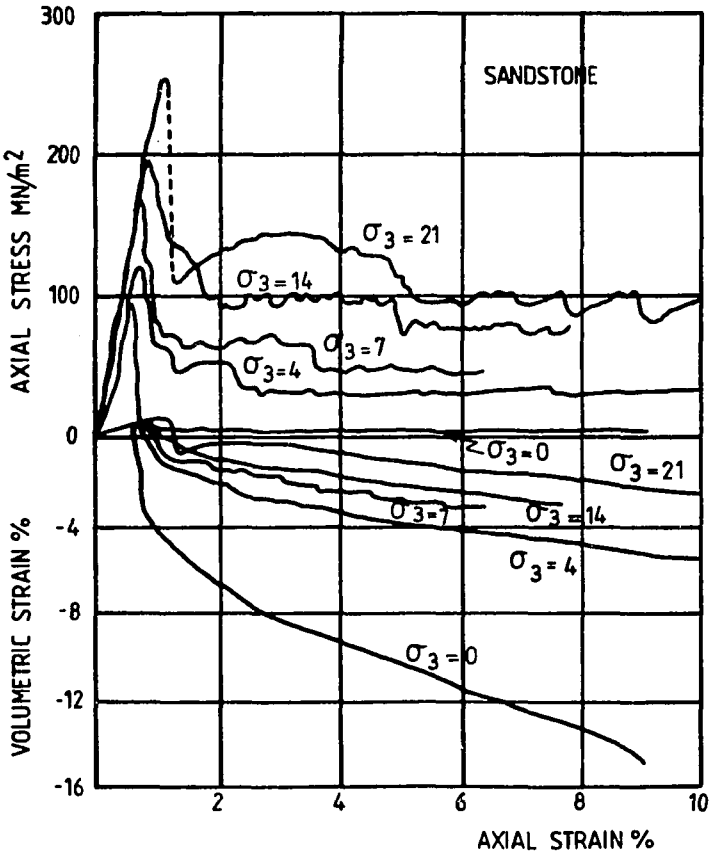

Figure 30. Axial Stress-Axial Strain and Volumetric Strain-Axial Strain Curves for Coal Measures Sandstone Specimens Tested in Triaxial Compression at Confining Pressures from 0 to 21 MN/m^2. (from Price, 1979)

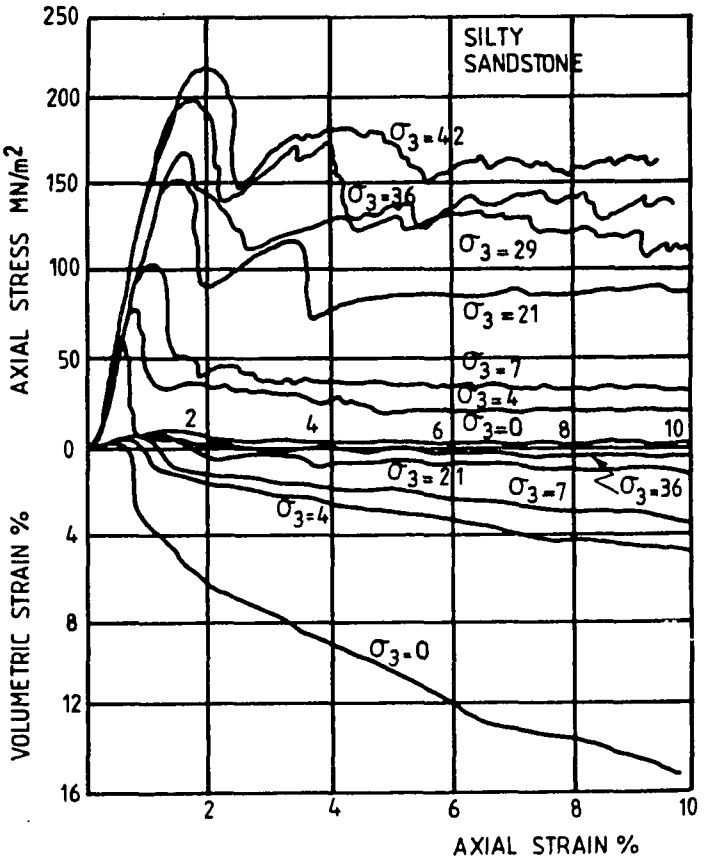

Figure 31. Axial Stress-Axial Strain and Volumetric Strain-Axial Strain Curves for Coal Measures Silty Sandstone Specimens Tested in Triaxial Compression at Confining Pressures from 0 to 42 MN/m^2. (from Price, 1979)

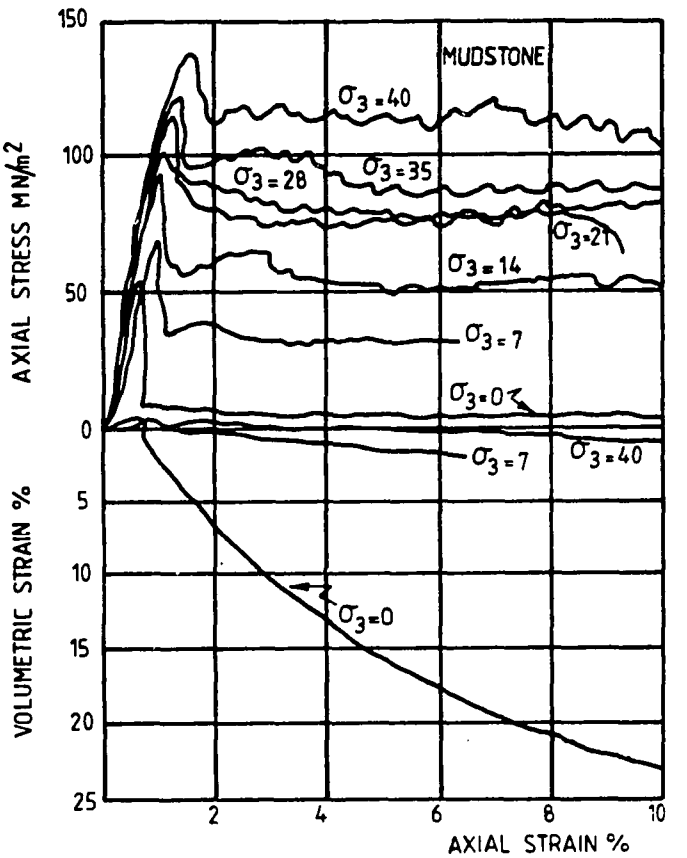

Figure 32. **Axial Stress-Axial Strain and Volumetric Strain-Axial Strain Curves for Coal Measures Mudstone Specimens Tested in Triaxial Compression at Confining Pressures from 0 to 40 MN/m^2. (from Price, 1979)**

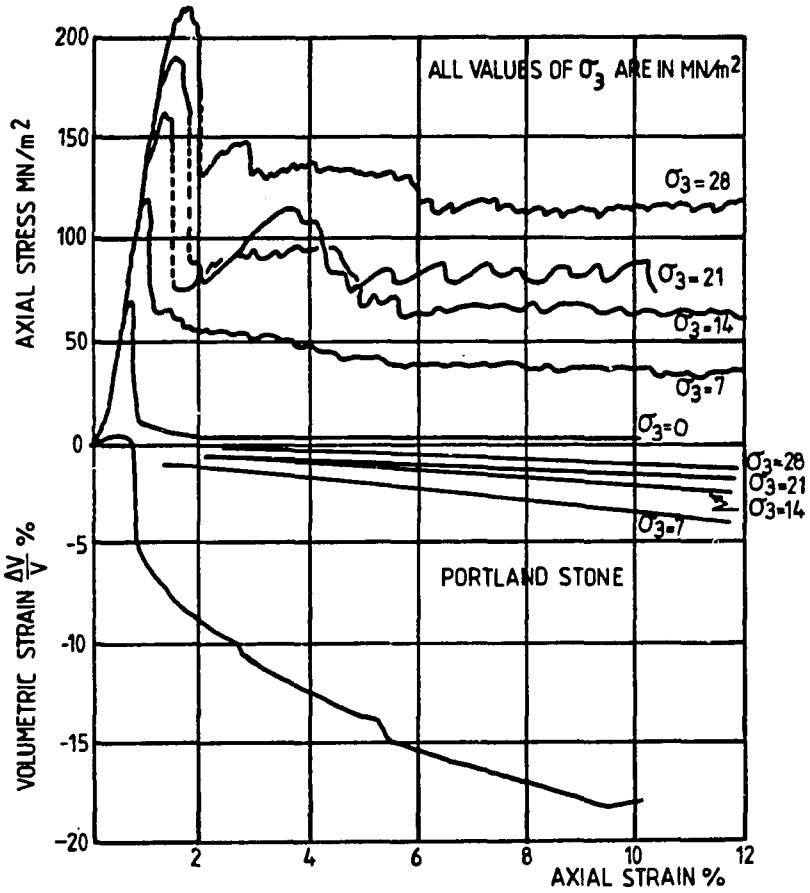

Figure 33. Axial Stress-Axial Strain and Volumetric Strain-Axial Strain Curves for Portland Stone Specimens Tested in Triaxial Compression at Confining Pressures from 0 to 28 MN/m^2. (from Price, 1979)

After fracture and immediate volumetric strain (dilation), the sample continues to strain (dilate) as additional energy is input to the system. Again, this is similar to the situation in a tunnel annulus as rock fracture progresses into the annulus. Energy associated with the immediate dilation of rock beyond will be the input energy for "strain softening" behavior in the already fractured near tunnel rocks.

The instantaneous volumetric strain as a function of total strain energy density at failure and "confinement" for the rocks of Figures 30-33 is illustrated in Figure 34. While not being conclusive evidence, it does show the influence of confinement (critical energy difference) on the rocks ability to do work (in fracture) against that confinement. For stable rock fracture in the tunnel annulus, Figure 34 illustrates that instantaneous volumetric strain will decrease rapidly for most rocks as the distance into the annulus increases. For an actual tunnel annulus, the amount of volumetric closure will probably be less than that estimated from the triaxial tests since the triaxial sample is free to "expand" in all directions (except axially) whereas the rock in the annulus will be free to expand only radially toward the opening. Small amounts of confinement will drastically limit the amount of volumetric closure as is shown by the σ_3 = 7MPa line on Figure 34. The confining strain energy (minimum $W_c = f(\sigma_2,\sigma_3$ only) vs. $\Delta V/V$ (Figure 35) shows an even more marked influence of confinement on the instantaneous volumetric strain (strain associated with fracture development). The reason that "confinement" influences

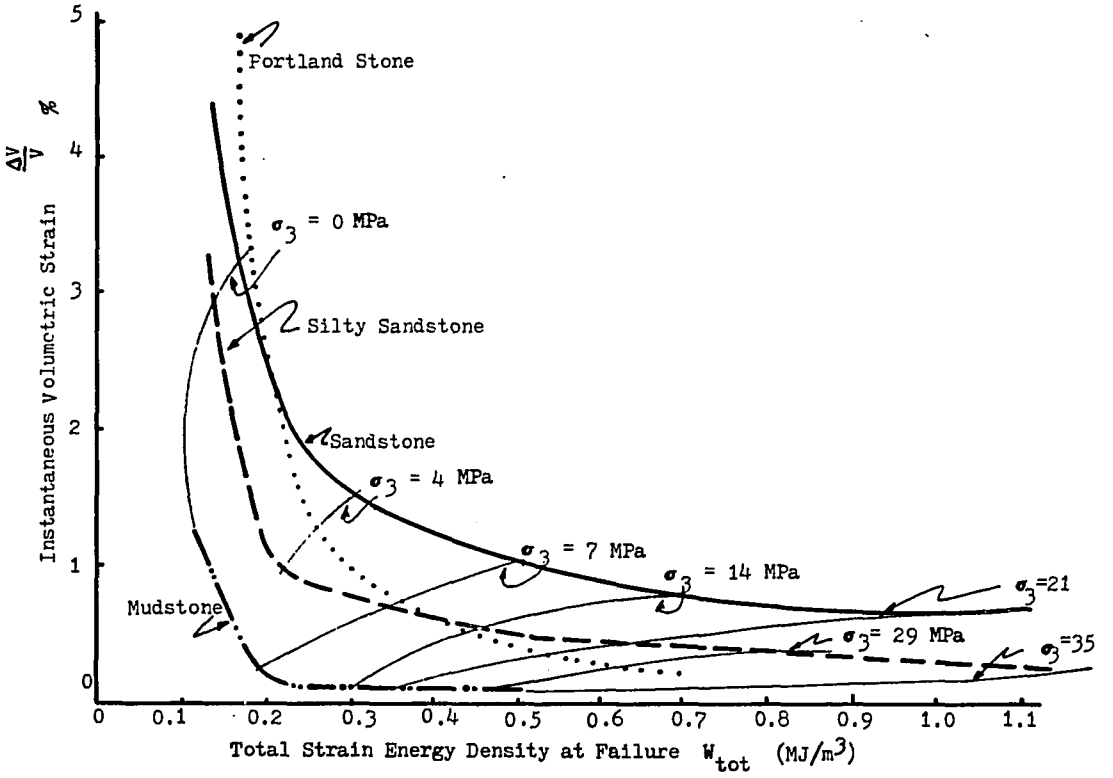

Figure 34. Total Strain Energy Density at Failure vs. Instantaneous Volumetric Strain for Four Coal Measures Rocks (Confining Pressure Superimposed). (Modified from Price, 1979)

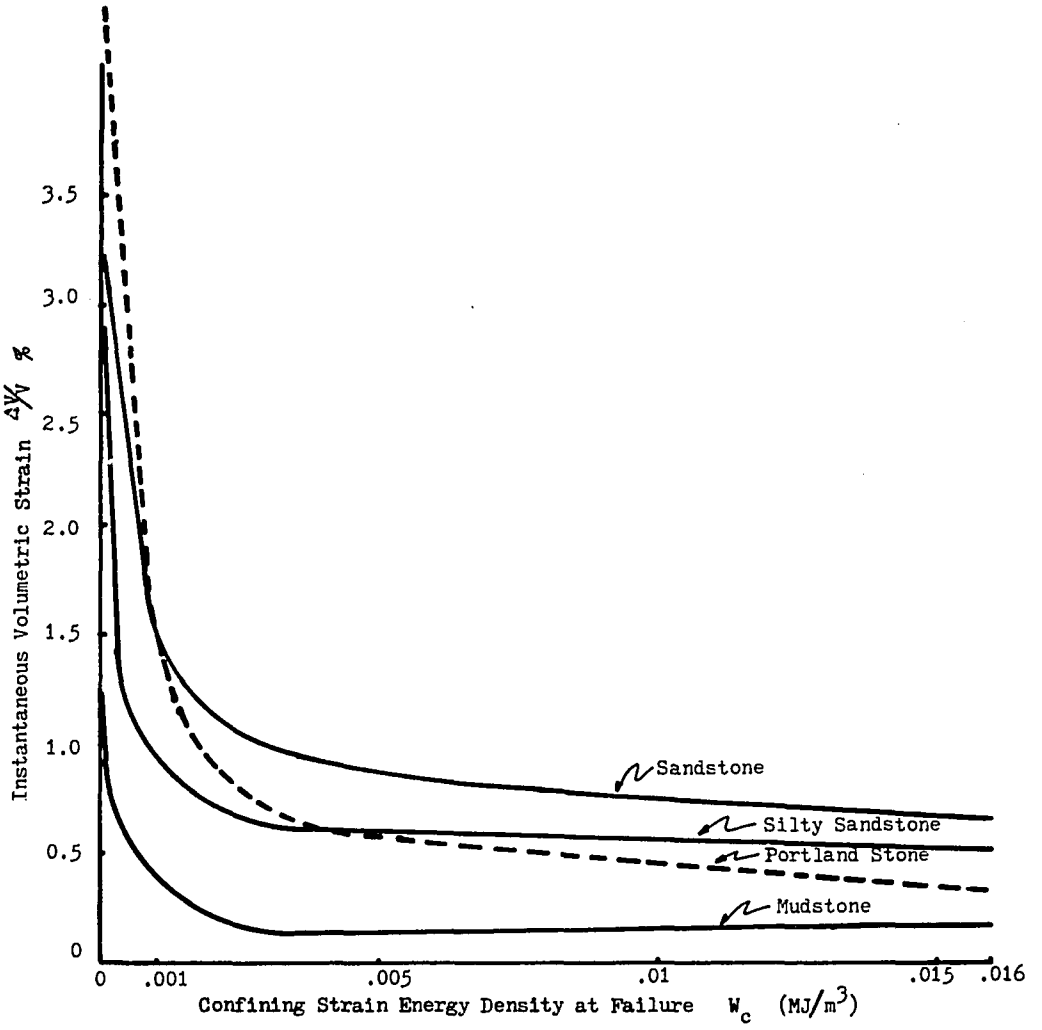

Figure 35. Variation of Instantaneous Volumetric Strain with Confining Energy. (Modified from Price, 1979)

the volumetric strain to such a great extent is that the kinetic energy released onto the fracture surface must do work against that confinement. Therefore, the kinetic energy must expend more energy to move the crack surface apart a given distance. If the surface energy requirements for a given rock type are indeed a constant, then the kinetic energy released per unit crack surface area is also a constant regardless of confinement and as such cannot move the opposite crack surfaces apart as great a distance as in a low confinement situation. The total volume change in the annulus (assuming the triaxial tests to properly model the rock behavior there) will be the integration of the volumetric strains over the expected confinements at failure along a radial distance from the tunnel boundary.

As is illustrated from Figures 34 and 35, a point will eventually be reached in which the rock will not change in volume upon fracture. This is essentially the critical state as defined in soil mechanics in which the material yields plastically at constant volume. True plastic behavior is not dealt with here although others (see Ladanyi, 1974) have modeled rock behavior in the tunnel annulus as such.

As was mentioned previously, the idea of instantaneous loading (instantaneous removal of all of the rock in the volume to be occupied by the tunnel) does not accurately describe the true loading mechanism, and, may even cloud the proper solution path.

For unfractured elastic rock, the initial development of an opening will release energy which will attempt to induce an equal

amount of strain energy in the annulus. The annulus will accept the energy up to the fracture resistance of the rock in the tunnel boundary layer. In other words, the rock in the annulus will store the released potential energy as strain energy and all points in the annulus will be displaced toward the excavation an amount equal to (assuming plane strain):

$$u_e = \frac{P_o r^2 (1 + \nu)(1 - 2\nu) + (P_o - P_i) a^2 (1 + \nu)}{Er}$$

where a = the radius of the tunnel

r = the radial distance from the tunnel centerline

P_o = the in-situ field hydrostatic stress

ν = Poisson's ratio

E = modulus of elasticity

P_i = internal pressure

with the displacements at the tunnel/rock interface being (with r = a and P = 0):

$$u_e = 2P_o a(1 - \nu^2)/E$$

This displacement is the manifestation of the maximum amount of the released energy which can be induced as strain energy in the annulus of a tunnel of radius a (with no internal pressure). Importantly, all points will displace a finite amount toward the tunnel.

As the tunnel progresses, more material will be removed, and, therefore, more energy will be released. This is different from most models in which the tunnel is developed instantaneously and the released energy must also instantaneously be accounted for. Realistically, the rocks in the annulus will be gradually loaded so that the released energy can be dissipated gradually. In most instances a point will be reached where the annulus has reached its maximum elastic energy storage capability and the addition of more energy will induce fracturing in the tunnel boundary layer. A finite increase in the amount of material removed will cause a finite increase in the released energy and induced energy. A finite annular thickness of rock will fracture, dilate, and provide a somewhat lower amount of "support" for the intact rock beyond, which simultaneously "relaxes" due to the lower confinement. In relaxing, the intact rock accepts some of the released energy until it reaches its energy storage capacity, and the process begins again. The released energy will eventually be accounted for as the fracturing process proceeds into the annulus. Fracturing will stop when all the released energy has been accounted for and a certain critical energy difference exists between the intact and adjacent fractured rock. It is possible that the intact rock at the fractured/intact boundary will always be at its maximum (below fracture) energy storage capacity. This might explain why the rock in a tunnel annulus continues to fail with time. The intact material is at a critical equilibrium with the energy stored in that volume, and as time progresses the rock will degrade and immediately lose its energy storage capacity and will fracture.

Considering the boundary displacements which occur as a result of these energy changes: part of the additional tunnel boundary displacements are due to the fracturing of the rock and some are due to initial and subsequential elastic displacements. The subsequential elastic displacement due to fracturing in a finite annular thickness is given by:

$$u_{ei} = \frac{P_o r^2 (1 + \nu)(1 - 2\nu) + (P_o - P_i) a^2 (1 + \nu)}{Er} \qquad (31)$$

For a circular tunnel the internal "pressure" is equal to the support provided to the intact rock by the fractured rock in the finite annulus. (The support P_i can be compared, in energy terms, to the residual energy stored in the newly fractured rock). The total amount of boundary displacement is therefore, given by:

$$u_{tot} = u_{el} + u_{f1} + u_{e2}$$

Fracturing will occur until a pseudo-equilibrium condition is reached in which no further released energy is available to be dissipated. Considering two annular thicknesses to have failed, the boundary displacement is:

$$u_{tot} = u_{el} + (u_{f1} + u_{e2}) + (u_{S12} + u_{f2} + u_{e3})$$

where u_{el} = Initial elastic boundary displacement for a tunnel of radius a.

u_{e2} = Subsequential elastic displacement at the fracture/intact boundary due to fracture in the 1st annulus.

u_{e3} = Subsequential elastic displacement at the fracture/intact boundary due to fracture in the 2nd annulus

u_{f1} = Displacement due to fracture in the 1st annulus

u_{f2} = Displacement due to fracture in the 2nd annulus

u_{S12} = Additional displacement in the 1st annulus due to fracture in the 2nd annulus

For n annular thicknesses, the total boundary displacement is:

$$u_{tot} = u_{e1} + (u_{f1} + u_{e2}) + (u_{S12} + u_{f2} + u_{e3}) + \ldots + (u_{S1n} + u_{S2n} + \ldots + u_{S(n-1)n} + u_{fn} + u_{e(n+1)}) \quad (32)$$

where: u_{e1} = the original elastic displacement

$(u_{f1} + u_{e2})$ = the additional displacement due to fracture in the 1st annular thickness

$(u_{S12} + u_{f2} + u_{e3})$ = the additional displacement due to fracture in the 2nd annular thickness

$(u_{s1n} + u_{S2n} + \ldots + u_{S(n-1)n} + u_{fn} + u_{e(n+1)}$ = the additional displacement due to fracture in the nth annular thickness

In the preceeding expressions:

$u_e, u_{e2}, \ldots u_{e(n+1)}$ = the elastic displacements for the original 1st - nth annular thickness.

u_{f1}, u_{f2}, $\ldots u_{fn}$ = the instantaneous displacements due to fracture in the 1st, 2nd - nth annuli.

u_{s1n}, u_{S2n}, $\ldots u_{S(n-1)n}$ = the "strain softening" displacements in the 1st, 2nd, (n-1)th annular thickness due to fracture and instantaneous displacement in the 2nd, 3rd, nth annuli.

Additionally:

u_{el}, u_{e2}, $\ldots u_{e(n+1)}$ = a function of elastic rock properties

u_{f1}, u_{f2}, $\ldots u_{fn}$ = a function of energy release properties, including residual energy storage characteristics

u_{s1n}, u_{S2n}, $\ldots u_{S(n-1)n}$ = a function of residual energy storage characteristics and "large strain" energy release characteristics

Equation (30) can be rewritten as:

$$u_{Tot} = u_{el} + U_1 + U_2 + \ldots + U_n = u_{el} + \sum_{i=1}^{n} U_i \qquad (33)$$

where: U_1 = Additional boundary displacements due to fracture in the 1st annulus.

U_n = Additional boundary displacements due to fracture in the nth annulus.

The contribution of the total boundary displacement due to fracture in the annular sections will decrease as the

pseudo-equilibrium condition is approached. For the preceeding method for determining the total closure (elastic and inelastic) around a tunnel to be used, a knowledge of the instantaneous residual energy storage characteristics and inelastic strain induced energy release characteristics must be known.

Additional Factors Affecting Strain Energy Storage and Dissipation in a Tunnel Annulus

In most instances a tunnel will not be driven in perfectly elastic homogeneous intact rock. Fractures, joints, ground water, and inelastic rock are commonly encountered in tunneling. The preceeding analysis does however, provide a logical starting point for the development of a method for tunnel design based on an energy criterion.

The influence of pre-existing fractures or joints on rock mass behavior has been considered by many workers (Deere, 1964; Hobbs, 1974; Bieniawski, 1973, 1976; Hoek and Brown, 1981). The existence of such structural features produces difficulty in determining the strain energy which can be stored and released by a tunnel annulus.

If the rock into which the tunnel is driven is not initially fractured or jointed, then any excess strain energy can be released through rock fracture and subsequent elastic relaxation as previously described. In addition, if joints are contained within the rock mass but are unfavorably oriented (for sliding along the fracture), fracture may remain the preferential energy release mechanism. Strain energy will probably "seek" the path of least resistance for its release so that if favorably oriented joints exist in the annulus,

energy release will first occur as frictional sliding along the joints. In this case little fracture of intact material aside from fracture surface shearing effects may take place.

For the case of rock with pre-existing fractures, a certain amount of rockmass elasticity can probably be expected for most degrees of fracturing. This rock mass elasticity will, in general, be a function of the fracture frequency. In this case, the most commonly presented data is based on moduli computed from seismic tests in near surface rocks subject to varying degrees of weathering. Figure 36 summarizes data obtained by Hobbs (1974) in chalk. The dynamic modulus is normalized in terms of the laboratory dynamic modulus measured from intact core samples of the chalk. The data illustrates a clear inverse relationship between in-situ modulus and fracture frequency. It appears that the rocks ability to behave elastically drastically decreases with increased fracture frequency. From this information it would seem that fracture frequency will influence in a like manner the amount of energy which can be released elastically through tunnel boundary deformations. Figure 37 illustrates the type of relationship which can be expected (given the information from Figure 36) for released energy (relative to perfectly elastic material) as a function of fracture frequency. Deere's (1964) rock classification scheme is superimposed on the abscissa for reference. These two Figures (36 and 37) are not, however, conclusive in terms of the rocks ability to store strain energy. The figures suggest that some of the total releasable energy will be released elastically, but

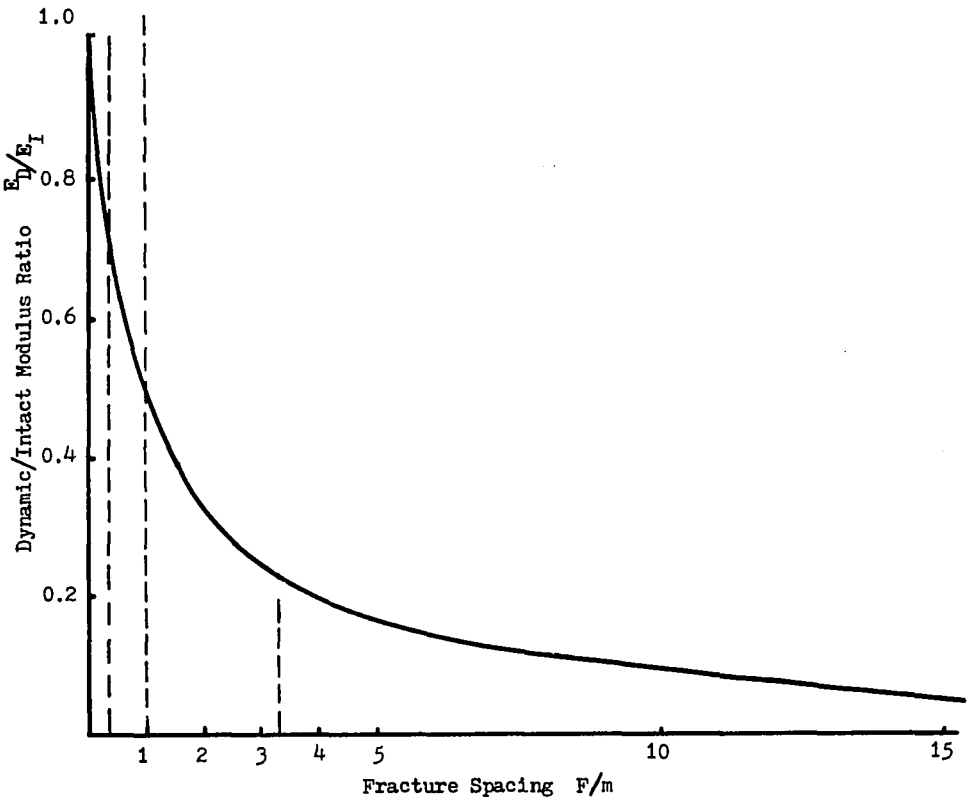

Figure 36. Influence of Fracture Spacing on Elastic Properties.

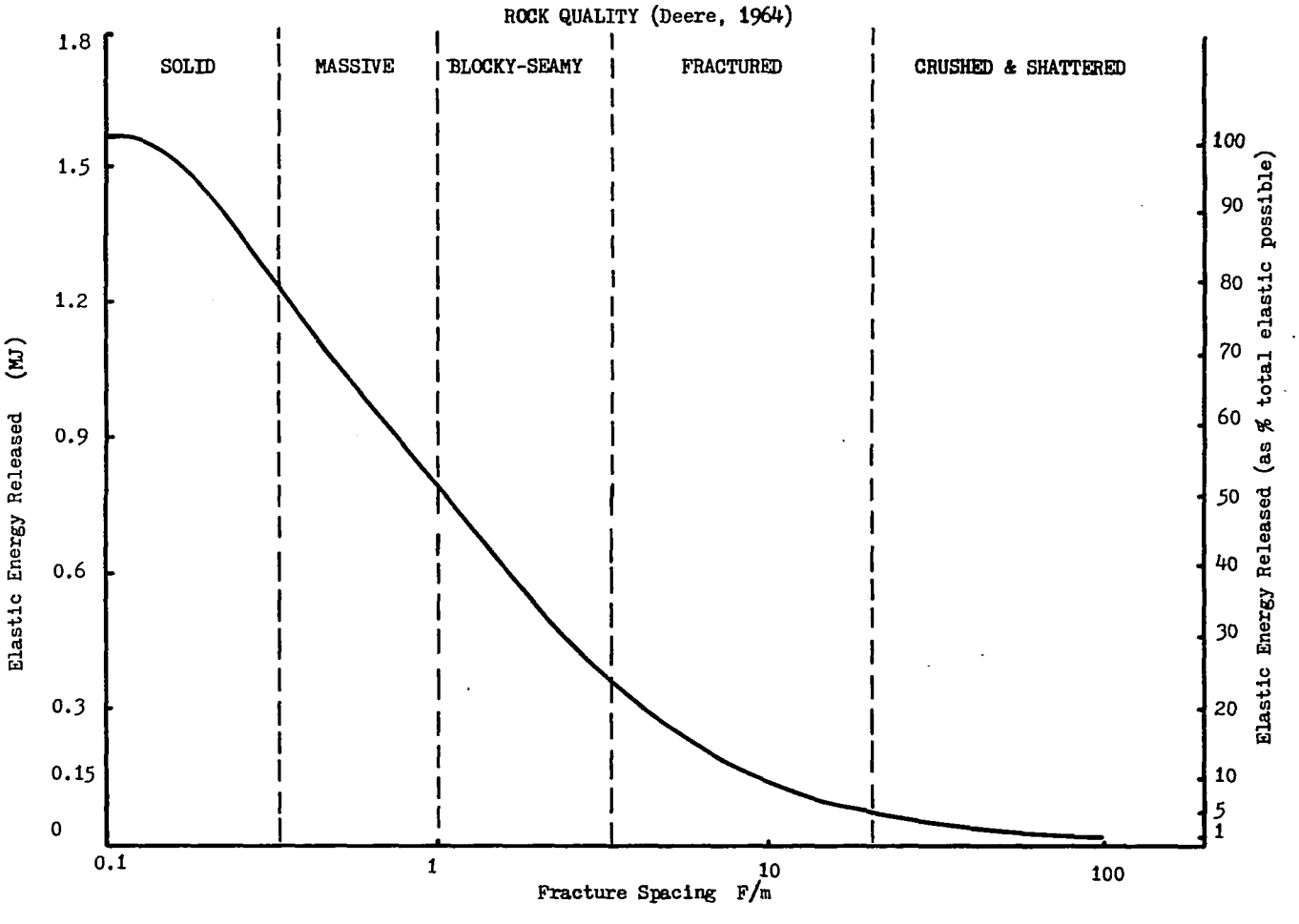

Figure 37. Elastic Energy Release vs. Fracture Spacing (Rock Quality (Deere, 1964) Superimposed).

that amount may be significantly less than intact rock. In the case of highly fractured rock, the majority of the releasable energy must therefore, be released inelastically as sliding on joints or plastic type deformation. The joint orientation may significantly influence the amount of energy which can be released elastically in a jointed rock mass. This type of behavior may best be analyzed using a joint energy-rock mass approach incorporating Bieniawski's (1974) approach.

The presence of jointed or unjointed inelastically responsive rock will also greatly influence the energy release characteristics associated with tunnel development. Many rock materials can dissipate (release) energy only through large inelastic deformation. Some materials do not have a tendency to form macroscopic cracks but rather deform as a result of atoms sliding past one another so that the overall behavior is similar to plastic behavior. In this case energy is lost mainly as heat energy and as a result of a change in potential energy associated with tunnel boundary deformations. The deformations can occur as true time-dependent deformations of creep. These materials require analyses other than those introduced here for elastic rock to adequately define expected annular displacements.

Finally, the presence of ground water can also greatly influence the ground response to tunneling. High water pressure in joints will tend to decrease resistance to movement along the joint thus presenting an easier energy release path there. Additionally, water will tend to accelerate the rock degradation process, causing the intact material to lose resistance to fracture. The complexity

associated with ground water precludes its incorporation in the energy analysis at this time.

Dynamic Energy

Dynamic energy changes affecting an underground structure occur in two forms, elastic and inelastic. Elastic changes are those associated with energy in the seismic range, whereas inelastic changes are associated with energy in excess of the seismic range. High energy shock waves will be developed near the explosive source and will eventually attenuate into the elastic "seismic type" dynamic energy at a distance from the source based on the energy dissipative characteristics of the rock.

The previously described static case relating distributed energy around a tunnel is an important addition to, or modification of, existing design concepts. However, it has limited applicability to the case of a tunnel subjected to true dynamic energy inputs. A seismic compression wave is the classic case of transient stress exceeding rock strength (resistance to fracture) without fracture actually occurring. An inelastic or shock wave, on the other hand, is a wave containing energy levels at or above those required to fracture the rock.

With reference to the previous "static" energy changes, it is important to note that any dynamic energy changes will be superimposed on those changes. In this case, any fracture due to static energy overloads will have occurred so that the resulting fractured rock carcass will be more susceptable to dynamic energy. This secondary

dynamic energy may then have a greater tendency to accelerate the fracture separated blocks into the opening than to create new fractures. The intact rock beyond the fractured zone will also be influenced by the transient dynamic energy input due to either blast or earthquake loads. In this way, the tenuous pseudo-equilibrium balance at the intact/fractured boundary can be upset by dynamic energy changes.

In the case of a tunnel subjected to dynamic energy from an explosive source, the basic criteria for tunnel damage can be examined with reference to the date collected and energy attenuation solutions computed for the Hardhat 5kt explosion in granite (see Rodean, 1971) and other similar explosions. These are summarized in Figure 38 as a plot of peak radial stress (or energy density) against the radial distance from an explosion, scaled to the cubed root of TNT equivalent in kilotons. This information (Hardhat) was obtained from stress meters placed approximately 150 feet below the ground surface at varying radial distances from the source. The results thus provide real information concerning the free-field transient stress (energy) associated with the detonation of a nuclear device. Figure 38 is a good device for illustrating the energy or stress decay in the wavefront some distance from the source, but will lose accuracy close to the source. The actual near-field pressure and temperature have been estimated theoretically and are so great that true measurement is impossible. Those measurements close to the boundary between elastic and non-elastic wave attenuation are the most accurate.

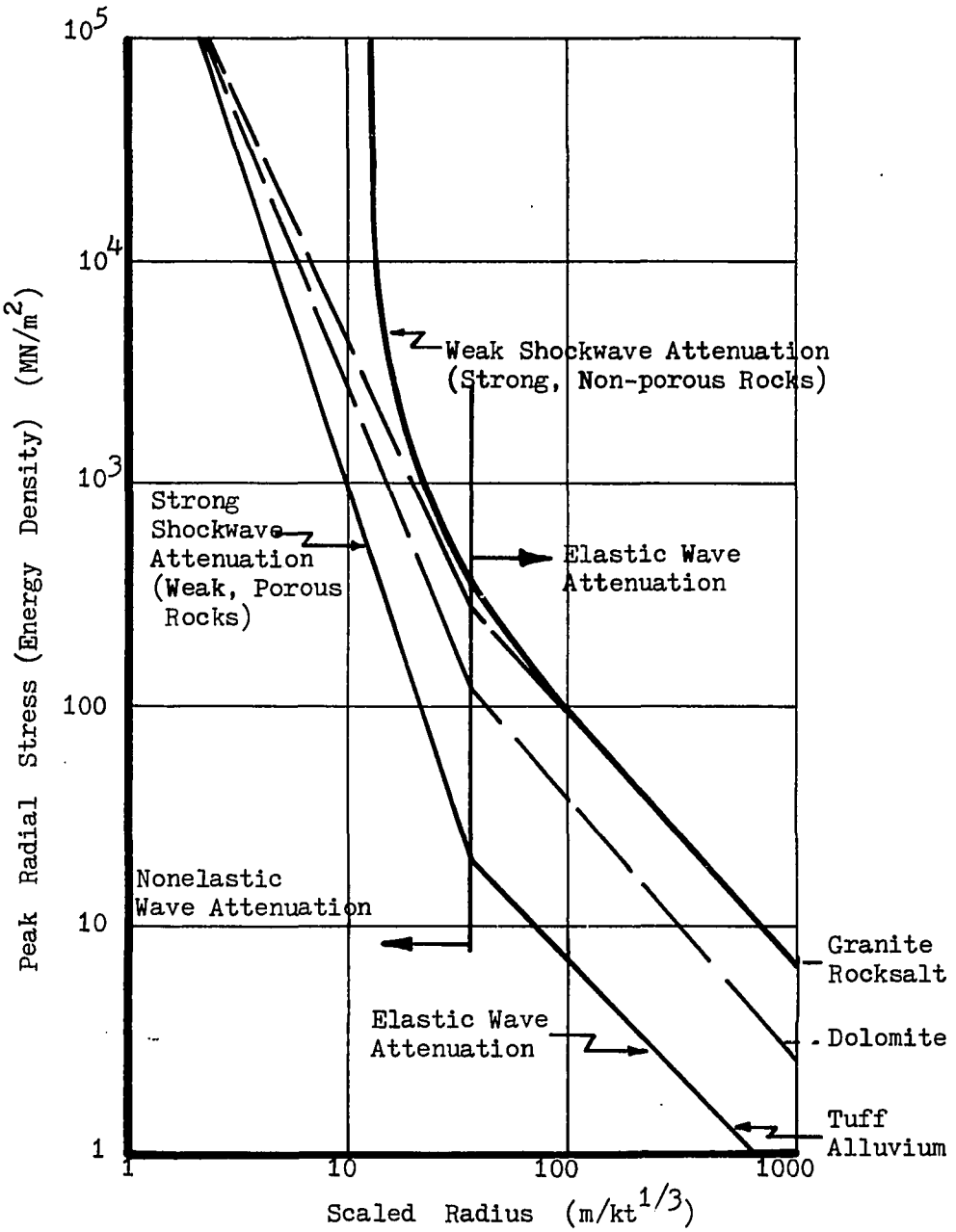

Figure 38. Theoretical Solutions (Solid Lines) and Data Envelopes (Dashed Lines) for Peak Stress or Energy Density Attenuation from an Explosive Source. (After Rodean, 1971)

Based on tests in granite, salt, dolomite, tuff and alluvium, the data were compared with three solutions for wave attenuation: weak shock attenuation (low energy losses in strong nonporous rocks), strong shock attenuation (high energy losses in weak, porous rocks), and elastic wave attenuation. There is very strong agreement with measured data with variations mainly in the weak shock wave attenuation close to the source. In Figure 38 the theoretical curves for the strong and weak shock wave attenuation are included as solid lines. The data for tuff and alluvium fit very closely the strong shock wave and elastic wave attenuation curves. The data for granite and salt fit the weak shock wave attenuation curve at the elastic/ inelastic boundary, but diverge from the weak shock solution so that the behavior of these rocks follows a line similar to the strong shockwave attenuation curve and is included in Figure 38 as a dashed line. The data for dolomite follows an intermediate (also dashed) line through both the elastic and inelastic region.

It can be argued therefore that upper and lower bound envelopes cover the data for shockwave attenuation from an explosive source. The upper bound envelope for nonelastic waves in strong, nonporous rocks has a relation between radial stress and scaled radius of the form:

$$\sigma = Kr^{-2} \tag{34}$$

The lower bound solution for nonelastic waves in weak porous rocks has a relation:

$$\sigma = Kr^{-3} \tag{35}$$

For elastic wave attenuation, both curves have the same slope equal to:

$$\sigma = Kr^{-1} \tag{36}$$

The power of r in each case is a measure of the attenuation of the energy in each type of rock. In the weaker rocks, the inelastic (shock) waves have a high attenuation rate, whereas the strong rocks have a relatively lower attenuation rate. In the case of elastic waves, the linear relation indicates geometrical attenuation with little energy lost to fracturing, friction, heat or other causes. This may be expected, owing to the relatively short distances considered. It should also be noted that the stress at which an apparent change from inelastic to elastic deformation takes place is very close to the compressive strength of the rocks, 300 MN/m^2 for "strong" rocks and 20 MN/m^2 for "weak" rocks, although the presence of salt as a strong rock indicates that some other factor, such as fracture toughness, may be important. The indication is, therefore, that beyond this elastic/inelastic transition, little significant free field rock damage will occur.

It is less easy to propose simple criteria based on loose relations between dynamic energy in the wave front and energy criteria for failure (fracture). The difference in slope between the inelastic attenuation and the elastic wave attenuation represents the energy dissipated in crushing, fracturing, heating, or permanently deforming

the rock. The actual amount of this energy may be estimated by subtracting the extension of the elastic wave attenuation curves from the inelastic curves in Figure 38. These then become (Figure 39) the envelope containing the energy lost or dissipated in the rock and ultimately remaining in the rock as potential, heat, or, most important, fracture surfaces. This ranges from nearly 10^5 MJ/m^3 at 2 m, scaled distance at zero at the elastic/inelastic boundary.

For a tunnel in rock the energy from an explosion can influence the performance of the tunnel. Obviously, a tunnel subjected to a high energy shock wave will require significant "hardening" to survive such an energy input. The fracturing of rock in the annulus due to the presence of energy in excess of the rock's threshold fracture energy will cause dilation of the annular rock toward the opening. It is this energy and dilation which may cause failure of the tunnel. Energy levels in the elastic range, although not causing rock fracture in the free field, may cause damage to rocks in the tunnel annulus.

It was mentioned previously that any dynamic energy input will occur after the static energy changes. This suggests that fracturing in the annulus will have occurred prior to the dynamic energy input. In this case, lower energy inputs (energy in the seismic range) can cause tunnel damage by imparting momentum to the fracture bounded blocks in the annulus. The energy in the dynamic wave will be manifested as kinetic energy in the broken material so that the energy in the block is given by:

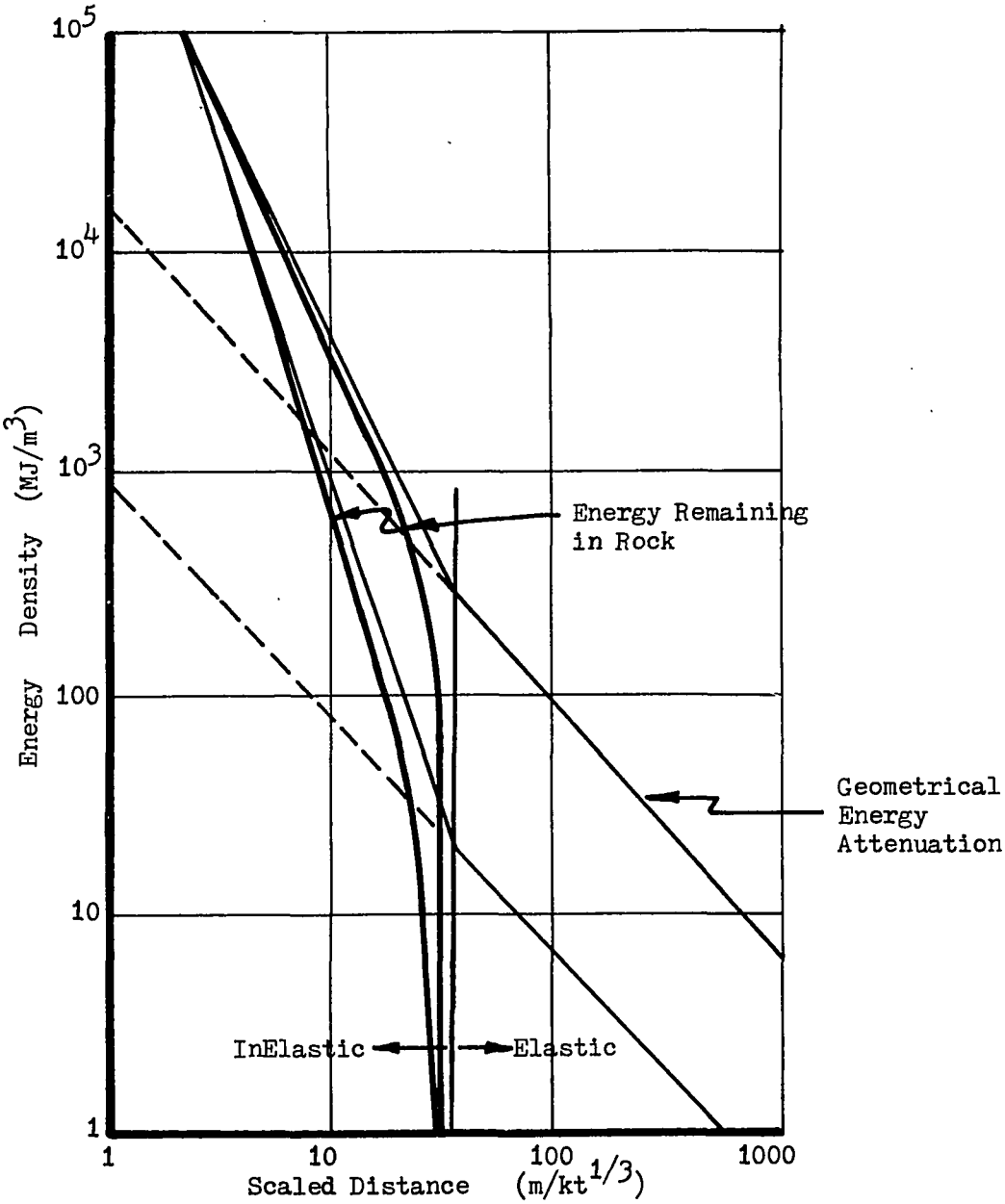

Figure 39. Envelopes Defining the Energy Lost During Wave Passage Through Strong and Weak Rocks Based on Figure 38.

$$W_B = (1/2)Qv^2 \qquad (37)$$

where: Q = weight of the fracture bounded block of rock,

v = velocity imparted to the block from the dynamic energy.

This velocity will be a function of the resistance to movement along the fractures in that a certain amount of energy will be dissipated, overcoming the frictional resistance there. Therefore, the orientation of any fractures which may have previously developed and the direction of energy movement will have a significant influence on the dynamic stability of a tunnel. The influence of these fractures on the tunnel stability may best be addressed through the use of probabilistic methods.

CHAPTER 3

LIMIT STATE DESIGN CONCEPTS

During the past 30 years increasing knowledge of the behavior of structural materials and the necessity to reduce weight and cost in increasingly sophisticated structures, has led to the introduction of limit state design. Limit state design is based on traditional design methods, but aims to reduce "safety factors" by considering variations in working stresses and strengths, both during and after construction, in a rational manner.

Limit state design originates from reinforced concrete design, in which the structural members performance is evaluated according to whether or not it has reached or exceeded certain limiting states of deformation or strength. The limit state design itself is the embodiment of ideas of the form and proportions of a structure and is required to satisfy:

a. That there is an adequate margin of safety against possible overload, defects in materials, and inadequacies in analytical and construction procedures.
b. That the structure will remain serviceable for the purpose for which it was designed during its useful life.
c. That there is a proper balance between safety and economy.

To achieve these requirements, the "characteristic" strengths and working stresses or loads used in the design should take into

account the variations in strengths and properties of the materials used in construction and the "probable" loads to which they will be subjected. In addition to the inbuilt margins of safety obtained by using these "characteristic" values, additional partial safety factors are used for the construction materials and for imposed or live loads. In concrete design all relevant limit states are considered in order to ensure an adequate degree of safety and serviceability, as required by a,b, and c above. The usual approach is to design on the basis of the most critical limit state and then to check that the remaining limit states will not be reached.

The limit states are commonly grouped into three main categories (Hughes, 1980):

(1) ULTIMATE LIMIT STATE - Represents complete collapse or rupture of one or more critical sections of the structure due to elastic or plastic instability from stress overloads. Characteristic of the ultimate limit state for reinforced concrete structures is the development of plastic deformations as the ultimate limit state is approached. Permanent deformations preclude elastic analysis since the strains become excessively large.

(2) SERVICEABILITY LIMIT STATES - Represent varying degrees of deformation, cracking, changes in slope, continuity, or vibration resulting in a general loss of performance capability. That is, the design has not failed according to the traditional sense of strength excess, but it has undergone changes which could result in "failure" based on a limit state criterion. Serviceability limit

states are, in general, repairable limits, in that, remedial action to regain performance is possible.

(3) OTHER LIMIT STATES - Such as fatigue and durability (due to recurring loads), impact, which in itself does not collapse the structure but which can reduce the structures resistance to the normal loading condition so as to cause collapse later, fire resistance, lighting, or any other factor which at some time can cause a loss of the structures performance capability.

Limit State Design Applied To Tunnels

The design of tunnels in rock is well suited to limit state design concepts. In reinforced concrete design, the structure is considered loaded by forces external to the region of consideration so that failure occurs as a result of localized rupture or by excessive deformation in that region. In tunnels, the structure is a composite of intact rock, fractured rock, and liner (support), all of which need not be present and all of which may have different characteristics. Additionally, the properties of the intact and fractured rock are not well known, and the interaction of the various composite sections is not well understood. A most conservative approach to tunnel design would be to cast a very thick liner for all possible tunnel conditions. This approach would provide an adequate margin of safety but would not satisfy the design requirements since the balance between safety and economy will have been upset. The obvious difference between limit state design of reinforced concrete structures and tunnels in rock is that the rock around the tunnel is

both a load carrying member and a load inducing member. This difference along with the variability and lack of knowledge of the rock/support characteristics makes adequate design of tunnels much more difficult. An accounting of this variability and lack of understanding can be taken care of through probabilistic methods (for the variability of materials and material characteristics) and through the use of energy methods to better describe the fracture and dilation characteristics in the tunnel annulus and how these characteristics interact with the support characteristics.

The performance standards relating to particular limit states will vary according to the prescribed use of the tunnel. High priority structures will be significantly more sensitive to deformations than low priority structures, and hence their deformation limit states will be much more strict. Ultimate or collapse limit states will however, be independent of the prescribed use of the tunnel as they are based solely on strength excess.

Barton et al. (1974) proposed the first limit state type of approach by suggesting the Excavation Support Ratio of increasing degrees of underground support for:

a. Temporary mine openings
b. Vertical shafts
c. Permanent mine openings; hydro tunnels; pilot headings for major excavations
d. Storage rooms, water treatment plants, minor road and railway tunnels, surge chambers, access tunnels

e. Power stations, major road and railway tunnels; civil defense chambers; portals; intersections, etc.

f. Underground nuclear power stations; railway stations; sports halls; public access facilities.

These were essentially a series of increasing factors of safety based on minimum deformation limit states in strong and shallow granites.

In general, the possible limit states for structures in rock can be considered as:

(A) ULTIMATE LIMIT STATE: For structures in rock represents complete collapse of the tunnel. The ultimate limit state for tunnels in rock would be reached in those instances when the fracture resistance of a significant volume of rock in the tunnel annulus is exceeded by the strain energy imposed upon that volume of rock. The volume of rock unfavorably influenced by the energy changes during and after excavation must be great enough to completely compromise the tunnel project. For instance, immediately following excavation, the release of energy causing redistributed stresses and strain energy will commonly exceed the rock fracture resistance in a finite thickness of the tunnel annulus. However, this does not presume that the failed rock will be great enough in volume or will even completely collapse into the opening. The energy overloads must be great enough to force this to happen. The ultimate limit state for tunnels could be considered to describe macroscopic catastrophic circumstances such as rockburst conditions and not microscopic (on the project level)

excess of rock strength. Upon reaching the ultimate limit state, the failure would be fairly rapid and complete.

In reinforced concrete design, the ultimate limit state can be reached by exceeding the strength of some key structural element. This can also occur for rocks: for instance, by exceeding the strength of a rock beam or plate near its supports. If this structural element supports weaker materials, then a catastrophic collapse can occur. This way the strength of a large volume of rock need not be exceeded, but rather may require only a small volume of key material.

Important to consider in evaluating the structure (tunnel) for attainment of any of the limit states is the influence of geologic discontinuities. The strength of the intact rock need not be exceeded, but rather, the strength along joints or fractures can, if properly oriented control the performance of the tunnel. The ultimate limit state can be reached if the strength along a significant (or key) number of these joints is exceeded.

The development of a carcass of fractured rock around the tunnel, or the presence of pre-existing fractures, will create a condition in which time-dependent behavior can occur. The broken material will tend to degrade under the influence of weathering, presumably becoming less structurally competent with time. This time dependent behavior could cause the tunnel(rock/linear system) to reach some of the various serviceability limit states as described below sometime after completion of the project.

(B) SERVICEABILITY LIMIT STATES - These several limit states represent deformations of the tunnel short of complete collapse which

affect the performance of the tunnel during its useful life. An extreme example might be complete closure resulting from time or transient related deformation over the useful life of the tunnel. In tunnel design, the serviceability limit states will largely be developed based on carcass deformations. Any number of these limit states can be defined and the ranges of tolerable deformations will be, in general, site specific. The following serviceability limit states can be considered.

(B-1) SEVERE LIMIT STATE - The limit state of most severe tunnel damage. Normal activity and use of the tunnel is hampered or stopped. Repairs would include removal of excess rock, replacement of supports, realignment of the tunnel and major repair of tracks and pipes. Deformations occur in the fractured carcass surrounding the tunnel and along favorably oriented joints in the tunnel vicinity. Since the deformations occur largely in the fractured (not intact) rock, the elastic analysis is not valid. Other models, most notably plastic analysis, have been used to estimate boundary displacements. These models do not provide an adequate fracture mechanism and therefore, probably do not describe well the fracture zone behavior in brittle rocks. An areal closure possibly in excess of 50% is envisaged, controlled by yielding supports. In the extreme case of time-dependent deformation, the closure can reach 100% and can, with the exception of the mode of failure and time of application, be indistinguishable from the ultimate state.

(B-2) MODERATE LIMIT STATE - A limit state describing less severe tunnel damage. The tunnel deformations result in a gradual

loss of serviceability with time (depending on the expected life of the structure). The deformations are less extreme than the severe limit state so that repairs are economical but given greater deformations they become intolerable and uneconomical. Medium cost repairs and replacement of some supports may be required to regain the performance capability as defined in the original design.

(B-3) MINOR LIMIT STATE - Characterized by minor deformations and carcass damage which requires minor repairs and realignment. Repairs are relatively inexpensive and infrequent resulting in a minor loss of tunnel performance capability.

(B-4) NO DEFORMATION LIMIT STATE - The limit state where sufficient support is made available to eliminate deformation completely. This situation represents an extreme example of a strict tunnel performance standard and as such will be applicable only to very important high-priority structures.

(B-5) SPECIAL LIMIT STATES - These limit states will represent any other important consideration which might affect the performance of the tunnel during its lifetime. These can include; vibrations, water drainage, ventilation, lighting, etc., which can have a major influence on the tunnel performance.

All of the various serviceability limit states (minimum-severe) can be used to gauge the performance of a given tunnel at a given time. Assuming that the carcass deformations are stable, then the structure will pass from the limit states of minor deformations to the limit states of more severe deformation. If

guidelines are in place (e.g., a limit state code of practice for tunnels), then, based on the rapidity with which the serviceability limit states are reached and exceeded, contingency plans for support changes or additions can be made.

The importance of time and economics should be emphasized in the application of limit state design concepts. The tunnel designer is charged with the task of providing both a safe and economical structure. To this end he must weigh the value of the end product (ore for mining, transportation speed for vehicular tunnels) with the cost of providing access (tunnel support) to that end. A mine opening would ideally remain functional only until the ore was removed. The cost of repairing or maintaining a tunnel may, at some time, become uneconomical so that the tunnel may be better left abandoned.

Tunnel supports can be designed to resist the deformations which will occur around an excavation, or they can be designed to control the deformations. In either case they have a major effect on the design and on the performance of the tunnel. The type of tunnel support can be determined after the performance standards for that tunnel have been established. Table 2 lists some common types of support and the deformations they are capable of assuming. Obviously, rockbolts will not be the support of choice if large deformations are expected and can be tolerated by the tunnel.

Inherent in limit state design of tunnels is the idea of performance. Performance is the realization of a certain amount of the design expectations. Many factors will affect the tunnel in

Table 2. Allowable Deformation (Expressed as Percentage of Vertical Height) of Typical Support Systems. (From Farmer, 1985)

Segmental lining	$\leq$ 1 %
Rockbolts	$\leq$ 2 %
Rockbolts plus shotcrete	3 %
Shotcrete	4 %
Square Rectangular Set	12 %
Rigid Arch	25 %
Yielding Arch	40 %

deleterious ways throughout the tunnels lifetime. These factors include:

a. Size and shape of the excavation - influences the released energy which will be applied to the surrounding rocks.

b. Location relative to other openings - proximity to other excavations can significantly increase the amount of energy which must be stored in the surrounding rocks to achieve stability.

c. Use of the tunnel - a tunnel can perform well only for the use for which it was designed. The performance standards for a vehicular tunnel would be peculiar to those for a mine opening.

d. Expected life of the tunnel - a tunnel of short life expectancy might be more tolerant of the attainment of minor or even moderate limit states.

e. Rock or ground conditions - a broad all encompassing categorization of intact rock and fractured (jointed) rock behavior.

f. Ground water conditions - can influence initial and long term tunnel behavior due to water pressure, strength reduction, and rock alteration.

g. Excavation quality - poor excavation quality control can accelerate the rock comminution process.

h. Stress regime - influenced by tunnel geometry and in-situ stress conditions.

i. Tunnel support - resistance to deformation, support/rock interaction characteristics with respect to the rock, resistance to ground water, etc.

The preceeding list is not all encompassing but does represent the difficulty associated with satisfying the original design performance standards of the tunnel. Unlike designing in reinforced concrete where the properties and reactions of the material are known within reasonable bounds, considerable variations exist in knowledge and material characteristics associated with tunnels in rock. These variations may best be approached through probabilistic methods which take into consideration those variations.

Energy Probability and Limit States

The purpose of limit state design is the achievement of acceptable probabilities that the structure being designed will not become unfit for the use for which it is required. In tunnels this would most likely be in terms of areal (or volumetric) convergence as previously described. The variation in many of the factors mentioned act to increase the uncertainties of the design process and can ultimately lead to an uneconomical or unsafe design.

In general, the uncertainties can be lumped into four main groups: (a) uncertainties in material properties, both intact and broken rock properties, and liner (support)-rock interactive properties, (b) uncertainties in the jointing orientation and joint material properties, (c) uncertainties in the actual loading

conditions, and (d) uncertainties in the analysis procedure. Type (a) and (b) uncertainties can be considered to be represented by various probabilistic distributions (e.g., normal, lognormal, uniform, Fisher, bivariate normal, etc.). Type (c) and (d) uncertainties are closely related and are not necessarily amenable to probabilistic or uncertainty analysis. They can best be minimized by choosing the analysis which most correctly models the actual rock behavior. All analytical models are based on an assumption of idealized rock behavior (e.g., plastic behavior of the broken material (Ladanyi, 1974; Bray, 1967), usually precluding, or describing only poorly, rock fracture mechanics. The use of strain energy principles can provide a link between the rock and tunnel behavior and limit state design concepts. Both strain energy and limit states contain, as essential components, the concept of deformation.

Probably the most important limit states for tunnels in rock are the serviceability limit states which describe tunnel performance in terms of percent areal (volumetric) closure. Strain energy, especially in the elastic range describes the energy changes around an excavation in terms of boundary deformations. Carrying the energy changes farther, the release of energy through both elastic and rock fracture (inelastic) will be manifested as a loss of potential energy in the system considered (tunnel and annulus). This loss in potential energy will occur as tunnel closure.

CHAPTER 4

CONCLUSIONS AND RECOMMENDATIONS FOR FURTHER RESEARCH

Most methods for evaluating the performance of tunnels in rock assume either idealized rock behavior or assume that the behavior can be described from an empirical knowledge of historical behavior of similar structures under similar rock conditions. Although each may adequately predict behavior in certain instances, neither approach is entirely satisfactory, since they tend to neglect the actual fracture mechanism in rock, which may be best be described in terms of an energy balance between the potential energy stored in the rock and the surface energy requirements for a crack to form or expand.

Strain energy is a concept which can take into consideration the potential for fracture development and as such may provide the most satisfactory solution to the problem of rock fracture around underground installations. The combination of the potentially more satisfying strain energy concepts with design requirements based on limit states can be the basis for a complete tunnel design program.

The largest obstacle in the strain energy analysis is the lack of understanding of the behavior, in strain energy terms, of rock in the annulus of a tunnel. The development of excess strain energy in the annulus of a tunnel can be described from elastic theory, and the initiation of fracture in the annulus may be defined with the aid of the term "fracture toughness". Fracturing beyond the tunnel boundary

layer, however, is not so easily defined. It is this fracturing which will control the tunnel boundary deformations, which in turn will define the tunnel's performance according to limit state design. Current laboratory testing programs do not satisfactorily model the conditions that may be expected in the annulus. To this end, current laboratory tests should be evaluated in strain energy terms and additional tests should be developed.

Recommendations

The importance of properly modeling both the distribution of strain energy and the rock's response to that energy cannot be underestimated. A rock testing program incorporating laboratory, scale model, and actual monitoring of existing tunnels should be undertaken to provide the parameters which can accurately describe the tunnel's behavior under the expected loading conditions.

Laboratory Testing

Laboratory testing programs should be developed to determine the energy release characteristics and the residual energy storage capability of rocks in a manner similar to that expected in a tunnel annulus. Questions that should be addressed include: the influence of the intermediate principal stress on rock fracture characteristics, the influence of the energy gradient or critical energy difference on fracture, the influence of the size of the "window" through which the energy changes will occur, the immediate (after fracture) energy storage capability, and the large displacement (strain-softening) energy storage capability.

The actual loading condition in the tunnel annulus will be that of true triaxial loading. Therefore, polyaxial devices should be employed to assess the influence of the intermediate principal stress on rock strength and fracture characteristics. This test can be used to estimate the influence of variations in the principal stresses on the dilational characteristics of rock.

Triaxial devices ($\sigma_2 = \sigma_3$) can be used in conjunction with polyaxial devices to determine the significance of σ_2 on the release of energy during fracture and fracture resistance. Triaxial testing devices are less expensive (as is the testing procedure) so that numerous tests can be made at reduced cost.

Triaxial and polyaxial tests should be performed on broken and fractured rock samples to determine the residual energy release and residual energy storage characteristics of rock in the annulus. The broken material can either be the post-fracture rock sample from triaxial or polyaxial tests or in-situ broken material.

Other tests can be envisaged which model more closely the loading conditions in the tunnel annulus. For instance, a test to determine the influence of the area ("window") through which fracture and displacement can occur. A common triaxial test allows energy release through a 360° "window". Fracturing in the annulus of a tunnel would allow energy release and dilation only toward the opening so that the area ("window") there would be proportionally smaller.

Other Testing

Ultimately, the testing program should model as closely as possible the conditions in the tunnel annulus. Therefore, larger scale testing programs would be desirable. To this end, scale model experiments may provide useful information. A large (9 x 9 x 3 ft) load frame is under development at the Waterways Experiment Station in Vicksburg, Mississippi. This load frame, when operational, will allow model size (2 ft diameter) tunnels constructed in plaster material to be loaded up to 2000 psi. This device will alleviate scale effects commonly encountered in laboratory testing. Additionally, the device may be altered to allow study of dynamic energy inputs on scale model tunnels.

The final recommendation is to study actual tunnels in rock so that correlations between laboratory testing and field behavior can be made. The influence of support, if any is used, must be incorporated in the evaluation.

APPENDIX A

TRIAXIAL TEST DATA

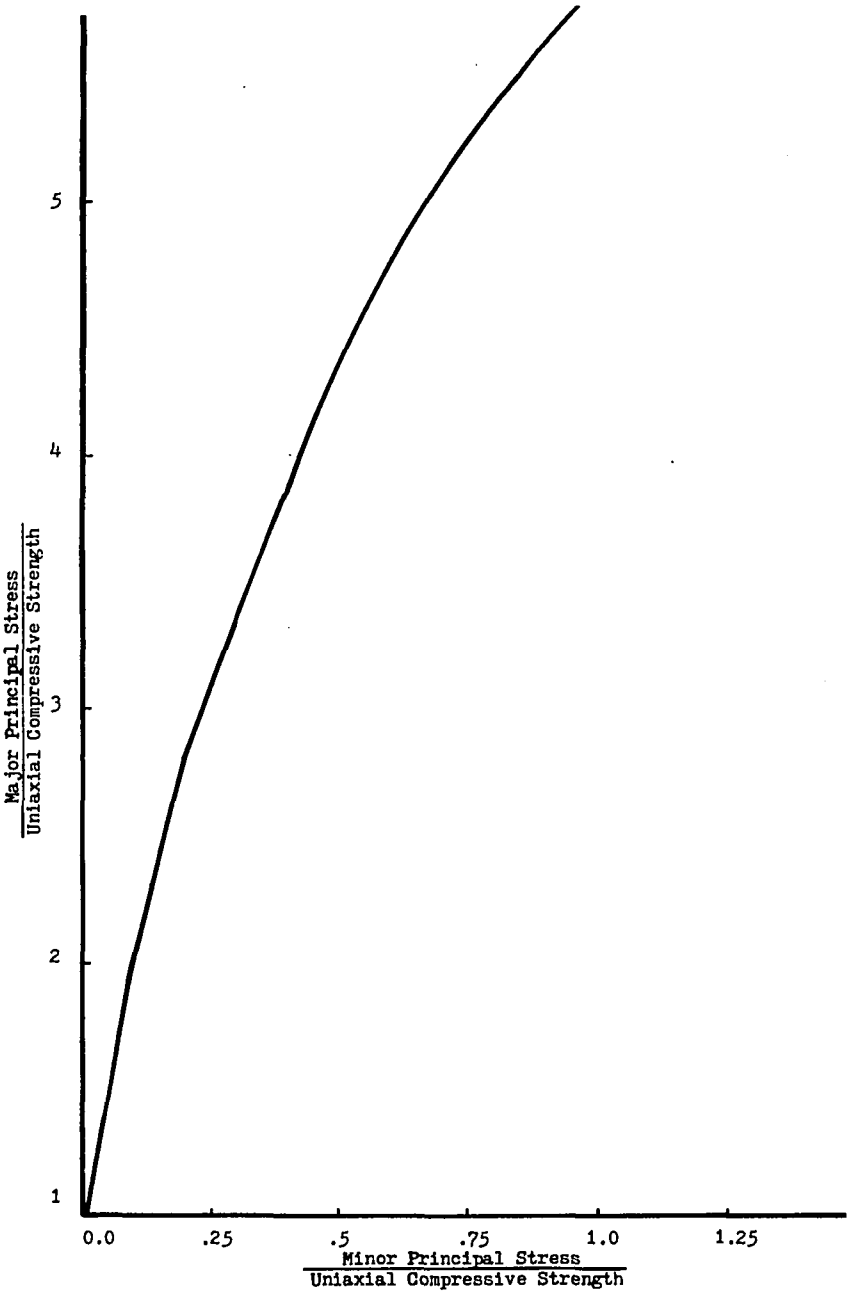

Figure A1. Relationship Between Normalized Major and Minor Principal Stresses at Failure for Granite. (from Hoek and Brown, 1981)

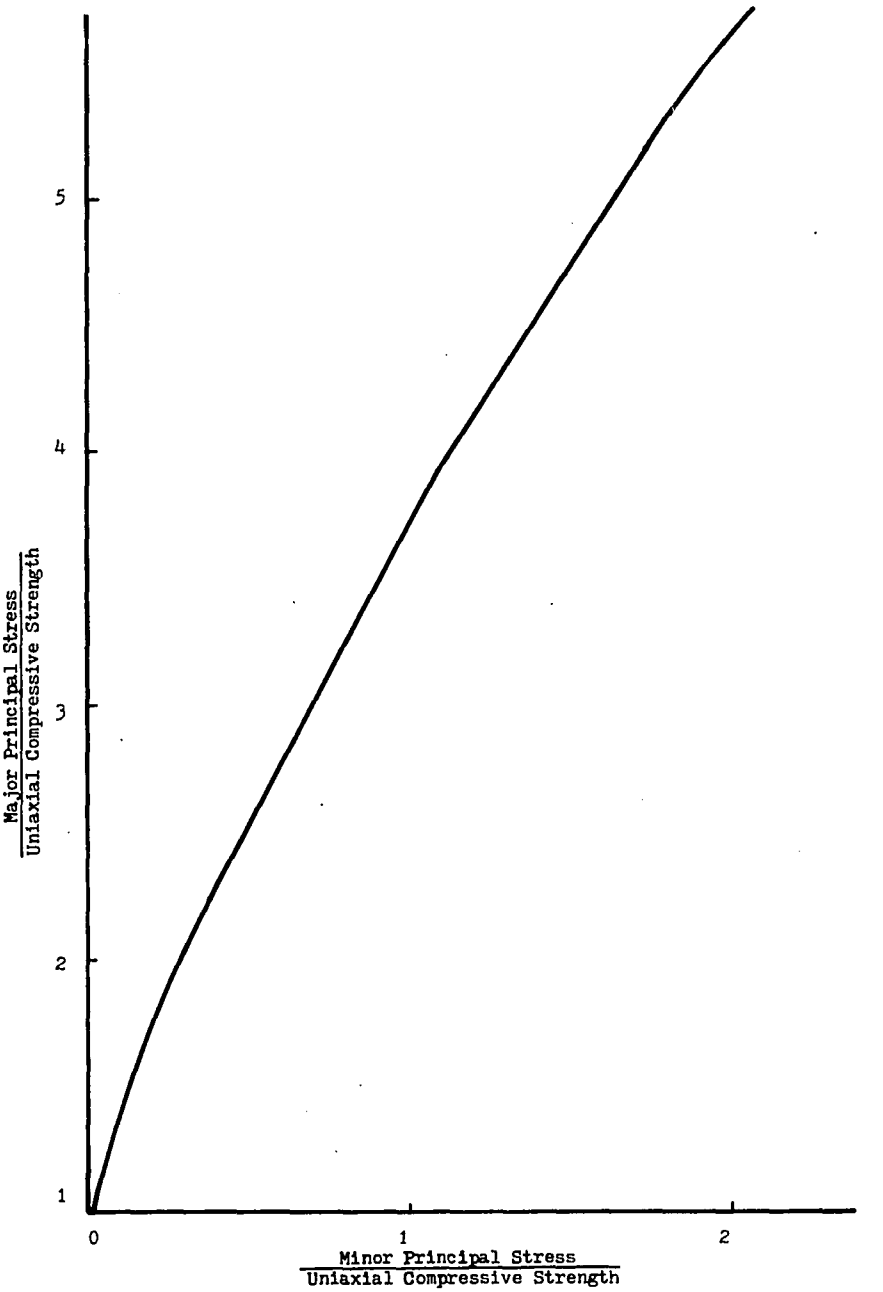

Figure A2. Relationship Between Normalized Major and Minor Principal Stresses at Failure for Limestone. (from Hoek and Brown, 1981)

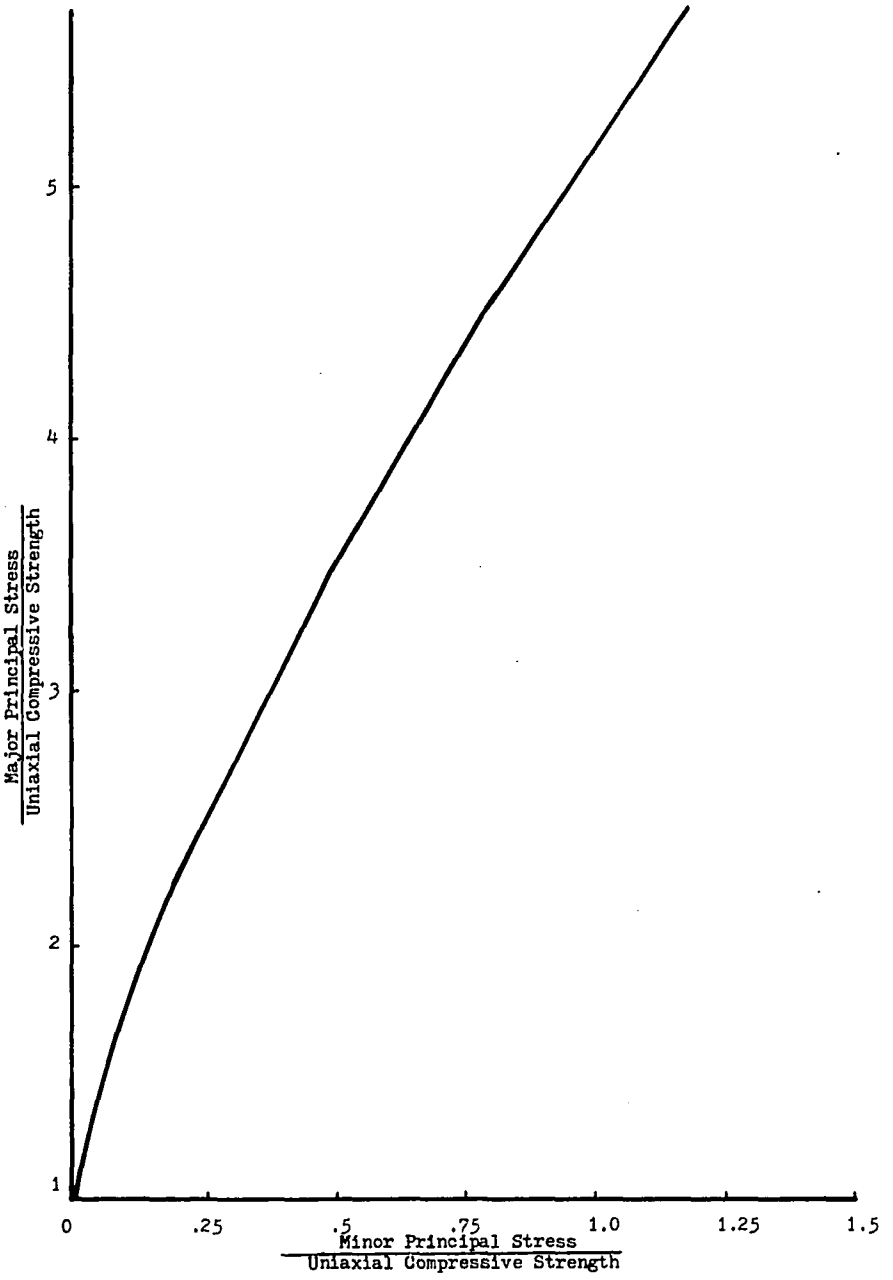

Figure A3. Relationship Between Normalized Major and Minor Principal Stresses at Failure for Sandstone. (from Hoek and Brown, 1981)

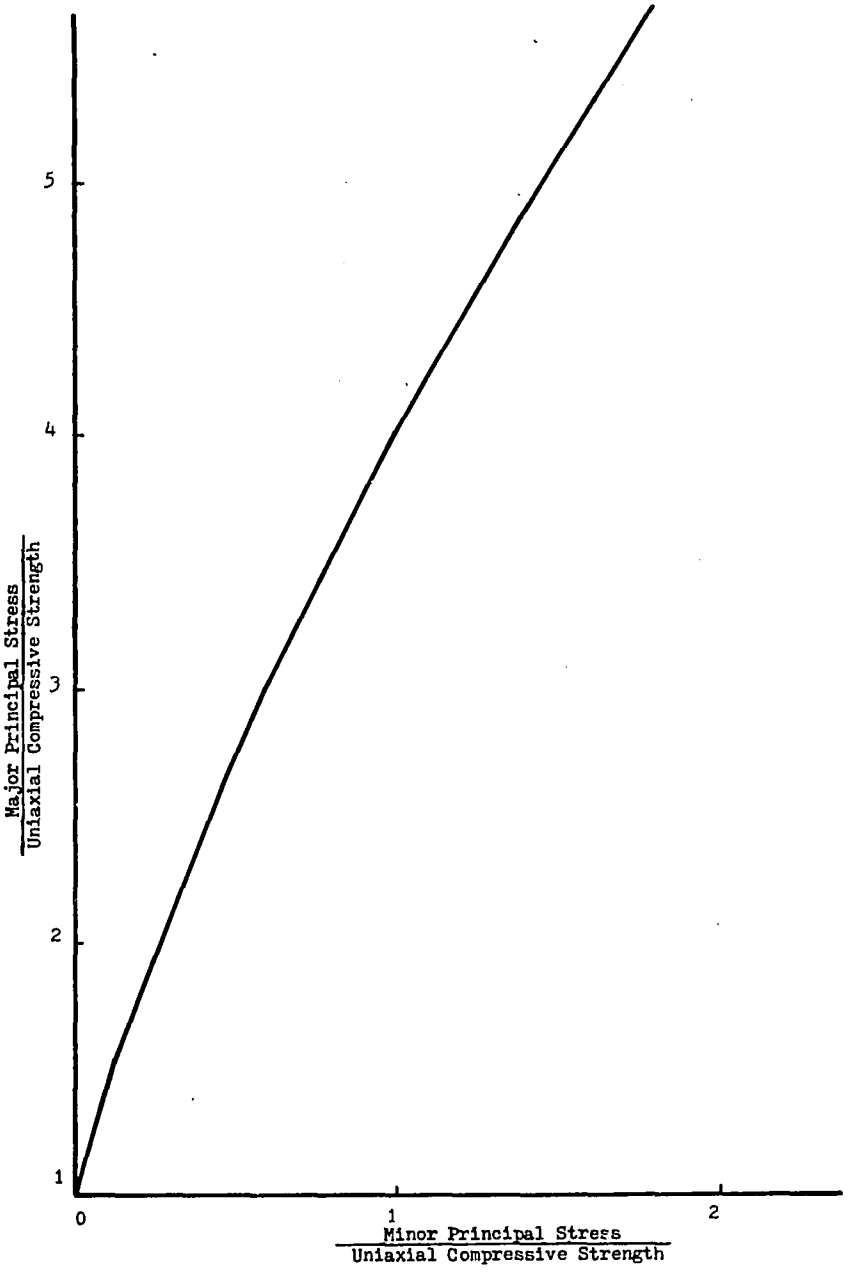

Figure A4. Relationship Between Normalized Major and Minor Principal Stresses at Failure for Mudstone. (from Hoek and Brown, 1981)

REFERENCES

Barton, N., Lien, R., and Lunde, J., "Engineering Classification of Rock Masses for the Design of Tunnel Supports," Norwegian Geotechnical Institute Publication, NR 106, 1974.

Bieniawski, Z.T., "Engineering Classification of Jointed Rock Masses," Transactions of the South African Institute of Civil Engineers, Vol. 15, 1973, pp. 335-344.

Bieniawski, Z.T., "Rock Mass Classifications in Rock Engineering," Proceedings of a Symposium on Exploration for Rock Engineering, Johannesburg, Vol. 1, 1976, pp. 97-106.

Brady, B.G.H. and Brown, E.T., "Energy Changes and Stability in Underground Mining: Design Applications of Boundary Element Methods," Transactions of the Institute of Mining and Metallurgy, London, 1981, pp. A61-68.

Brady, B.G.H. and Brown, E.T., Rock Mechanics for Underground Mining, George Allen and Unwin, London, 1985.

Bray, J.W., "A Study of Jointed and Fractured Rock - Part II: Theory of Limiting Equilibrium," Felsmechanik und Ingenieurgeologie (Rock Mechanics and Engineering Geology), Vol. V, No. 4, 1967, pp. 197-216.

Brown, E.T., Bray, J.W., Ladanyi, B. and Hoek, E., "Ground Response Curves for Rock Tunnels," Journal of the Geotechnical Engineering Division, Vol. 109, No. 1, ASCE, 1983, pp. 15-39.

Cook, N.G.W., "The Design of Underground Excavations," Proceedings of the Eighth Symposium on Rock Mechanics, University of Minnesota, 1966, in Failure and Breakage of Rock, C. Fairhurst (Ed.), 1967, pp. 167-193.

Daemen, J.J.K., "Problems in Tunnel Support Mechanics," Underground Space, Pergamon Press, 1977, pp. 163-172.

Deere, D.U., "Technical Description of Rock Cores for Engineering Purposes," Rock Mechanics and Engineering Geology, Vol. 1, No. 1, 1964, pp. 16-22.

Deere, D.U. and Miller, R.P., "Engineering Classification and Index Properties for Intact Rock," Air Force Weapons Laboratory Report, AFWL-TR-65-16, Kirtland, New Mexico, 1966.

Dickenson, C.M. and Lindberg, H.E., "Scale Model Experiments Investigating the Response of Protective Structures to Nuclear Attack Loading," Proceedings of the Twenty-fifth U.S. Symposium on Rock Mechanics, Northwestern University, Evanston, Illinois, June 25-27, 1984, pp. 829-837.

Dowding, C.H., "Seismic Stability of Underground Openings," Proceedings of the First International Symposium on Storage in Excavated Rock Caverns, Rock Store 77, Stockholm, Sweden, Pergamon Press, Vol. 2, 1978, pp. 231-238.

Farmer, I.W., Engineering Behavior of Rocks, Second Edition, Chapman and Hall, London, 1983.

Farmer, I.W., Coal Mine Structures, Chapman and Hall, London, 1985.

Fenner, R., "Untersuchungen zur Erkenntnis des Gebirgsdruckes, Gluckauf," (Study of Ground Pressures), Technical Translation 515, NRC Division of Building Research, Vol. 74, 1938, pp. 691-696; 705-715.

Friedman, M., Handin, J. and Alani, G., "Fracture Surface Energy of Rocks," International Journal of Rock Mechanics and Mining Science, Vol. 9, 1972, pp. 757-766.

Hobbs, D.W., "The Behaviour of Broken Rock Under Triaxial Compression," International Journal of Rock Mechanics and Mining Science, Vol. 7, 1970, pp. 125-148.

Hobbs, N.B., "The Prediction of Settlement of Structures on Rock," Conference on Settlement of Structures, Cambridge, 1974, pp. 579-610.

Hoek, E. and Brown, E.T., Underground Excavations in Rock, Institute of Mining and Metallurgy, London, 1981.

Hughes, B.P., Limit State Theory for Reinforced Concrete Design, Third Edition, Pitman, London, 1980.

Jaeger, J.C. and Cook, N.G.W., Fundamentals of Rock Mechanics, Third Edition, Chapman and Hall, London, 1979.

Joachim, C.E., "Tunnel Destruction: State of the Art," Proceedings of the 1979 Rapid Excavation and Tunneling Conference, Atlanta, Georgia, June 18-21, 1979, pp. 1507-1517.

Kirsch, G., "Die Theorie der Elastizitat und die Bedurfinisse der Festigkeitslehre," Zeitschrift des Vereines Deutscher Ingenieure, Vol. 42, 1898, p. 797.

Krech, W.W., "The Energy Balance Theory and Rock Fracture Energy Measurements for Uniaxial Tension," Proceedings of the Third Congress of the International Society of Rock Mechanics, Vol. II, Part A, 1974, pp. 167-173.

Ladanyi, B., "Use of the Long-term Strength Concept in the Determination of Ground Pressure on Tunnel Linings," Proceedings of the Third Congress of the International Society of Rock Mechanics, Vol. II, Part B, 1974, pp. 1150-1156.

McClintock, F.A. and Walsh, J.B., "Friction on Griffith Cracks Under Pressure," Proceedings of the Fourth U.S. Congress on Applied Mechanics, 1962, pp. 1015-1021.

Muskhelishvili, N.I., Some Basic Problems of the Mathematical Theory of Elasticity, Fourth Edition, Translated by J.R.M. Radok, Published by Groningen Noordhoff, 1953.

Owen, G.N., Scholl, R.E. and Brekke, T.C., "Earthquake Engineering of Tunnels," Proceedings of the 1979 Rapid Excavation and Tunneling Conference, Atlanta, Georgia, June 18-21, 1979, pp. 709-721.

Price, A.M., "The Effect of Confining Pressure on the Post-yield Deformation Characteristics of Rocks," Ph.D. Thesis, University of Newcastle-Upon-Tyne, U.K., 1979.

Rodean, H.C., "Nuclear Explosion Seismology," U.S. Atomic Energy Commission, Oak Ridge, Tennessee, 1971.

Timoshenko, S.P., Strength of Materials - I: Elementary Theory and Problems, Third Edition, Van Nostrand, Princeton, New Jersey, 1958.

Timoshenko, S.P. and Goodier, J.N., Theory of Elasticity, Second Edition, McGraw-Hill, Inc., New York, 1951.

Wiebols, G.A. and Cook, N.G.W., "An Energy Criterion for the Strength of Rock In Polyaxial Compression," International Journal of Rock Mechanics and Mining Science, Vol. 5, 1968, pp. 529-549.

Wilson, A.H., "The Stability of Tunnels in Soft Rocks at Depth," Proceedings of a Conference on Rock Engineering, Newcastle-Upon-Tyne, U.K., 1977, pp. 511-527.

Wilson, A.H., "The Stability of Underground Workings in the Soft Rocks of the Coal Measures," Ph.D. Thesis, University of Nottingham, U.K., 1980.